METHOD DEVELOPMENT FOR PILOT PRODUCTION OF ASTRAGALOSIDE VII

A Thesis Submitted to
the Graduate School of Engineering and Sciences of
İzmir Institute of Technology
in Partial Fulfilment of the Requirements for the Degree of

MASTER OF SCIENCE

in Bioengineering

by
Mustafa Ünver KURT

December 2019
İZMİR

We approve the thesis of **Mustafa Ünver KURT**

Examining Committee Members:

Prof. Dr. Erdal BEDİR
Department of Bioengineering, İzmir Institute of Technology

Prof. Dr. Ali ÇAĞIR
Department of Chemistry, İzmir Institute of Technology

Assoc. Prof. Dr. Derya GÜLCEMAL
Department of Chemistry, Ege University

19 December 2019

Prof. Dr. Erdal BEDİR
Supervisor, Department of Bioengineering
İzmir Institute of Technology

Assoc. Prof. Dr. Engin ÖZÇİVİCİ
Head of the Department of Bioengineering

Prof. Dr. Mehtap EANES
Dean of the Graduate School of
Engineering and Sciences

ACKNOWLEDGMENTS

I am kindly grateful to my supervisor Prof. Dr. Erdal BEDİR, who has always been an example for us with his scientific knowledge, experiences, perspective, and ethical understanding from the moment I met in my undergraduate education, until now. I do not doubt that he has undeniably contributed to the formation of my talents and thinking.

I am thankful to Prof. Dr. Ali ÇAĞIR and Assoc. Prof. Dr. Derya GÜLCEMAL for listening to me patiently in my thesis presentation and contributing to my thesis.

I would like to express my gratitude to Göklem ÜNER, who helped me keep my hope freshly for tomorrow, for her unchanging patience, support, and eternal love during my thesis studies. Also, I thank to my family, who has been supporting and encouraging me in all my life, even though we have been away from each other for many years.

My friendly thanks to all members of Natural Product Chemistry Laboratory for their helps, understandings, patience, and guidance. Nevertheless, I must especially thank to Nilgün YAKUBOĞULLARI for activity results of AST VII, to Eyüp BİLGİ and Emre GEZER for the sleepless days we were working together and his invaluable contribution to production at semi-pilot scale, and to Melis KÜÇÜKSOLAK for her guidance on project management and everything.

Thanks to everyone in BIONORM for seeing me as a part of their family. Also special thanks to Hürcan ATMACA, Dr. Özgür TAĞ and Duygu ARSLAN for letting us to use UHPLC-CAD system and their helps during quantitative analysis. In addition, I am thankful to BIYOMER for permitting us to use HPLC-DAD system and some laboratory devices.

This thesis was performed as a part of 116Z958 project (1003 Program, PI: Erdal BEDİR) funded by The Scientific and Technological Research Council of Turkey (TÜBİTAK).

ABSTRACT

METHOD DEVELOPMENT FOR PILOT PRODUCTION OF ASTRAGALOSIDE VII

Based on the promising adjuvant properties comparable to most widely used adjuvants Alum and *Quillaja* saponins (including QS-21), our team has decided to carry out advance studies to develop Astragaloside VII (AST VII) as a new vaccine adjuvant and/or an immunotherapeutic agent. To do so, one of the most important steps is establishing efficient isolation and purification processes to obtain AST VII at large scale.

In this thesis, starting from laboratory scale to semi-pilot scale, it was aimed to optimize the production steps of AST VII from *Astragalus trojanus*. Factor screening (1 categorical and 3 numerical) and optimization studies were performed using experimental design, based on which methanol (MeOH) as solvent, 1:20 (g/mL) as plant:solvent ratio, 0.5-1.0 mm as plant particle size and 8-10 hours for extraction time were selected yielding 0.36 percent g AST VII/g plant. To enrich AST VII in extract, pre-purification studies were performed such as liquid-liquid extraction, resin fractionation and precipitation. The results showed that the resin (D-101) fractionation employing water, 20 percent EtOH and EtOH was superior. To enrich AST VII up to 85-90 percent purity, several chromatographic steps using normal (employing EtOAc:MeOH:Water and Chloroform:MeOH:Water systems) and reversed phase (C18; employing MeOH:Water systems) silica gel were used. In last step, a precipitation method was developed using MeOH and acetone affording 98 percent purity. Developed method at lab scale (3.5 g) was successfully transferred to semi-pilot scale (about 100 g) with minor modifications, and a crucial step towards large-scale isolation (kg) of AST VII was accomplished.

ÖZET

ASTRAGALOSİDE VII MOLEKÜLÜNÜN PİLOT ÜRETİMİNE YÖNELİK METOTLARIN GELİŞTİRİLMESİ

Ekibimiz, en yaygın kullanılan adjuvanlar Alum ve *Quillaja* saponinlerle (QS-21 dahil) karşılaştırılabilir umut verici adjuvan özelliklerine dayanarak, yeni bir aşı adjuvanı ve /veya bir immünoterapötik ajan olarak AST VII'yi geliştirmek için ileri çalışmalar yapmaya karar vermiştir. Bunu yapmak için, en önemli adımlardan biri, AST VII'yi büyük ölçekte elde etmek amacıyla verimli izolasyon ve saflaştırma işlemleri geliştirmektir.

Bu tezde, laboratuvar ölçeğinden yarı pilot ölçeğe kadar, *Astragalus trojanus*'tan AST VII'nin üretim aşamalarını optimize etmek amaçlanmıştır. Faktör tarama (1 kategorik ve 3 nümerik) ve optimizasyon çalışmaları, deneysel tasarım kullanılarak gerçekleştirilmiştir. Bu çalışmalar sonunda, yüzde 0.36 g AST VII/g bitki verimine ekstraksiyonda ulaşmak için, çözücü olarak MeOH, bitki:solvent oranı olarak 1:20 g/mL, bitki parçacık oranı olarak 0.5-1.0 mm, ekstraksiyon süresi olarak 8–10 saat esas alınmıştır. Hedef molekülü zenginleştirmek için, sıvı-sıvı ekstraksiyon, reçine fraksiyonlama ve çöktürme gibi ön saflaştırma çalışmaları yapılmıştır. Sonuçlar, Su, yüzde 20 EtOH ve EtOH kullanılan reçine (D-101) fraksiyonlamanın üstün olduğunu göstermiştir. AST VII'nin saflığını yüzde 85-90'a çıkarabilmek için, normal (EtOAc:MeOH:Su ve Kloroform:MeOH:Su sistemleri kullanılan) ve ters faz (C18; MeOH:Su sistemleri kullanılan) silika jel kullanılan birkaç kromatografik aşama kullanılmıştır. Son adımda, yüzde 98 saflığa MeOH ve aseton kullanılan bir çöktürme yöntemi ile ulaşılmıştır. Laboratuar ölçeğinde (3.5 g) geliştirilen yöntem, küçük modifikasyonlarla yarı pilot ölçeğe (yaklaşık 100 g) başarıyla aktarılmış ve AST VII'nin büyük ölçekli izolasyonuna (kg) yönelik önemli bir adım aşılmıştır.

TABLE OF CONTENTS

LIST OF FIGURES ix

LIST OF TABLES xi

LIST OF CHROMATOGRAMS xii

LIST OF SPECTRA xiii

ABBREVIATIONS xiv

CHAPTER 1. INTRODUCTION 1

1.1. Vaccine and Adjuvant 1

1.2. Saponin 4

1.3. Isolation and Purification of Some Commercial Saponins 6

1.4. *Astragalus* and Astragaloside VII 9

CHAPTER 2. MATERIALS AND METHODS 14

2.1. Materials 14

2.1.1. Materials for Optimization Studies at Laboratory Scale 15

2.1.2. Materials for Production of AST VII at Laboratory Scale 20

2.1.3. Materials for Production of AST VII at Semi-Pilot Scale 20

2.2. Methods 21

2.2.1. Methods for Optimization Studies at Laboratory Scale 24

2.2.1.1. Optimization of Extraction 24

2.2.1.1.1. Comparison of Parts of Plant Material 24

2.2.1.1.2. Design of Experiment 24

2.2.1.1.3. Extraction Studies 26
2.2.1.2. Optimization of Pre-purification Step 28
2.2.1.2.1. Liquid-Liquid Extraction 28
2.2.1.2.2. Resin Fractionation 30
2.2.1.2.3. Saponin Precipitation 33
2.2.1.3. Optimization of Purification 33
2.2.1.4. Optimization of Final Purification 34
2.2.2. Methods for Production of AST VII at Laboratory Scale 34
2.2.2.1. Extraction Step 35
2.2.2.2. Pre-purification Step 37
2.2.2.3. Purification Step 38
2.2.3. Methods for Production of AST VII at Semi-Pilot Scale 41
2.2.3.1. Extraction Step 41
2.2.3.2. Pre-purification Step 43
2.2.3.3. Purification Step 44

CHAPTER 3. RESULTS AND DISCUSSIONS 47
3.1. Results of Optimization Studies at Laboratory Scale 47
3.1.1. Optimization of Extraction 47
3.1.1.1. Comparison of Parts of Plant Material 47
3.1.1.2. Extraction Studies 49
3.1.1.3. Design of Experiment 53
3.1.2. Optimization of Pre-purification 60
3.1.2.1. Liquid-Liquid Extraction 60
3.1.2.2. Resin Fractionation 64
3.1.2.3. Saponin Precipitation 67
3.1.3. Optimization of Purification 68

3.1.4. Optimization of Final Purification 70
3.2. Results from the Production of AST VII at Laboratory Scale 70
3.2.1. Extraction Step 70
3.2.2. Pre-purification Step 70
3.2.3. Purification Step 71
3.3. Results from the Production of AST VII at Semi-Pilot Scale 73
3.3.1. Extraction Step 74
3.3.2. Pre-purification Step 74
3.3.3. Purification Step 75

CHAPTER 4. CONCLUSION 81

REFERENCES 84

LIST OF FIGURES

Figure **Page**

Figure 1. Chemical structure of QS-21 isolated from *Quillaja saponaria Molina* 7
Figure 2. Chemical structure of glycyrrhizic acid from licorice 8
Figure 3. Chemical structure of betulinic acid isolated from plane tree 9
Figure 4. Chemical structure of AST VII 11
Figure 5. Photos of plant material before and after sieving 15
Figure 6. Photos of the lyophilization process and displaying drying conditions 22
Figure 7. Photo of Soxhlet-type extraction system 26
Figure 8. Formulae of calculations 27
Figure 9. Photos of SCES loaded with EtOAc and H_2O 29
Figure 10. Photos of resin fractionation studies 30
Figure 11. Isolation of AST VII from *A.trojanus* at laboratory scale 35
Figure 12. Soxhlet-like extraction system using a rotary evaporator 36
Figure 13. Photos of resin column 37
Figure 14. Photos of silica column 38
Figure 15. Photos of RP-C_{18} column 39
Figure 16. Photo of column subjected with AST VII rich fraction 40
Figure 17. Photo of lyophilization for pure AST VII fractions 41
Figure 18. Isolation of AST VII at semi-pilot scale 42
Figure 19. Photos of extraction 43
Figure 20. Photos of resin column 44
Figure 21. Photos of silica column 45
Figure 22. Photos of RP-C_{18} column 46
Figure 23. Photos of precipitation studies 46
Figure 24. TLC profiles of the MeOH extracts of *A. trojanus* 48
Figure 25. ANOVA table and R^2-values for factor screening studies 54
Figure 26. Plots for factor screening 55
Figure 27. Comparisons of percent yield of AST VII versus main factors 55

Figure **Page**

Figure 28. Model formation in Design Expert 7.0.0 58
Figure 29. ANOVA table and R^2-values for factor optimization studies 58
Figure 30. Plots for factor optimization 59
Figure 31. 3D surface graph for the percent yield of AST VII 59
Figure 32. TLC profiles for EtOAc:H_2O partition in SCES 60
Figure 33. TLC profiles of n-BuOH:H_2O partition in SCES 62
Figure 34. TLC profiles of EtOAc:H_2O partition in SF 62
Figure 35. TLC profiles of n-BuOH:H_2O partition in SF 63
Figure 36. TLC profiles of the fractions under UV_{365} 65
Figure 37. TLC profiles of fractions obtained after resin column 65
Figure 38. TLC profiles of first kinetic study 66
Figure 39. TLC profiles of precipitation studies with crude extract 67
Figure 40. TLC profile of precipitation studies with [4-18] obtained after resin column 68
Figure 41. TLC profiles of fraction of [Fr: 23-61] spotted on different adsorbents and developed with different mobile phase system 69
Figure 42. TLC profiles of some fractions obtained after resin column 71
Figure 43. TLC profiles of AST VII rich fractions 71
Figure 44. TLC profiles of the AST VII richest fraction 72
Figure 45. TLC profiles of combined fractions after RP-C_{18} column 73
Figure 46. TLC profiles of main fractions obtained in different stages during the isolation of AST VII 73
Figure 47. TLC profiles of combined fractions after first silica column 75
Figure 48. HPTLC profile of AST VII obtained from precipitation of [Fr: 51-79] 78
Figure 49. The flow chart of developed method for isolating AST VII in high purity from *A.trojanus* 82

LIST OF TABLES

Table **Page**

Table 1. Run sheet sorted by standard number (STD) for screening.....16
Table 2. Run sheet sorted by standart number for optimization.....19
Table 3. Analysis method for UHPLC studies 22
Table 4. Analysis method for HPLC studies 23
Table 5. Development of resin column for determination of elution system 31
Table 6. Development of resin column.....31
Table 7. Amounts of extract and resin in first kinetic study.....32
Table 8. Amounts of extract and resin in second kinetic study 32
Table 9. AST VII content in the roots and aerial parts determined by UHPLC-DAD.....49
Table 10. Percent yield of AST VII data for factor screening.....49
Table 11. Percent yield of AST VII data for factor optimization.....53
Table 12. UHPLC results of EtOAc:H_2O partitions in SCES 61
Table 13. UHPLC results of n-BuOH:H_2O partitions in SCES.....61
Table 14. UHPLC results for EtOAc:H_2O partitions in SF 63
Table 15. UHPLC results of n-BuOH:H_2O partitions in SF.....64
Table 16. UHPLC results of fractions obtained after resin column.....66

LIST OF CHROMATOGRAMS

Chromatogram **Page**

Chromatogram 1. UHPLC-CAD chromatograms of *Astragalus trojanus* extract 13

Chromatogram 2. UHPLC-CAD chromatogram of the MeOH extract of both plant parts 48

Chromatogram 3. UHPLC-CAD chromatogram of four samples 57

Chromatogram 4. UHPLC-CAD chromatogram of MeOH extract of *A.trojanus* and pure AST VII 74

Chromatogram 5. HPLC-DAD chromatogram of [Fr: 62-81] isolated from first silica column 76

Chromatogram 6. HPLC-DAD chromatogram of [Fr: 28-36] isolated from RP-C_{18} silica 76

Chromatogram 7. HPLC-DAD chromatogram of [Fr: 61-67] isolated after second silica column 77

Chromatogram 8. HPLC-DAD chromatogram of [Fr: 61-67] purified after precipitation 77

LIST OF SPECTRA

Spectrum **Page**

Spectrum 1. ^{1}H NMR spectrum of AST VII obtained from precipitation of [Fr: 51-79] 78

Spectrum 2. Expanded ^{1}H NMR spectrum of [Fr: 51-79] 79

Spectrum 3. ^{13}C NMR spectrum of AST VII obtained from precipitation of [Fr: 51-79] 79

Spectrum 4. Expanded ^{13}C NMR spectrum of [Fr: 51-79] 80

ABBREVIATIONS

^{13}C NMR	Carbon Nuclear Magnetic Resonance
^{1}H NMR	Proton Nuclear Magnetic Resonance
A.trojanus Stev.	*Astragalus trojanus* Steven
ACN	Acetonitrile
ACS	American Chemical Society
Adj. R^2	Adjusted R^2
ANOVA	Analysis of Variance
APC	Antigen-Presenting Cell
AST IV	Astragaloside IV
AST VII	Astragaloside VII
BBD	Box-Behnken Design
BIOMER	Biotechnology and Bioengineering Application and Research Center
BIONORM	Bionorm Natural Products Production and Marketing Corp.
CAD	Charged Aerosol Detector
CC	Column Chromatography
$CHCl_3$	Chloroform
DAD	Diode Array Detector
DNA	Deoxyribonucleic Acid
DOE	Design of Expert
DT	Diphtheria-Tetanus
EtOAc	Ethyl Acetate
EtOH	Ethanol
Fr	Fraction
GFD	General Factorial Design
GSK	Glaxo Smith Kline
H_2O	Water
HIV	Human Immunodeficiency Virus
HPLC	High-Performance Liquid Chromatography

IFN- γ	Interferon- γ
IL-2	Interleukin-2
ISCOM	Immunostimulant Complex
MeOH	Methanol
N/A	Not Available
n-BuOH	n-Butanol
NDV	Newcastle Disease Virus
NMR	Nuclear Magnetic Resonance
Pred. R^2	Predicted R^2
QS-21	*Quillaja saponaria Molina*-fraction21
RP	Reversed Phase
RSM	Response Surface Methodology
SCES	Single-Current Extraction System
SF	Separation Funnel
SN	Standard Number
SS	Stainless Steel
STD	Standard
tert-BuOH	tert-Butanol
TLC	Thin Layer Chromatography
UHPLC	Ultra-High-Performance Liquid Chromatography
UPW	Ultra-Pure Water
UV	Ultraviolet
VLC	Vacuum Liquid Chromatography

CHAPTER 1

INTRODUCTION

1.1. Vaccine and Adjuvant

The goal of vaccination is to establish a strong, protective and long-term immune response to infections. Live vaccines, prepared with weakened infectious agents but reproduction of which are still in progress, proliferate in the recipient after a period of time and produce immunity close to the response of natural infection without clinical findings and complications. Therefore, live vaccines do not require the use of adjuvants. Dead vaccines, prepared with inactive or highly purified infectious agents, are less immunogenic and require the use of adjuvants to produce adequate immunization. Further, in "combined" vaccines, where purified antigens from different microorganisms or from multiple strains of the same microorganism are co-administered, strong "adjuvants" are needed to achieve an equal immune response for each antigen with fewer injections (Petrovsky and Aguilar 2004, Gupta and Siber 1995, Lee and Nguyen 2015).

Adjuvant means "adjuvare" in Latin, which means that an enhancer or a helper and enhances the immune response when inoculated with the antigen. They are not immunogenic and do not form antibodies (O'Hagan 2000). The concept of vaccine adjuvant was first introduced by Ramon (Ramon 1925). One year after Ramon described adjuvants in 1925, Glenny et al. showed the adjuvant effect of aluminum salts with diphtheria toxoid adsorbed to aluminum (Glenny 1926). Since then, aluminum compounds (aluminum hydroxide and aluminum phosphate) have been the most commonly used vaccine adjuvant and have been the first adjuvant to be licensed for using in many human vaccines: diphtheria-tetanus (DT), diphtheria-tetanus-pertussis, DT combined hepatitis B virus or inactive poliovirus , hepatitis A, *Streptococcus pneumonia*, meningococcus and human papillomavirus vaccine (Ramon 1925, 1926, Arda et al. 1994, Diker 1998, Yurdakök and İnce 2008).

Today, there is a strong need for potential adjuvants to provide an appropriate immune response (cellular, fluid response) in vaccine applications. Important roles of adjuvants in vaccination are:

- ✓ To establish a more potent and long-term desired immune response type (Th_1/Th_2) in a short time;
- ✓ To increase immunogenicity of inactive, high purity or recombinant antigens;
- ✓ To reduce the number of immunizations or the amount of antigen required for protective immunity;
- ✓ To regulate the usefulness of vaccines in neonates, the elderly or those with weak immune systems;
- ✓ To act as an antigen delivery system for the removal of antigens from the mucosa;
- ✓ To provide a strong immune response against each antigen in combined vaccines (Rajput et al. 2007)

An ideal adjuvant with potential use in the vaccine industry should: provide cellular and/or fluid immune response; produce long-term immunity; be safe and have little side effects; not cause mutagenicity/carcinogenicity/teratogenicity and autoimmunity; be biodegradable, inexpensive and have a long shelf life (Aguilar and Rodriguez 2007). The antigen to be used in the selection of the adjuvant should be determined by the type of immune response required (Th_1, Th_2), the species to be vaccinated, the route of administration and the side effects. A good fluid immune response is required for toxins, whereas a Th_1-weighted immune response based on cellular response is required for intracellular bacteria, viruses and cancer antigens (Glenny 1926, Aguilar and Rodriguez 2007).

According to Edelman, the 2000 classifications of the adjuvants as mucosal and parenteral depending on the origin, mode of action, physicochemical properties and route of administration is as follows:

1. Active immunostimulants: Enhancing immune response to antigen
2. Carrier: Provides T cell help to immunogenic proteins

3. Vehicle adjuvants: Oil emulsions or liposomes that stimulate the immune response and form a carrier medium for antigens (Edelman 2000)

According to their types, adjuvants are classified as aluminum salts, emulsion type adjuvants, saponin based adjuvants, bacterial adjuvants, carbohydrate adjuvants, liposomes, cytokines, virus-like particles and polymeric (Nanotechnological) adjuvants (Reddy and Couvreur 2009). Newly developed adjuvants have contributed greatly to the development of therapeutic vaccines due to their high efficacy. In addition to preventing infection, the use of vaccines in disease treatments is a revolution in medicine. Diseases in which therapeutic vaccine development studies are currently underway are chronic infectious diseases (Herpes Simplex Virus, HIV, Hepatitis C Virus, Hepatitis B Virus, *Helicobacter pylori*), malignancies (melanoma, breast cancer, colon cancer) and allergic or autoimmune (multiple sclerosis, type1 diabetes, rheumatoid arthritis) diseases. The novel adjuvant formulations comprise two or more adjuvant mixtures having different mechanisms of action. For example, a mixture of alum with saponin or monophosphoryl lipid A (Stewart-Tull 1989, Spriggs and Koff 1990, O'Hagan 2000).

Side effects of adjuvants can be local or systemic. Local side effects; pain, local inflammation, swelling, necrosis at the injection site, damage to the lymph nodes, granuloma, ulcer and abscess formation, while systemic side effects; nausea, fever, arthritis, uveitis, eosinophilia, allergy, anaphylactic shock, immunotoxicity (Lindblad 1995, Gupta 1998, Roberts 2000).

As previously specified, Alum compounds are adjuvants commonly used in human and animal vaccines. Aluminum hydroxide and aluminum phosphate having different physical properties than mineral salts are frequently used as adjuvants. Potassium aluminum sulfate is the most preferred adjuvant in the vaccine industry under the name "Alum". Alum is also partially used in the purification of protein antigens, tetanus and diphtheria toxins. Two common methods are used when preparing the vaccine with aluminum compounds that are legal to be added to human vaccines, depending on the physical and chemical characteristics of the antigen: In situ precipitation of Alum compounds or adsorption of the antigen to the aluminum gel (Aprile and Wardlaw 1966, Gupta 1998, O'Hagan 2000).

Mechanisms of action of aluminum compounds are as follows:

1. Warehouse mechanism: The adjuvant and adsorbed antigen remain at the injection site. The antigen is released slowly to stimulate antibody production
2. Inflammation mechanism: Adjuvant causes local inflammation. Antigen-presenting cells (APCs) are rapidly directed to the site and encounter high concentrations of antigen
3. Mechanism to facilitate antigen uptake: Adsorption converts soluble antigen into particulate form, and then APCs absorb these particles by phagocytosis. Aluminum compounds lead to local granulomas containing antibody-producing plasma cells, and also alternatively activate the complement system, the use of Th_2 immune response profile and the use of freeze-sensitive (non-lyophilized) aluminum compounds. In addition, Alum induces the formation of immunoglobulin E (IgE) antibody response due to certain allergic reactions in humans (O'Hagan 2000, Lindblad 1995, Gupta 1998).

1.2. Saponin

Saponins are secondary metabolites found in plant or marine organisms carrying sugar units on a high molecular weight triterpenic (30-carbon) or steroidal (27-carbon) core. For centuries, they have been used as soap (Saponin comes from the Latin word "sapo = soap") because of the foaming properties of the plants that carry these compounds and are also used for fishing because of their toxicities towards cold-blooded organisms. Saponins have been the subject of intensive research for centuries because of their use in traditional medicine (especially in India and China). Based on these studies, many saponin-including plants have been among the most widely consumed products in the dietary supplement market (*Ginseng, Astragalus, Tribulus, Centella,* etc.). Recently, the saponin-including products have started to be used in the livestock industry both against infections and to increase productivity (such as *Yucca* saponin preparations used in poultry) (Yeo and Kim 1997).

One of the effects of saponins on the immune system is to increase the level of specific immune response to the vaccine substances via adjuvant properties (Sun, Xie, and Ye 2009). Saponins of plant origin enhance response of immune system cells such as neutrophils, monocytes and lymphocytes (Chaves-Mora et al. 2007). Although the cytokine modulating effects of herbal medicines is well-known, it has been reported to result in different levels of cytokine (IL-2, interleukin-4, interleukin-6 and IFN-γ) secretion depending on the drug dose (Nalbantsoy et al. 2011, Nalbantsoy et al. 2012, Yesilada et al. 2005). The adjuvant activity of saponins varies according to the hydrophobic aglycone skeleton and hydrophilic side sugar chains. Adjuvant activity is also thought to be associated with branched sugar chains, aldehyde groups, or acyl residues in aglycone (Sun, Xie, and Ye 2009). To date, studies with saponins have found that bidesmosidic saponins (carrying two sugar chains) are more effective than monodesmosidics (carrying a single sugar chain) or aglycones without sugar chains. Unfortunately, there are no studies on tridesmosidic saponins since the number of them in nature is limited. All of the tridesmosidic saponins in nature have been found in *Astragalus* genus by Bedir and his coworkers (Bedir et al. 1999a).

The adjuvant effect of saponins was first demonstrated in 1936. Later, saponin obtained from the tree called *Quillaja saponaria* grown in South America have been used as an adjuvant in the vaccine industry (Donnelly 1997). *Quillaja saponaria Molina* is an important milestone for saponin research focusing on adjuvant activity (Richou, Jensen, and Belin 1964). *Quillaja saponins* are commonly used alone or in combination with aluminum salts, liposomes, oil in water emulsions and amphipathic proteins, which are immunostimulant complexes, and also used with lipids that form detergent/lipid/saponin complexes known as immunostimulant complex (ISCOM) (Garçon, Chomez, and Van Mechelen 2007).

Today, saponin fractions obtained from this tree are available in two different forms: Quil A and QS-21 (*Quillaja saponaria Molina*-fraction 21). For many years, Quil A has been used as an adjuvant in veterinary medicine, especially against foot and mouth disease. In addition, the serological response to Ephemeral Fever containing Quil A vaccine in cattle was found to be better than other adjuvants such as dextran sulfate or aluminum hydroxide. A pure saponin is also used as an adjuvant in cat leukemia recombinant vaccine (Diker 1998, O'Hagan 2000, Roberts 2000). Although Quil A has been used successfully in veterinary medicine for many years, it is not preferred in human vaccines due to its toxic and heterogeneous nature.

QS-21 is obtained by purification of Quil A by reverse phase chromatography. It has been reported to be less toxic and produce a stronger cellular immune response. It is currently being used in humans as an adjuvant in HIV, Alzheimer, Varicella zoster diseases, DNA and other cancer vaccines (Cox et al. 1999). Among the mechanisms of action of the adjuvant are shown to be developing cytotoxic T cell response, inducing cytokines, and directly activating phagocytosis by macrophages. In addition, its strong cellular and humoral immune response and low dose activity have been reported as the most important advantages. However, the pain at the injection site, hemolysis, toxic and irritant properties are among the disadvantages (Coffman, Sher, and Seder 2010, Sivakumar et al. 2011). QS-21 has been used to generate a strong cellular response as an alternative to aluminum adjuvants. It stimulates Th_1 cytokines (IL-2, IFN-γ) and IgG2α antibodies (Kensil et al. 1993).

In contrast, ISCOM, a complex adjuvant containing antigen, cholesterol and phospholipid with saponin derivatives, enhances both cellular and humoral immune responses. Clinical trials have been reported in human-produced HIV and influenza vaccines. Another complex adjuvant, ISCOMATRIX is a mixture that resembles ISCOM but does not contain antigen and produces only a humoral type immune response. It has been tried in animal experiments and recently in human studies; reliable and effective. It has been found that the humoral immune response increases potency, speed and duration of action and also reduces the dose of antigen required. Due to these properties, it is an adjuvant that may be preferred for combined vaccines.

Studies on the use of these newly developed adjuvants in human vaccines are in progress (Garcon and Van Mechelen 2011). Clinical studies of QS-21 adjuvant systems proceed as QS-21 (Pfizer, Phase II), AS01 (Glaxo Smith Kline (GSK), Phase III), AS02 (GSK, Phase III),and AS15 (GSK, Phase III) (Lee and Nguyen 2015, Rajput et al. 2007).

1.3. Isolation and Purification of Some Commercial Saponins

Saponins can be used in food, cosmetics, pharmaceutical/health applications as high-value added products. Therefore, increasing data of their health benefits have motivated research on method development for the production of saponins at commercial-

scale from natural sources. Some commercially produced saponins and a sapogenin were given below as a result of this researches.

To isolate QS-21 (Figure 1), a well-known vaccine adjuvant, the extract of *Quillaja saponaria Molina* bark, Quil-A, was obtained by dialysis against H_2O. Then the aqueous extract was dissolved/suspended in MeOH and filtered. To purify methanol-soluble extract, several chromatographic stages using normal phase silica gel (employing $CHCl_3$:MeOH:H_2O (62:32:6) system) and RP-C_4-HPLC; (employing isocratic separation in 40 mM acetic acid in MeOH:H_2O (58:42) system) were conducted (Kensil and Marciani 1991)

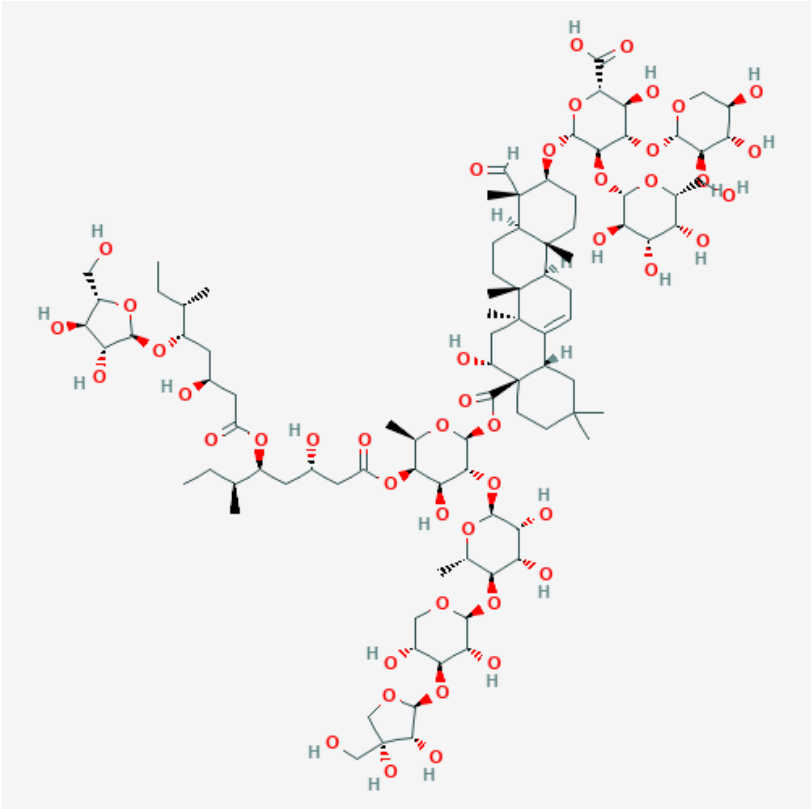

Figure 1. Chemical structure of QS-21 isolated from *Quillaja saponaria Molina* (Source: Marty-Roix et al. 2016, Fernández-Tejada 2017, National Center for Biotechnology Information. PubChem Database. Unii-61H83wzx3U)

To obtain glycyrrhizic acid (Figure 2) in crude form, which mostly used in food, medicine, and cosmetics fields, 700 kg licorice was extracted at 80°C with 4900 kg of hot

H2O for 7.5 h in a counter-current circulation extraction system which involves 6 extractors. To remove impurities inside of the extract, precipitation was carried out by cooling to 20℃. Subsequently, the supernatant was precipitated with 30% sulfuric acid during 2.5 h to adjust 1.7 pH. After the acid precipitation, 3.0 pH was adjusted by washing with H_2O three times. Then the liquid was filtered via a frame filter box and the obtained wet product was dried. As a result, 53.31 kg crude glycyrrhizic acid containing 25.23 g crude licorice acid product was achieved (Zhiming et al. 2017).

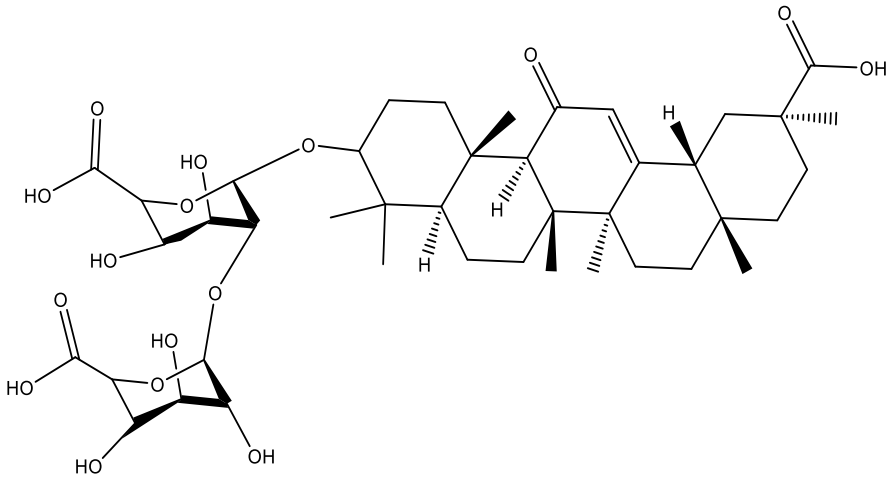

Figure 2. Chemical structure of glycyrrhizic acid from licorice (Source: Zhiming et al. 2017)

To produce betulinic acid (Figure 3), which is a potent anti-HIV and anti-cancer agent, the extraction of plane tree bark was performed in an extraction apparatus which involves three extractors, a distillate receiver, and an evaporator in series-connected. In extraction procedure, 1950 kg powdered plane bark was soaked with 780 L H_2O and then loaded to each extractor, equally. Subsequently, the plant material was extracted with 2.5 m^3 of warm toluene:(+-)-2-pentanol:MeOH mixture (88:7:5) for each individual extractor during 20 h. After the extract was dried by an evaporator, the crude extract was refluxed with 1430 L 2-propanol for 30 min. Then, the solution was combined with 11 kg kieselguhr and 24 kg activated charcoal and filtered into a crystallizer. The filtrate was cooled to 10℃ overnight for crystallization and the solution was filtered again. Thus, 43.4 kg of betulinic acid in crude form (83.9% content according to HPLC-UV) was achieved.

To further purification of betulinic acid, the same procedure was repeated by using 930 L dichloromethane and 325 L MeOH instead of 2-propanol with 11 kg kieselguhr and 22 kg activated charcoal at 5°C. As a result, 28.9 kg pure betulinic acid (93.8% content according to HPLC-UV) was obtained (Puder et al. 2007).

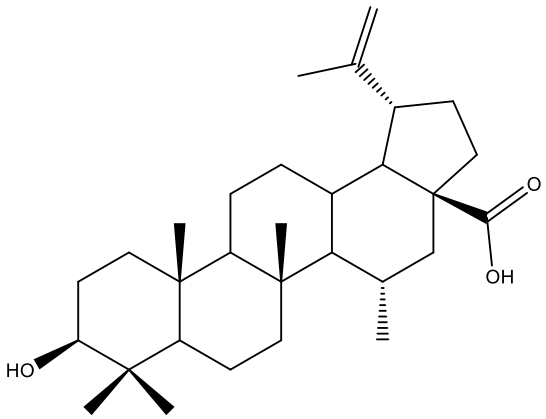

Figure 3. Chemical structure of betulinic acid isolated from plane tree (Source: Puder et al. 2007)

To produce ginsenosides at lab scale, which reported as anti-cancer molecules from *Panax ginseng*, the herbal powder were processed with a reflux extraction three times by using 85% EtOH. Saponins in the extract was enriched using D-101 macroporous adsorption resin. Elution was performed employing H_2O and 60% EtOH. Several chromatographic steps using normal [employing n-BuOH:EtOAc:H_2O (2:3:5) system] and reversed phase [C_{18}; employing MeOH:H_2O (75:25) system] silica gel were performed. It was reported that the method can be applied to industrial scale (Zhang 2015).

1.4. *Astragalus* and Astragaloside VII

Astragalus genus, which is a member of *Fabaceae* family, is the largest genus among vascular plants with approximately 2500 species in the world. There are 372

species in North America and 133 species in Europe. In Turkey, *Astragalus* genus is represented by approximately 447 species in the flora and is distributed in almost every region of Anatolia. They are prickly, sometimes thorn less, pennate-leaved perennial plants that generally grow at heights of 800-3000 m. The flowers are yellow, white or pink in butterfly shape. Spiky species can be easily noticed from a distance, especially with the clusters made in the form of pillows (Davis and Plitmann 1970, Gülcemal, Aslanipour, and Bedir 2019, Zeybek 1985, Davis 1970).

The roots of *Astragalus* species (especially *A. microcephalus, A. brachycalyx and A. gummifer*) are commercially important due to the fact that they give gum tragacanth drogs (emulsifying agent and thickener), also a product exported for many years from Turkey. However, it is not collected and exported anymore because of laborious collection and loss of its economic value.

Among the *Astragalus* species, the well-known species in the world is *A. membranaceus*, which grows in China and Mongolia. Formulations rich in polysaccharides and saponins, prepared from roots in traditional Chinese medicine, are the most commonly used drugs in cancer and immune system treatments. The cultivation of this plant is vast in China and Mongolia, and the plant is presented to the world market from these countries. Although many species grow wildly in Turkey, traditional use of Astragalus is not a common practice. The roots of these plants were realized to be used only in wound healing and blood cancer treatments in Southeastern Anatolia (Bedir et al. 1999a, b, Bedir, Calis, et al. 2001, Bedir, Tatli, et al. 2001, Bedir, Pugh, et al. 2000). As well, the roots are used by the villagers as animal feed during the cold winter months and above ground parts are used as firewood (Zeybek 1985).

Phytochemical studies on *Astragalus* species revealed cycloartane saponins, polysaccharides, flavonoids, pterocarpans, ionone glycosides, aliphatic nitro compounds and indolizidine alkaloids. As a result of the biological activity screenings, it is found that the compounds responsible for the effects could be classified in two groups: cycloartane saponins and polysaccharides (Mamedova and Isaev 2004).

The genus *Astragalus* stands out as the richest genus of cycloartanes in the plant kingdom. More than half of the saponins of about 650 cycloartane groups obtained to date have been obtained from *Astragalus* species. As noted above, the Turkish flora inhabits about 450 species with almost 1/6 of *Astragalus* members on Earth.

Studies on Turkish *Astragalus* species, more than 190 cycloartane type saponins including more than 90 new metabolites were obtained (Bedir et al. 1998, Bedir et al.

1999a, Bedir, Calis, and Khan 2000, Bedir, Calis, et al. 2000, Bedir, Pugh, et al. 2000, Bedir, Tatli, et al. 2001, Bedir, Calis, et al. 2001, Tabanca et al. 2005, Polat et al. 2009, Polat et al. 2010, Horo et al. 2010, Horo et al. 2012, Gülcemal et al. 2011, Gülcemal et al. 2012, Gülcemal et al. 2013, Karabey, Khan, and Bedir 2012, Djimtombaye et al. 2013). In parallel with these phytochemical studies, the effects of *Astragalus* extracts and pure saponins on macrophage activation and inflammatory cytokine expression were investigated. Based on the fact that folk remedies prepared from some *Astragalus* roots are used in the treatment of blood cancer in the Southeastern Anatolia Region, the purified compounds were tested against cancer cell lines (NCI panels); however, no significant activity was found. Based on the assumption that the effect on cancer could be via stimulation on the immune system, our studies have been shifted towards immune modulation. AST VII (Figure 4), a trisaccharidic cycloartane, showed noteworthy induction of IL-2 (139.6%), one of the cytokines playing an important role in the immune response against cancer (Yesilada et al. 2005).

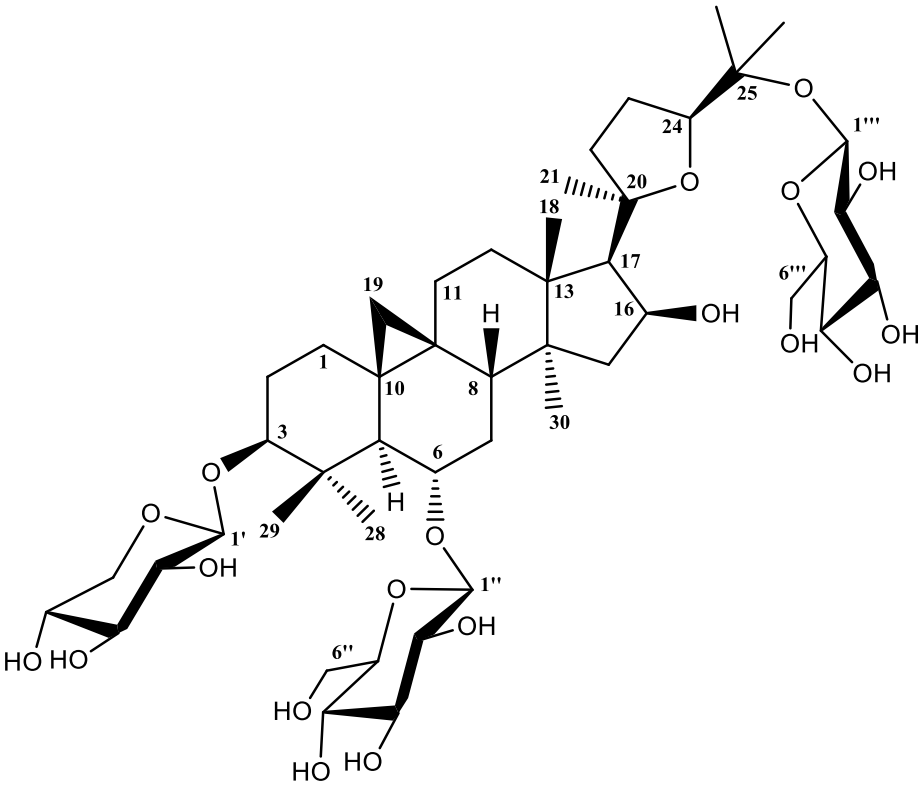

Figure 4. Chemical structure of AST VII (Source: Kitagawa, Wang, and Yoshikawa 1983, Bedir et al. 1999a)

The effects of AST VII were confirmed as an immunostimulant by in vivo studies (TUBITAK Project No: 109T637). Mouse vaccination studies have shown that AST VII enhances the Th_1-weighted immune response compared to groups treated with bovine serum albumin as a model antigen. These studies was continued to test adjuvant effects of AST VII in animal vaccines in cooperation with a vaccine company. Studies were carried out in comparison to Alum adjuvant in a vaccine containing 2 antigens consisting of *Clostridium perfringens* type C Beta Toxoid and *Escherichia coli* K99 bacterial antigen. The results showed that AST VII significantly increased the immune response to the toxoid antigen by 3-fold compared to the Alum adjuvant. Later, a TEYDEB project was initiated to carry out advanced preclinical and clinical studies with the vaccine company (ATAFEN). The clinical studies showed that AST VII had potent adjuvant properties for veterinary (Clostridial) vaccines (1507-TEYDEB, Project No: 7130545).

A further study was designed to see the effectiveness of the molecule in viral vaccines as well as bacterial vaccines. Our group conducted in vitro and in vivo studies with Newcastle disease virus (NDV) which is a major problem in poultry (TÜBİTAK Project No: 1139B411402292). When the inactivated NDV vaccine was administered to rats with AST VII, a higher immune response was obtained than the inactivated NDV vaccine without adjuvant. In inactivated NDV vaccines with AST VII and AST VII formed by different combinations of adjuvants (Monophosphoryl lipid A-MPL, squalene, *Astragalus* polysaccharide) induced a predominant Th_1 immune response, generally increasing IFN-γ, immunoglobulin G (IgG) production and stimulating splenocyte proliferation. In addition, some formulations of AST VII showed an equivalent or higher effect in inducing the immune system compared to the fat adjuvants used in commercial NDV vaccines. In the light of these data, AST VII has been shown to have high potential for use as an adjuvant not only in bacterial but also in viral vaccines.

Moreover, AST VII possess good potential for the vaccine industry as an adjuvant because of its following advantages: High solubility in H_2O, low molecular weight compared to other potent adjuvants (QS-21=1990.13 atomic mass unit (amu); AST VII=946 amu), higher chemical stability and good lyophilization properties.

In the analytical studies, the highest amount of AST VII was determined in *Astragalus trojanus* (0.2%), an endemic species (Chromatogram 1). For this reason, *A. trojanus* was selected as starting plant material in this thesis.

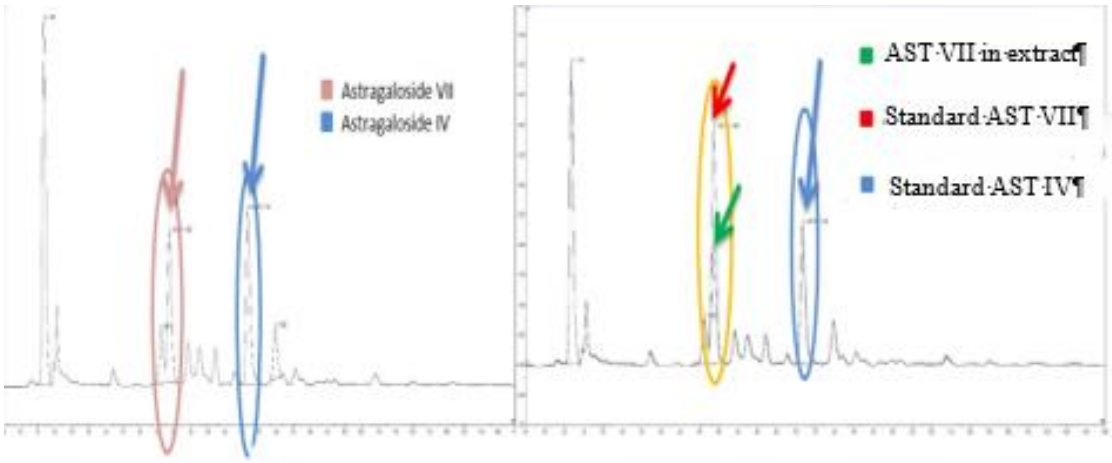

Chromatogram 1. UHPLC-CAD chromatograms of *Astragalus trojanus* extract

CHAPTER 2

MATERIALS AND METHODS

2.1. Materials

The materials used were briefly described in this section and grouped under three main headings:

- Materials for optimization studies at laboratory scale
- Materials for production of AST VII at laboratory scale
- Materials for production of AST VII at semi-pilot scale

In all studies, the qualitative controls were carried out on thin layer chromatography (TLC) plates (Silicycle, Normal Phase Silica Gel Plate; TLA-R10011B-323; Merck, High-Performance Normal Phase Silica Gel Plate, 1.05548.0001; Merck, Normal Phase Silica Gel Plate, 1.05554.0001; Merck, Reversed-Phase Silica Gel Plate, 1.05559.001). The chloroform ($CHCl_3$):MeOH:H_2O, ethyl acetate (EtOAc):MeOH:H_2O, MeOH:H_2O, and acetonitrile (ACN):H_2O mixtures were used as mobile phases for development (Camag, 10*11*4.5, 20*22*6). For visualization of bands, 20% sulfuric acid (Sigma Aldrich, ACS Grade) was sprayed onto the TLC plates followed by heating with a heat gun (Bosch, Easy Heat 500). Ultraviolet (UV) cabin (Vilber, CN-15.LM) furnished with (365 nm light) source was used for imaging of the saponin spots. To obtain dried samples, freeze dryers (Christ, Alpha 1-2 LDplus; Labconco, Freezone 6) were used.

Quantitative analysis of all samples and purity check of AST VII were carried out on ultra-high-performance liquid chromatography (UHPLC) (Thermo Fisher, Dionex Ultimate 3000) and high-performance liquid chromatography (HPLC) (Agilent, 1200). Both systems included consisted of four pumps, automatic sample injection sections, column ovens, solvent reservoir areas, and charged aerosol detector (CAD) /UV detectors. Column was developed with gradient ACN (Sigma Aldrich, GC grade):ultra-pure water (UPW) mixtures as mobile phase. The analyses were performed on UHPLC

(Thermo Fisher, HYPERSIL ODS; 100:4:3) and HPLC systems (Merck, Chromalith C_{18}, 100:4.6:3). For detection, CA (Corona™ Veo™ Charged Aerosol Detector, Thermo™)) as well as UV-diode array detector (DAD) and UV-DA detectors were utilized.

2.1.1. Materials for Optimization Studies at Laboratory Scale

BIONORM supplied *Astragalus trojanus* Stev. roots, which was harvested from Kozak Plateau-Bergama in August- September period in 2017. The roots and aerial parts were separately dried in shade, and then powdered by a grinder (Spice & Herb Grinder, IC-25B), which was followed by mechanical sieving (Baz Makina, BZ-004/SH) (Figure 5).

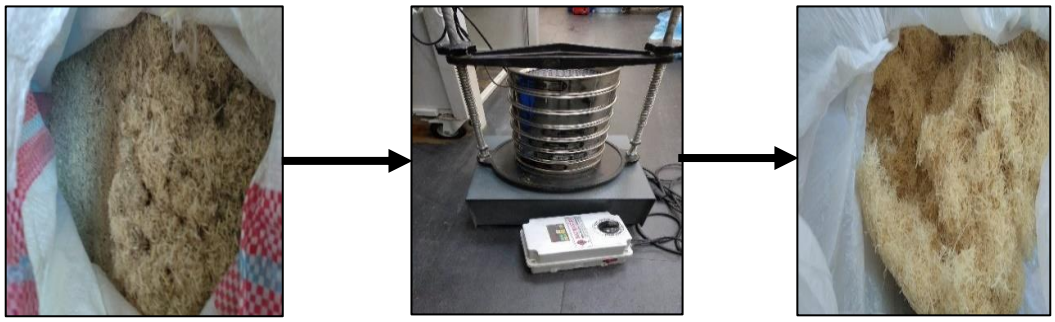

Figure 5. Photos of plant material before and after sieving

Design Expert 7.0.0 software was used to prepare run sheets (Table 1 and 2), whereas Microsoft Office 365 Excel-was used for plotting of data obtained via quantitative analysis. MeOH (Sigma Aldrich, ACS grade), ethanol (EtOH) (Isolab, ACS grade), 50% EtOH:H_2O mixture and n-butanol (n-BuOH) (Vwr, ACS grade) were used for extraction. The extraction process was performed on a Soxhlet system (V = 70 mL, Heating mantle (Isolab, I.608.16.250), Chiller (PolyScience, BS-SHK4450CH-1CE)). The extracts were concentrated on a rotary evaporator system (Buchi, R-100).

Table 1. Run sheet sorted by standard number (STD) for screening (Blocking using, 3 repetitions)

STD Number	Run Number	Block	Factor 1- Solvent	Factor 2- Time (h)	Factor 3- Plant:Solvent Ratio (g/mL)	Factor 4– Plant Particle Size (mm)	Response 1– Percent Yield of AST VII (g/g)
1	61	Block 1	MeOH	4	0.1	2-5	
2	65	Block 2	MeOH	4	0.1	2-5	
3	27	Block 3	MeOH	4	0.1	2-5	
4	80	Block 1	EtOH	4	0.1	2-5	
5	66	Block 2	EtOH	4	0.1	2-5	
6	24	Block 3	EtOH	4	0.1	2-5	
7	14	Block 1	50% EtOH:H_2O	4	0.1	2-5	
8	70	Block 2	50% EtOH:H_2O	4	0.1	2-5	
9	41	Block 3	50% EtOH:H_2O	4	0.1	2-5	
10	96	Block 1	n-BuOH	4	0.1	2-5	
11	8	Block 2	n-BuOH	4	0.1	2-5	
12	58	Block 3	n-BuOH	4	0.1	2-5	
13	75	Block 1	MeOH	12	0.1	2-5	
14	71	Block 2	MeOH	12	0.1	2-5	
15	32	Block 3	MeOH	12	0.1	2-5	
16	10	Block 1	EtOH	12	0.1	2-5	
17	29	Block 2	EtOH	12	0.1	2-5	
18	6	Block 3	EtOH	12	0.1	2-5	
19	16	Block 1	50% EtOH:H_2O	12	0.1	2-5	
20	53	Block 2	50% EtOH:H_2O	12	0.1	2-5	
21	94	Block 3	50% EtOH:H_2O	12	0.1	2-5	
22	20	Block 1	n-BuOH	12	0.1	2-5	
23	88	Block 2	n-BuOH	12	0.1	2-5	
24	50	Block 3	n-BuOH	12	0.1	2-5	
25	9	Block 1	MeOH	4	0.03	2-5	
26	79	Block 2	MeOH	4	0.03	2-5	
27	74	Block 3	MeOH	4	0.03	2-5	
28	46	Block 1	EtOH	4	0.03	2-5	
29	93	Block 2	EtOH	4	0.03	2-5	
30	23	Block 3	EtOH	4	0.03	2-5	
31	42	Block 1	50% EtOH:H_2O	4	0.03	2-5	

(cont. on next page)

Table 1. (cont.)

STD Number	Run Number	Block	Factor 1- Solvent	Factor 2- Time (h)	Factor 3- Plant:Solvent Ratio (g/mL)	Factor 4– Plant Particle Size (mm)	Response 1– Percent Yield of AST VII (g/g)
32	82	Block 2	50% EtOH:H_2O	4	0.03	2-5	
33	44	Block 3	50% EtOH:H_2O	4	0.03	2-5	
34	76	Block 1	n-BuOH	4	0.03	2-5	
35	95	Block 2	n-BuOH	4	0.03	2-5	
36	35	Block 3	n-BuOH	4	0.03	2-5	
37	11	Block 1	MeOH	12	0.03	2-5	
38	40	Block 2	MeOH	12	0.03	2-5	
39	51	Block 3	MeOH	12	0.03	2-5	
40	33	Block 1	EtOH	12	0.03	2-5	
41	54	Block 2	EtOH	12	0.03	2-5	
42	31	Block 3	EtOH	12	0.03	2-5	
43	49	Block 1	50% EtOH:H_2O	12	0.03	2-5	
44	22	Block 2	50% EtOH:H_2O	12	0.03	2-5	
45	90	Block 3	50% EtOH:H_2O	12	0.03	2-5	
46	91	Block 1	n-BuOH	12	0.03	2-5	
47	3	Block 2	n-BuOH	12	0.03	2-5	
48	48	Block 3	n-BuOH	12	0.03	2-5	
49	59	Block 1	MeOH	4	0.1	0.5-1	
50	63	Block 2	MeOH	4	0.1	0.5-1	
51	60	Block 3	MeOH	4	0.1	0.5-1	
52	5	Block 1	EtOH	4	0.1	0.5-1	
53	77	Block 2	EtOH	4	0.1	0.5-1	
54	87	Block 3	EtOH	4	0.1	0.5-1	
55	89	Block 1	50% EtOH:H_2O	4	0.1	0.5-1	
56	43	Block 2	50% EtOH:H_2O	4	0.1	0.5-1	
57	47	Block 3	50% EtOH:H_2O	4	0.1	0.5-1	
58	15	Block 1	n-BuOH	4	0.1	0.5-1	
59	78	Block 2	n-BuOH	4	0.1	0.5-1	
60	34	Block 3	n-BuOH	4	0.1	0.5-1	
61	57	Block 1	MeOH	12	0.1	0.5-1	
62	81	Block 2	MeOH	12	0.1	0.5-1	
63	2	Block 3	MeOH	12	0.1	0.5-1	

(cont. on next page)

Table 1. (cont.)

STD Number	Run Number	Block	Factor 1-Solvent	Factor 2-Time (h)	Factor 3-Plant:Solvent Ratio (g/mL)	Factor 4–Plant Particle Size (mm)	Response 1–Percent Yield of AST VII (g/g)
64	18	Block 1	EtOH	12	0.1	0.5-1	
65	68	Block 2	EtOH	12	0.1	0.5-1	
66	7	Block 3	EtOH	12	0.1	0.5-1	
67	56	Block 1	50% EtOH:H_2O	12	0.1	0.5-1	
68	67	Block 2	50% EtOH:H_2O	12	0.1	0.5-1	
69	45	Block 3	50% EtOH:H_2O	12	0.1	0.5-1	
70	52	Block 1	n-BuOH	12	0.1	0.5-1	
71	36	Block 2	n-BuOH	12	0.1	0.5-1	
72	55	Block 3	n-BuOH	12	0.1	0.5-1	
73	62	Block 1	MeOH	4	0.03	0.5-1	
74	19	Block 2	MeOH	4	0.03	0.5-1	
75	13	Block 3	MeOH	4	0.03	0.5-1	
76	21	Block 1	EtOH	4	0.03	0.5-1	
77	85	Block 2	EtOH	4	0.03	0.5-1	
78	73	Block 3	EtOH	4	0.03	0.5-1	
79	17	Block 1	50% EtOH:H_2O	4	0.03	0.5-1	
80	37	Block 2	50% EtOH:H_2O	4	0.03	0.5-1	
81	4	Block 3	50% EtOH:H_2O	4	0.03	0.5-1	
82	92	Block 1	n-BuOH	4	0.03	0.5-1	
83	83	Block 2	n-BuOH	4	0.03	0.5-1	
84	1	Block 3	n-BuOH	4	0.03	0.5-1	
85	72	Block 1	MeOH	12	0.03	0.5-1	
86	38	Block 2	MeOH	12	0.03	0.5-1	
87	64	Block 3	MeOH	12	0.03	0.5-1	
88	28	Block 1	EtOH	12	0.03	0.5-1	
89	84	Block 2	EtOH	12	0.03	0.5-1	
90	12	Block 3	EtOH	12	0.03	0.5-1	
91	39	Block 1	50% EtOH:H_2O	12	0.03	0.5-1	
92	86	Block 2	50% EtOH:H_2O	12	0.03	0.5-1	
93	69	Block 3	50% EtOH:H_2O	12	0.03	0.5-1	
94	25	Block 1	n-BuOH	12	0.03	0.5-1	
95	30	Block 2	n-BuOH	12	0.03	0.5-1	
96	26	Block 3	n-BuOH	12	0.03	0.5-1	

Table 2. Run sheet sorted by standart number for optimization (no blocking, 5 center points)

STD Number	Run Number	Block	Factor 1– Time (h)	Factor 2- Plant:Solvent Ratio (g/mL)	Factor 3–Plant Particle Size (mm)	Response 1– Percent Yield of AST VII (g/g)
1	11	Block 1	8	0.1	0.75	
2	13	Block 1	12	0.1	0.75	
3	14	Block 1	8	0.03	0.75	
4	9	Block 1	12	0.03	0.75	
5	15	Block 1	8	0.05	0.50	
6	16	Block 1	12	0.05	0.50	
7	2	Block 1	8	0.05	1.00	
8	8	Block 1	12	0.05	1.00	
9	17	Block 1	10	0.1	0.50	
10	12	Block 1	10	0.03	0.50	
11	3	Block 1	10	0.1	1.00	
12	6	Block 1	10	0.03	1.00	
13	7	Block 1	10	0.05	0.75	
14	1	Block 1	10	0.05	0.75	
15	5	Block 1	10	0.05	0.75	
16	10	Block 1	10	0.05	0.75	
17	4	Block 1	10	0.05	0.75	

For liquid-liquid extraction studies in pre-purification step, both EtOAc (Carlo Erba, ACS grade):H_2O and n-BuOH:H_2O mixtures were partitioned using a separation funnel (SF) (V = 250 mL) or a single current extraction system (SCES) with 4 extractors (each one, V = 160 mL). Peristaltic pump (Thermo Scientific, FH100DX) was used to obtain a continuous circulation on SCES. For resin fractionation studies, cartridge column (V = 50 cm^3) was loaded with D-101 resin adsorbent, and elution was performed with H_2O, H_2O:EtOH mixtures and EtOH. D-101 resin (Extrepure Resin, HS Code: 39013913) was preferred due to its advantages such as easy regeneration, and high performance to cost ratio. For saponin precipitation studies, acetone (Vwr, ACS grade) was used and speed vac (Thermo Scientific, SPD121P) was utilized to centrifugation of samples.

In purification steps, conventional open column chromatography (CC) with normal phase silica gel (Merck, 1.07734.9025) and RP-C_{18} silica gel (Merck, 1.09303.0500) was utilized. A vacuum pump (ISOLAB, 622.12.001) was used for RP-C_{18} silica gel columns. To separate molecules, EtOAc:MeOH:H_2O and $CHCl_3$:MeOH:H_2O mixtures in normal phase silica gel columns, and MeOH:H_2O and ACN:H_2O mixtures in RP-C_{18} silica gel columns were used as mobile phases. To obtain AST VII, ACN (Fisher Scientific, ACS grade), MeOH, EtOH, and acetone were used as precipitation solvents, whereas EtOH was utilized as a crystallization solvent.

2.1.2. Materials for Production of AST VII at Laboratory Scale

The raw material used was the same as mentioned in 2.1.1. Extraction process was carried out with MeOH (Carlo Erba, ACS grade) in a rotary evaporator of 20 L volume (Zhengzhou Greatwall, R-1020). The extract was obtained by evaporating on the same rotary evaporator (R-1020).

Resin fractionation was selected for pre-purification step. The adsorbent and elution solvents were the same as mentioned in 2.1.1. Fractionation was performed in a stainless-steel (SS) single bag filter container (Proses T.İ.M, V = 80 L).

Chromatographic separation was started with a SS column (Femak Kazan, V = 10 L) and EtOAc:MeOH:H_2O mixtures were used as mobile phase. Further purification studies were performed in glass columns with different volumes. In these steps, $CHCl_3$ (Carlo Erba, ACS grade):MeOH:H_2O and MeOH:H_2O mixtures were used as mobile phase. For solvent evaporation, the R-1020 system was used.

2.1.3. Materials for Production of AST VII at Semi-Pilot Scale

The extracted plant material was the same as mentioned in 2.1.1. Pilot-scale SS extractor (SS 316, 2000 L) having a mixer was used for MeOH (Ergen Kimya) extraction.

The extract was dried in vacuum using rotary evaporators (V=50 L, Senco, R5003KE2) within BIONORM.

For resin fractionation, the adsorbent and elution solvents were the same as mentioned in 2.1.1. Fractionation was performed in a glass column (Goel Scientific, V = 100 L). A vacuum pump (Vacubrand, MZ 2C NT) was operated during D-101 resin column experiment. The solvent was evaporated using R-1020 rotary system.

Purification steps were performed with the glass column using silica and a SS column using RP-C_{18} silica gel mentioned in 2.1.2, respectively. Solvents mentioned in 2.1.2 were employed as mobile phase throughout CCs. A vacuum pump (Vacubrand, ME 1C) was utilized during SS column.

To remove impurities, MeOH and acetone were used in the final purification step. Drying of the final product was started in a forced convection oven (JSR, JSOF-050) and proceeded with a freeze dryer mentioned in 2.1.

^{1}H and ^{13}C NMR Spectrometers (Varian MERCURY plus AS-400 (400 MHz)) were used in order to confirm the pure compound whether it is AST VII.

2.2. Methods

The methods used during the thesis studies were briefly described in this section and grouped under three main headings:

- Methods for optimization studies at laboratory scale
- Methods for production of AST VII at laboratory scale
- Methods for production of AST VII at semi-pilot scale

In all headings, the samples were spotted on a TLC plate for qualitative control. Spots were made with a glass Pasteur pipette to 1-1.5 cm above the lower end of the plate with 0.5 or 0.7 cm intervals. Development distance of the samples was about 6 cm. After developing and evaporating the residual solvent on the plate, UV-active compounds were spotted under UV_{254} and UV_{365}. To detect the spots, 20% sulfuric acid was sprayed onto the TLC plates followed by heating until the spots became visible. The visualized spots were also examined under UV_{365}. To extracts were concentrated under vacuum at 50°C using a rotary evaporator prior to freeze drying process. The extracts were dissolved in

H_2O or 65% tert-BuOH:H_2O mixture followed by freezing at -20°C. Then the frozen samples were placed onto the freeze dryer for compete drying (Figure 6).

For sample preparation of quantitative analysis, 10 mg of each lyophilized sample was dissolved in 5 mL HPLC grade MeOH to afford 2000 ± %8 ppm concentration. The vials (20 mL) were kept in the sonicator to obtain a homogeneous solution. 1 mL homogenous solutions were pipetted and transferred into the HPLC vials. If the samples had any insoluble particles, a filtration procedure was performed involving 0.45 µm polytetrafluoroethylene (PTFE) syringe filter.

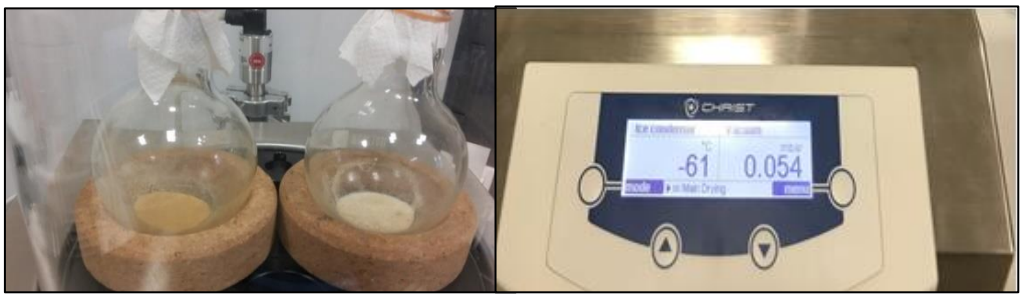

Figure 6. Photos of the lyophilization process and displaying drying conditions

For purging operation; A (UPW) and then solvent B (ACN) were passed through the system at a flow rate of 4.0 mL/min. Column conditioning was performed with 30% B. Each sample set together with AST VII and MeOH as standard and blank were placed to HPLC tray. UHPLC and HPLC analyses were carried out according to conditions given below (Tables 3 and 4).

Table 3. Analysis method for UHPLC studies

Retention Time (min)	**Flow Rate (mL/min)**	**A%**	**B%**
0.00	0.75	70	30
1.50	0.75	70	30
11.50	0.75	45	55
13.00	0.75	45	55
13.01	0.75	70	30
15.00	0.75	70	30

Analysis conditions for UHPLC studies

Column Temperature: 35°C

Detection: UV-DAD: 203, 205, 210, 254 nm and CAD

Sample Volume: 5 µL

Method Time: 15 min

Wash Time: 5 min (ACN; 0.5 mL/min)

Conditioning Time: 5 min

A Phase: UPW

B Phase: ACN

Table 4. Analysis method for HPLC studies

Retention Time (min)	Flow Rate (mL/min)	A%	B%	C%
0.00	0.75	70	30	0
1.50	0.75	70	30	0
11.50	0.75	45	55	0
13.00	0.75	45	55	0
13.01	0.75	0	0	100
16.00	0.75	0	0	100
16.01	0.75	70	30	0
18.00	0.75	70	30	0

Analysis conditions for HPLC studies

Column Temperature: 35°C

Detection: UV-DAD: 203, 205, 210, 254 nm and CAD

Sample Volume: 20 µL

Method Time: 18min

Wash Time: 5 min (ACN; 0.5 mL/min)

Conditioning Time: 5 min

A Phase: UPW

B Phase: ACN

C Phase: MeOH

2.2.1. Methods for Optimization Studies at Laboratory Scale

In this section, method development for isolation and purification steps of AST VII at laboratory scale was explained.

2.2.1.1. Optimization of Extraction

Experimental matrix was generated via statistical optimization approach using Design of Expert (DOE) program to determine the optimal conditions for the process. Since BIONORM where pilot-scale production of AST VII would take place has Soxhlet-like extraction system, the extraction method was not considered as a parameter in optimization.

2.2.1.1.1. Comparison of AST VII Content in Plant Parts

Roots and aerial parts of *A. trojanus* were dried in the shade and cut into small pieces with secateurs. One g of each sample was weighed in 50 mL falcon tubes and was extracted with 10 mL of MeOH in an ultrasonic bath at 40°C for 30 min. The extracts were dried under vacuum at 50°C by a rotary evaporator. The dry extracts were dissolved in MeOH at a concentration of 16 mg/mL and qualitatively compared on TLC plates. In addition, quantitative assessment of the extracts was performed with UHPLC equipment on freeze dried samples.

2.2.1.1.2. Design of Experiment

General factor design was selected for the screening of 4 different parameters in

which 1 categorical and 3 numerical parameters (n=4) were entered as given below;

- Factor A, solvent, with 4 levels: MeOH, EtOH, 50% EtOH:H_2O, and n-BuOH (categorical factor)
- Factor B, time, with 2 levels: 4 and 12 h
- Factor C, plant:solvent ratio with 2 levels: 0.03 and 0.1 g/ml
- Factor D, plant particle, with 2 levels: between 0.5-1 and 2-5 mm

All experiments were performed randomly and independently according to DOE's run-in triplicate and to prevent biases between replicates a blocking strategy was employed. As a response, percent yield of AST VII was used to analyze the results statistically.

Responses that obtained from experiments were entered in Result-1 column of the related row after the determination of percent yield of AST VII of each sample (calculation was shown in 2.2.1.1.3 as an example). Analysis of variance (ANOVA) with square root transformation was performed for response and the graphics containing statistical correlation of data and factors were obtained.

Excel program was used to plot graphics to interpret correlation between percent yield of AST VII versus main factors. To do that the averages of triplicates were used for each block. Prior to this process, the responses of the experiments which were determined as outliers were removed.

Box-Behnken design (BBD), a Response Surface Methodology (RSM) was selected for the optimization of 3 different numerical parameters (n=3) which were entered as follow;

- Factor A, time, with 2 levels: 8 and 12 h,
- Factor B, plant:solvent ratio, with 2 levels: 0.03 and 0.1 g/ml,
- Factor C, plant particle, with 2 levels: 0.5 and 1 mm.

Studies were carried out with 5 center points and without using blocking strategy. As a response, percent yield of AST VII was used to analyze results statistically.

Responses that obtained from the experiments were entered in Result-1 column of the related row after determining percent yield of AST VII of each sample (calculation was shown in 2.2.1.1.3 as an example). ANOVA was performed and the results and

graphics, especially a 3D surface graph, containing statistical correlation between factors compared to responses were obtained.

2.2.1.1.3. Extraction Studies

Studies were performed based on the order of DOE's run sheet as shown in Table 1 for factor screening. In all experiments solvent volume was kept constant at 125 mL and the amounts of plant material were determined according to Table 1 for each ratio.

Weighed plant materials were transferred to the cartridges. The cartridges were wetted with the solvent and placed in the Soxhlet extractors which were settled into a mantle heater (Figure 7). Extraction of the plant material was stopped at planned time point. The extracts of worked samples were used in further experiments.

Subsequently, the samples were lyophilized and then were used to prepare UHPLC samples according to the preparation method specified in 2.2 for the quantitative analysis. After analyses, the chromatograms were examined, and the percent yield of AST VII was calculated using the peak area of AST VII at UV-DAD (205 nm) or CAD according to formulae given in Figure 8. The calculated data was entered into the Result-1 column of the relevant row in Table 10.

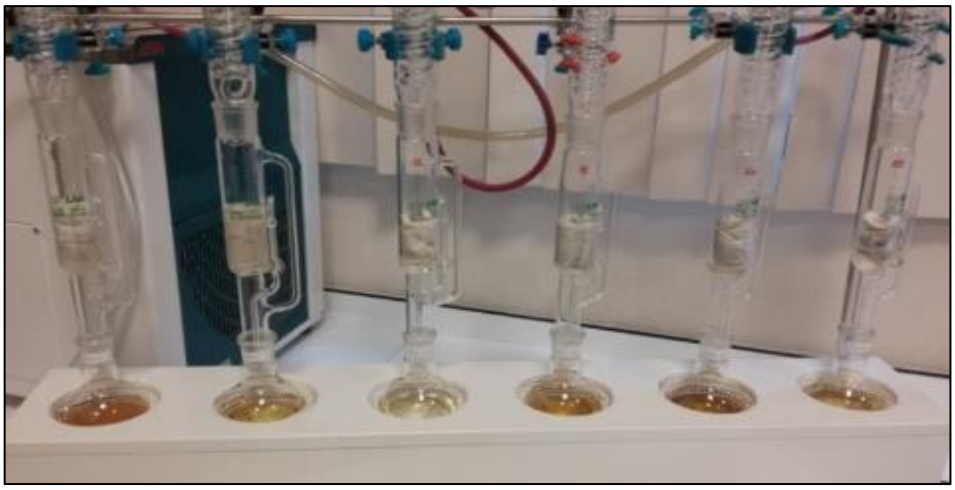

Figure 7. Photo of Soxhlet-type extraction system

Calculation of percent yield of extraction

$$\text{Percent Yield of Extraction (g extract/g plant)} = \frac{\text{Amount of Extract (g)}}{\text{Amount of Plant Material (g)}} \times 100$$

Calculation of Percent of AST VII in the extract using peak area at UV-DAD (205 nm) or CAD

$$\text{Percent of AST VII in the Extract (g AST VII/g extract)} = \frac{\text{Concentration of Standart Solution (ppm) x Purity of Standart x Peak Area of Sample at UV-DAD or CAD}}{\text{Concentration of Sample Solution (ppm) x Peak Area of Standart at UV-DAD or CAD}}$$

Calculation of percent yield of AST VII

$$\text{Percent Yield of AST VII (g AST VII/g plant)} = \text{Percent of AST VII in the Extract} \times \text{Percent Yield of Extraction} \times 100$$

Figure 8. Formulae of calculations

The calculations related to the extract of root of *A.trojanus* mentioned in Table 9 was presented below as an example;

- Calculation of percent yield of extraction

$$\text{Percent Yield of Extraction} = \frac{0.0681\text{g}}{1\text{ g}} \times 100$$

$$= 6.81\%\ \text{g/g}$$

- Calculation of percent yield of AST VII in the extract using peak area at UV-DAD(205 nm) or CAD

$$\text{Percent of AST VII in the Extract} = \frac{9.9\text{ ppm} \times 98.1 \times 0.1176}{2140\text{ ppm} \times 0.1274}$$

$$= 0.42\%\ \text{g/g}$$

- Calculation of percent yield of AST VII

Percent Yield of AST VII	=	0.0042 (g/g)	x	0.0681 (g/g)	x 100	
	=		0.031% g/g			

Extraction studies were performed based on the order of DOE's run sheet as shown in Table 2 for factor optimization. In experiments, the same methodology applied in factor screening studies was used. The calculated yield values were entered in the Result-1 column of the relevant row in Table 11.

2.2.1.2. Optimization of Pre-purification Step

The pre-purification studies aimed to enrich the target molecule in the extract before proceeding to further purification steps. The methods used during these steps were briefly described in this section and grouped under three main headings as:

- Methods for liquid-liquid extraction
- Methods for resin fractionation
- Methods for saponin precipitation

2.2.1.2.1. Liquid-Liquid Extraction

The partitions were carried out in two ways (SCES and SF) to examine processes efficiencies. The crude extract was extracted with n-BuOH and EtOAc, separately.

For the EtOAc:H_2O partition in SCES, 5 g of extract was dissolved and/or suspended in 400 mL of H_2O. Each extractor was supplied with approximately 80 mL of H_2O (heavy phase) via a peristaltic pump. Then, 500 mL of EtOAc (light phase) was fed to the system through the lower inlet. At this point; since density difference between phases acts as driving force for the travelling of the light phase through heavy phase, the light phase flows across the system till reaching the top outlet of the 4^{th} extractor and fed

to the system repeatedly with pump. Sampling of the heavy and light phase was carried out from 1st and 4th extractor, respectively by using injector at every 5 min and this process continued for 30 min. Samples were compared by using TLC.

The same process was performed with n-BuOH as the light phase instead of EtOAc, but operation time was increased to 60 min (Figure 9). Both partition processes were triplicated.

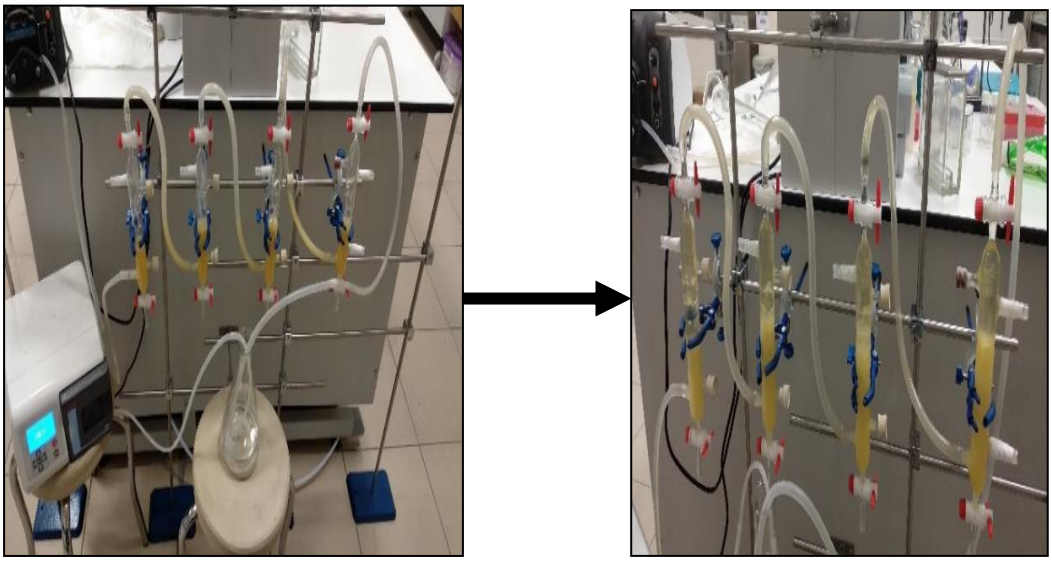

Figure 9. Photos of SCES loaded with EtOAc and H_2O

For the EtOAc:H_2O partition in SF, 1 g of extract was dissolved and/or suspended in 120 mL of H_2O. 80 mL of EtOAc was added over the H_2O. SF was gently shaken to increase extraction efficiency and valve of the SF was opened occasionally to remove the accumulated gas. The H_2O phase was taken from the lower outlet and the EtOAc phase was taken from the upper inlet, after achievement of proper phase separation. Same procedure was repeated onto the H_2O phase 2 more times with the same volume of fresh EtOAc. Each EtOAc phases from extraction processes were separately concentrated by means of a rotary evaporator. The obtained extracts were lyophilized, and phytochemical profiles were controlled with both qualitative and quantitative analysis mentioned in 2.2.

The same process was performed with n-BuOH instead of EtOAc as the light phase. Both partition processes were triplicated.

2.2.1.2.2. Resin Fractionation

Resin fractionation was carried out in 2 steps. Firstly, the mobile phase (EtOH:H_2O mixtures) which would be used in isolation was optimized and then, the fractionation was performed on crude extract with this optimized elution systems.

20 grams of wet D-101 resin (stocked in EtOH) was cleaned with 300 mL of EtOH in a beaker. Impurities and unfunctional resin particles which were suspended or floated in EtOH were removed and then, the usable resin was loaded onto a cartridge column (V=35 cm^3) (Figure 10). For the purpose of conditioning, 6 column volumes of H_2O were passed. 100 mg of extract was suspended in 2 mL of H_2O and subjected to the D-101 resin column. Elution was done as gradient, starting from H_2O to EtOH by increasing 10% of EtOH (Table 5). Fractions were collected in 250 mL Erlenmeyer flasks. Phytochemical profile was controlled qualitatively.

After determination of the elution system, 100 grams of wet D-101 resin (stocked in EtOH) was cleaned with 500 mL of EtOH in a beaker and usable resin was loaded onto a glass column (V=175 cm^3). For the purpose of conditioning, 4 column volumes of H_2O were passed. 7.5 g of extract was suspended in H_2O and subjected to the D-101 resin column. Fractions were collected in 250 mL Erlenmeyer flasks (Table 6). Phytochemical profile was controlled with both qualitative and quantitative analysis mentioned in 2.2.

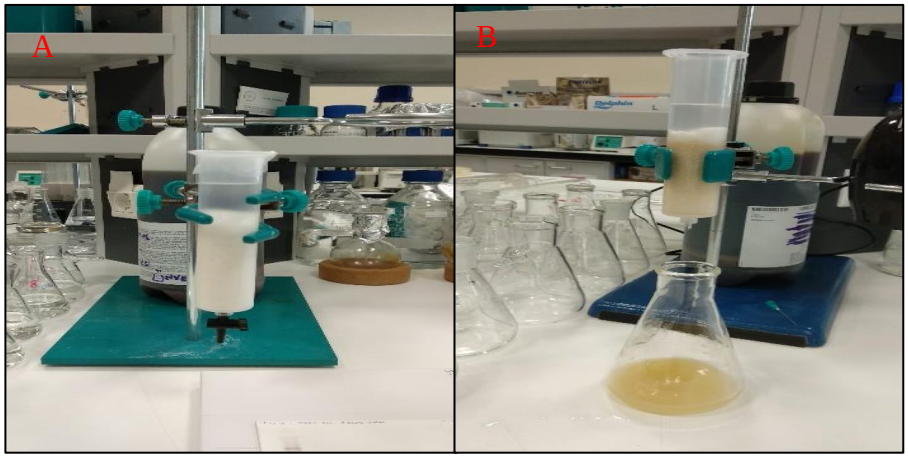

Figure 10. Photos of resin fractionation studies; A) Cartridge column loaded with resin B) Elution of crude extract with H_2O

Table 5. Development of resin column for determination of elution system

SOLVENT VOLUME (mL)	SOLVENT	FRACTION NUMBER
210	H_2O	1-2
100	10% EtOH:H_2O	3-4
100	20% EtOH:H_2O	5-6
100	30% EtOH:H_2O	7-8
100	40% EtOH:H_2O	9-10
100	50% EtOH:H_2O	11
50	60% EtOH:H_2O	12
50	70% EtOH:H_2O	13
50	80% EtOH:H_2O	14
50	90% EtOH:H_2O	15
50	EtOH	16
70	EtOH	Wash

Table 6. Development of resin column

SOLVENT VOLUME (mL)	SOLVENT	FRACTION NUMBER
700	H_2O	1-2-3-4
2400	75% EtOH:H_2O	5-6-7-8-9-10-11-12-13-14
650	EtOH	15-16-17-18

Since comparison the results of the liquid-liquid extraction, resin fractionation and saponin precipitation (given below) was indicated that resin fractionation was superior in the pre-purification step, kinetic study for resin was performed. The mass of resin was kept constant at 500 mg and mass of the extract was varied depending on the ratio of extract and resin from 1:5 to 1:50 (Table 7). The extracts dissolved in 2 mL of H_2O was immersed in an ultrasonic bath at 60ºC for 40 min to ensure a homogeneous solution. Subsequently, extracts were transferred into vials containing resin, and were centrifuged (1500 rpm, 3 h, 35℃) in a vacuum-free speed vac. After centrifugation, the supernatant parts (~1.7 mL in each sample) were taken by syringes and transferred into Eppendorf tubes. Pellets were dispersed into EtOH and immersed in an ultrasonic bath at 40ºC for

30 min to detect adsorbed molecules by resin. The comparisons of chemical contents of the phases was done with TLC.

Table 7. Amounts of extract and resin in first kinetic study

The ratio of Extract:Resin	Amount of Extract (mg)	Amount of Resin (mg)
1:5	99.9	501.0
1:10	50.2	501.0
1:15	33.6	500.6
1:20	25.3	500.0
1:25	19.9	502.9
1:30	16.8	502.3
1:35	14.6	500.5
1:40	12.7	500.2
1:45	11.3	498.9
1:50	10.1	502.6

According to results from first kinetic study, the second kinetic study for resin was done with different ratio (from 1:1 to 1:10 ratio). The mass of extract was kept constant at 500 mg and the mass of the wet resin varied depending on the ratio (Table 8). The extract dissolved in 10 mL of H_2O was immersed in an ultrasonic bath at 60ºC for 40 min to ensure a homogeneous solution. The same procedure of first kinetic study was used for following process.

Table 8. Amounts of extract and resin in second kinetic study

The ratio of Extract:Resin	Amount of Extract (mg)	Amount of Resin (mg)
1:1	507.8	507.1
1:2	501.8	1019.9
1:3	502.3	1512.7
1:4	505.0	2005.8
1:5	500.0	2503.8
1:6	507.1	3012.3

(cont. on next page)

Table 8. (cont.)

The ratio of Extract:Resin	Amount of Extract (mg)	Amount of Resin (mg)
1:7	500.2	3510.4
1:8	504.2	4033.1
1:9	506.6	4504.6
1:10	503.8	5038.4

2.2.1.2.3. Saponin Precipitation

200 mg of MeOH extract and saponin rich fraction [Fraction (Fr): 4-13] taken from D-101 resin were tested to precipitate. Both samples were dissolved in ~5 mL of H_2O with the help of heat and 9 mL of acetone were slowly added onto them. At the point where precipitation began, the solution was stored at -20ºC for 12 hours. To separate precipitated saponins from liquid, centrifugation was performed (9000 rpm, 20 min, +4°C). Phytochemical profiles of both supernatants and pellets were compared with both qualitative and quantitative analysis mentioned in 2.2.

2.2.1.3. Optimization of Purification

The optimization of the column adsorbent type (silica or RP-C_{18}-Silica) and the mobile phase system to be used in the further purification studies made according to the TLC profiles of saponin rich fraction [Fr: 23-61] obtained from D-101 resin fractionation. During chromatographic studies, the following mobile phase systems were used:

- <u>For the Silica Surface</u>

  - EtOAc:MeOH:H_2O 100:15:10
    100:17.5:13.5
    100:20:15
    100:25:20

- $CHCl_3$:MeOH:H_2O 80:20:2
  70:30:3
  61:32:7
  60:40:10

- For the RP-C_{18} Silica Surface

  - ACN: H_2O 40:60
    60:40
  - MeOH:H_2O 60:40
    80:20

2.2.1.4. Optimization of Final Purification

To optimize the final purification step, precipitation and crystallization were performed. In precipitation studies, 100 mg of [Fr: 32-107] [Fr: 71-110] [Fr: 37-54] [Fr: 23-61] -the fraction combination of each purification step can be followed from Figure 11- were weighed for each solvent (EtOH, ACN, acetone, and MeOH) and solvents were added until full solubility was achieved. In the meantime, samples were heated and expose to ultrasonic vibration. Then, samples were kept at +4 ºC till precipitation of AST VII was observed. In crystallization studies, one g of [Fr: 51-70] [Fr: 37-54] [Fr: 23-61] was weighed and ~40 mL of EtOH was added until obtaining a saturated solution. The sample was kept at +4 ºC for overnight. Phytochemical profiles of samples were controlled qualitatively.

2.2.2. Methods for Production of AST VII at Laboratory Scale

Isolation of AST VII was shown in Figure 11. The methods used during the production of AST VII were explained below in the subheadings of this section.

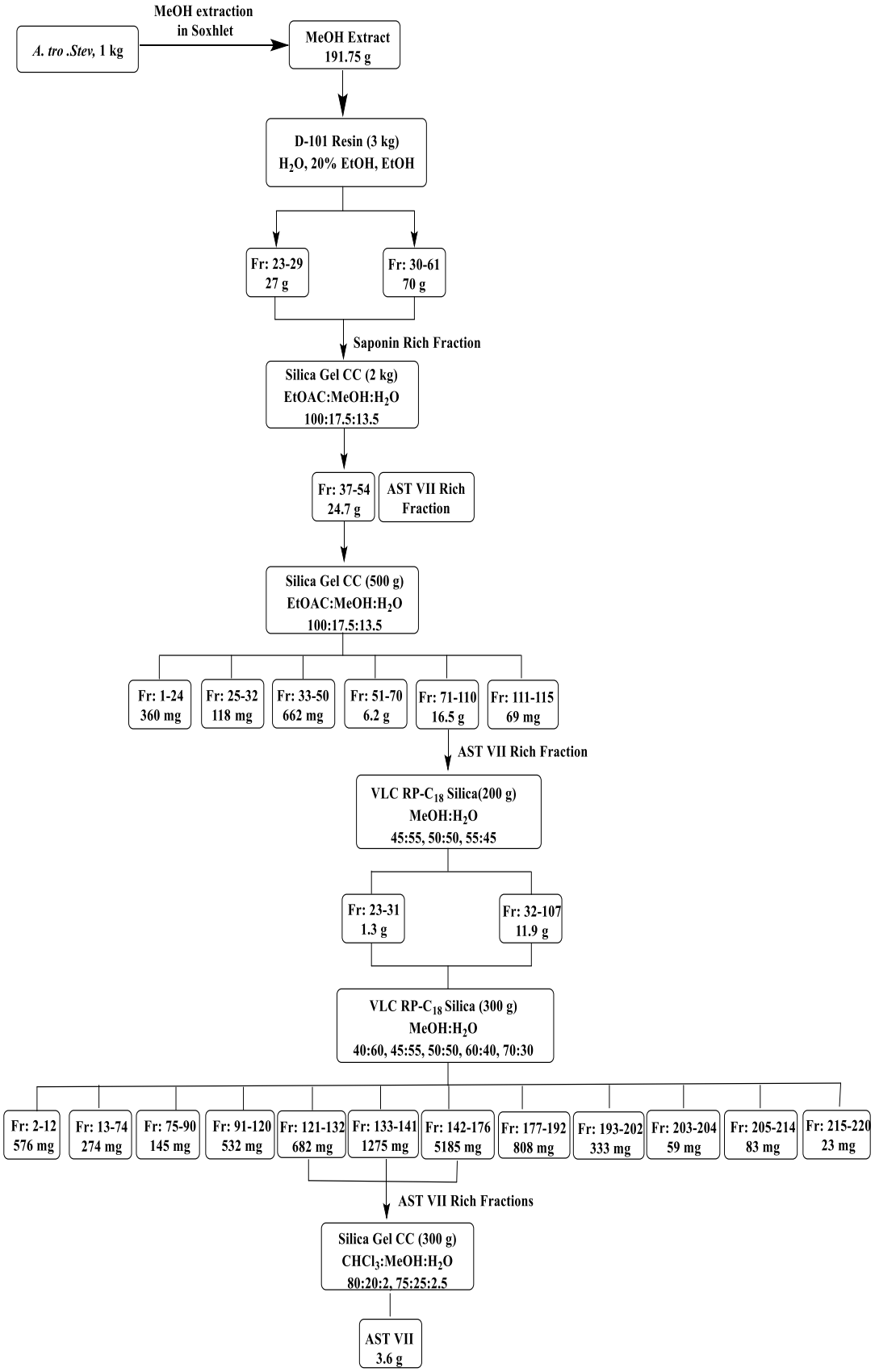

Figure 11. Isolation of AST VII from *A.trojanus* at laboratory scale

2.2.2.1. Extraction Step

500 g of the plant which had optimized particle size was extracted with 10 L of MeOH in a rotary evaporator. In this process, it was aimed to mimic the Soxhlet type extraction system. For this purpose, the plant was loaded on a cheesecloth in the receiving flask of the rotary and the solvent was put in the evaporating flask. Rotation and temperature set to 60 rpm and 45℃ (Figure 12).

Figure 12. Soxhlet-like extraction system using a rotary evaporator

During extraction, evaporated MeOH was condensed on the plant material till accumulation of the solvent reached to predetermined level. The collected extract was then fed to the evaporating flask, so extract was concentrated and thus extraction was continued as in Soxhlet. This process was repeated for 7 times to finish the extraction of each batch. In this step, 2 batches were done.

2.2.2.2. Pre-purification Step

3 kg of wet resin was loaded into a bag filter placed in container mentioned in 2.1.2 (V = 20.4 L) and column was conditioned by 80 L of H_2O. 500 g of wet resin was added to 191.75 g of MeOH extract suspended in H_2O and mixed by rotation until the extract was adsorbed by the resin. It was kept in a forced convection oven at 70℃ to remove the solvent. Then dried resin which adsorbed the extract was loaded to column. Elution was performed using H_2O (until removing of whole sugars), 6 L of 20% EtOH:H_2O mixture (for UV-active molecules), and 30 L of EtOH. Fractions were collected in 1 L Erlenmeyer flasks (Figure 13). Phytochemical profiles of the fractions were tracked with TLC. After fractionation, the saponin rich fractions were combined and extracts were concentrated by removal of the solvents.

Figure 13. Photos of resin column; A) Single bag filter container as a column, B) Top view of column, C) Fraction collection, D) Saponin rich fractions

2.2.2.3. Purification Step

Isolation studies on the saponin rich fraction were started with open CC using SS column (V = 4 L). 1.6 kg of silica gel in column was conditioned with 13.1 L of EtOAc:MeOH:H_2O (100:17.5:13.5). Fully adsorption was achieved via addition 400 g of silica gel to 107 g of saponin rich fraction which was dissolved in MeOH and mixed by rotation. It was kept in a forced convection oven at 50°C to remove MeOH. The dried silica gel which adsorbed the extract was loaded to the column. Mobile phase was developed using 52.4 L of EtOAc:MeOH:H_2O (100:17.5:13.5) as isocratic to give subfractions. Phytochemical profiles of the fractions were tracked with TLC. The column was washed by 28 L of MeOH when TLC results were indicated that AST VII spots disappeared. All fractions were collected in 1 L Erlenmeyer flasks (Figure 14).

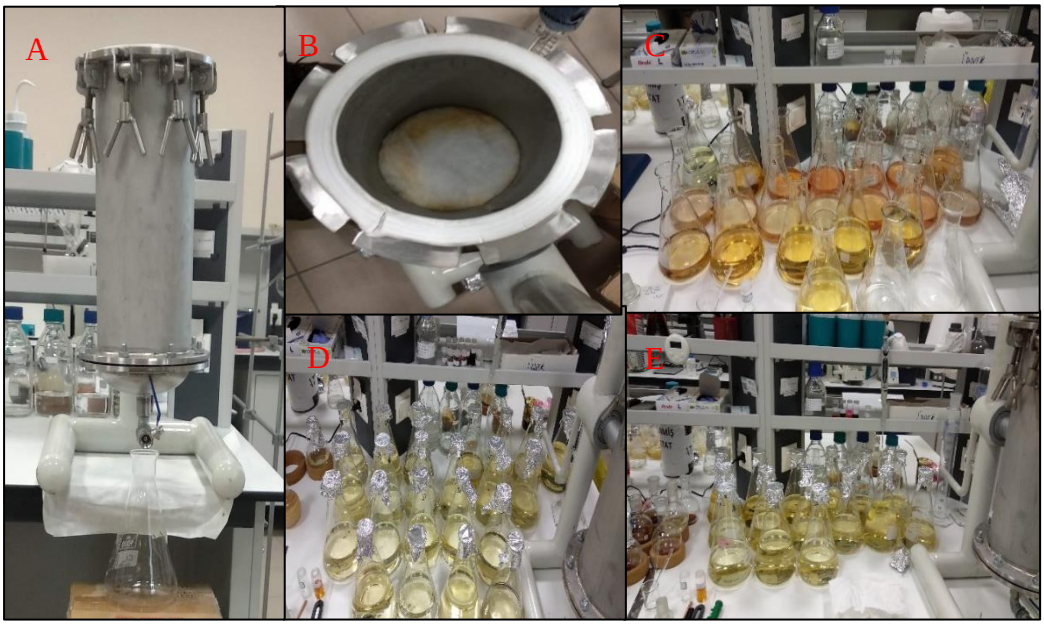

Figure 14. Photos of silica column; A) SS column, B) Top view of column, C) [Fr: 1-19], D) [Fr: 25-46], E) [Fr: 39-54]

To decide which adsorbent would be preferred in the further step, 50 mg of [Fr: 37-54] was subjected to vacuum liquid chromatography (VLC) using RP-C_{18} silica gel

(V = 30 cm^3) developing with MeOH:H_2O (40:60; 300 mL, 45:55; 100 mL, 50:50; 100 mL, 60:40; 300 mL) and MeOH (120 mL) to give subfractions. Also, 50 mg of same fraction was submitted to an open column using silica gel (V = 60 cm^3) employing EtOAc:MeOH:H_2O (100:17.5:13.5, 500 mL) and MeOH (200 mL) to give subfractions. Sample to adsorbent ratio was 1:400 for both RP-C_{18} silica gel and silica gels columns. According to comparison results of these columns 'phytochemical profiles it had been decided to continue with silica gel CC.

350 g of silica gel that was conditioned with EtOAc:MeOH:H_2O (100:17.5:13.5) was loaded into a glass column (V = 1 L) (Figure 15). 24.7 g of AST VII rich fraction was dissolved in MeOH:H_2O mixture and 150 g of silica gel was added and mixed by rotation till completing of adsorption. It was kept in a forced convection oven at 50°C to remove the solvent. The dried silica gel which adsorbed the AST VII rich fraction was loaded to the column. Mobile phase was developed using 32.75 L of EtOAc:MeOH:H_2O (100:17.5:13.5). as isocratic to give subfractions. Phytochemical profiles of the fractions were tracked with TLC. The column was washed by 2 L of MeOH when TLC results were indicated that AST VII spots disappeared. All fractions were collected in 250 and 500 mL Erlenmeyer flasks.

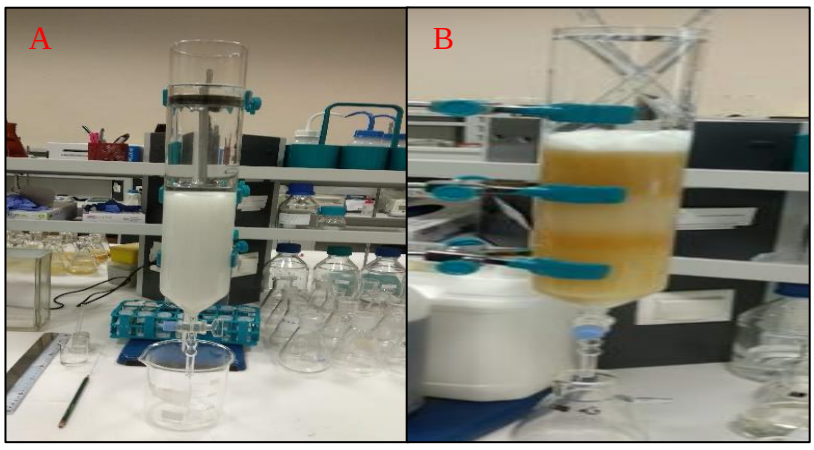

Figure 15. Photos of RP-C_{18} column; A) Column loaded with silica gel, B) Developed column

The chemical profiling performed on an HPTLC plate coated with silica gel showed that the purity of the fraction was not at the desired levels. Therefore, chemical

profile of fraction was controlled with RP-C_{18} silica plate developed with both MeOH:H_2O (75:25) and ACN:H_2O (40:60) to determine further purification steps. Hence, further purification was continued with VLC using RP-C_{18} silica.

300 g of RP-C_{18} silica gel dissolved with MeOH was seated in a glass column (V = 600 cm^3) and was conditioned with MeOH:H_2O (40:60). Then, 13.2 g of AST VII rich fraction dissolved in MeOH:H_2O (40:60) was subjected to the column (Figure 16). Mobile phases were developed using MeOH:H_2O (40:60;8.5 L, 45:55; 13 L, 50:50; 2 L, 60:40; 15.9 L, 70:30; 5 L) as gradient to give subfractions which were collected in 500 mL Erlenmeyer flasks. Phytochemical profiles of the fractions were tracked with TLC. The column was washed by 2 L of MeOH when TLC results were indicated that AST VII spots disappeared.

Figure 16. Photo of column subjected with AST VII rich fraction

For final purification, 300 g of silica gel was loaded into a glass column (V=650 mL) and conditioned with 2 L of $CHCl_3$:MeOH:H_2O (80:20:2). 7.1 g of AST VII rich fraction dissolved with mobile phase system was subjected to the column as liquid spotting. The column was developed using $CHCl_3$:MeOH:H_2O (80:20:2, 75:25:2.5) as gradient. The column was washed with MeOH. All fractions were collected in 10 cm glass tubes. Supposedly, pure AST VII fractions were combined according to TLC results and then these fractions were dried in freeze dryer (Figure 17).

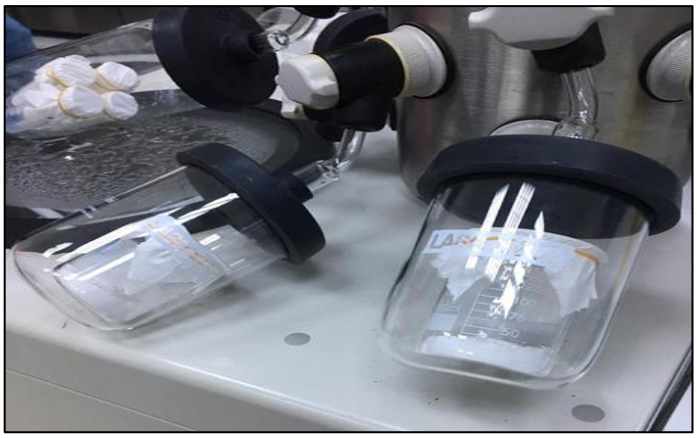

Figure 17. Photo of lyophilization for pure AST VII fractions

2.2.3. Methods for Production of AST VII at Semi-Pilot Scale

In concept of scale-up, the isolation of AST-VII from 100 kg of plant was aimed. The flowchart of isolation for 100 kg plant was shown in Figure 18. In this scale, the purification steps used in laboratory scale were partially modified. Particularly, instead of EtOAc:MeOH:H_2O systems which were found to be insufficient in isolations with silica gel CC, $CHCl_3$:MeOH:H_2O systems were preferred. On the other hand, precipitation procedure was successfully incorporated for final product obtaining step. The methods used during the production of AST VII were explained below.

2.2.3.1. Extraction Step

100 kg of *A. trojanus.* was extracted with 700 L of MeOH in a steel extractor having mixer within BIONORM with 2.5h extraction time. This step was repeated one more time to the pulp obtained from first extraction. End of process, the extract was separated by filtration. MeOH in the extract was evaporated under vacuum at 60°C by rotary evaporators (Figure 19). Percent content of AST VII was determined by quantitative analysis.

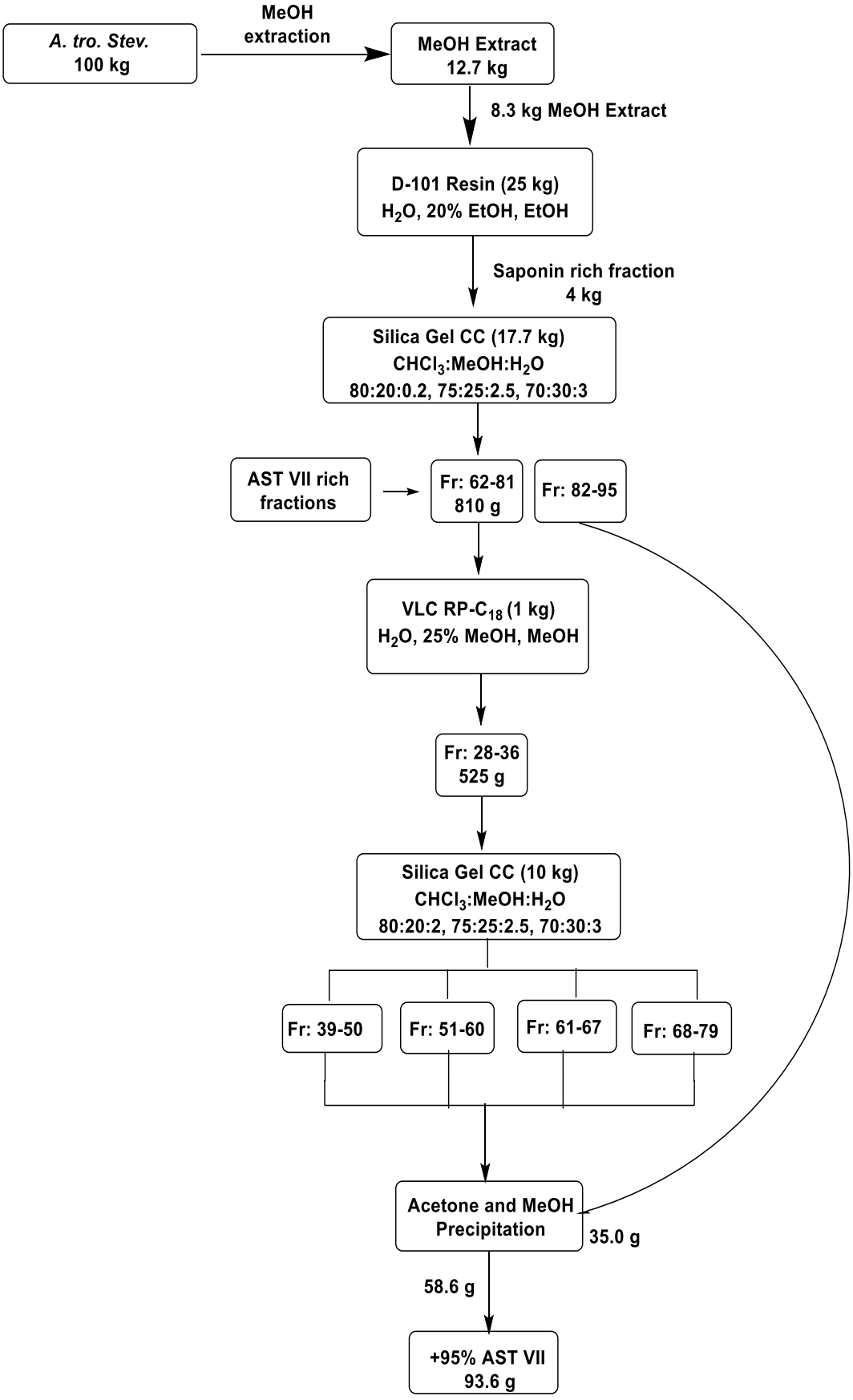

Figure 18. Isolation of AST VII at semi-pilot scale

Figure 19. Photos of extraction; A) Top view of extractor, B) Evaporation, C) The crude extract

2.2.3.2. Pre-purification Step

25 kg of wet D-101 resin was loaded in a glass column (V = 42 L) mentioned in 2.1.3 and to remove impurities that may coming from previous studies performed with same resin, it was washed with 45 L of EtOH. Then the resin was conditioned with 90 L of H_2O. 8.3 kg of crude extract was applied to the column. This process was performed in 2 steps. In the first step, 4.1 kg of the extract was suspended with 10 L of H_2O. 5 kg of wet resin was added to the extract and mixed by rotation until the extract was adsorbed by the resin. The extract adsorbed onto the resin was subjected to the column as dry spotting. Under vacuum, fractions were obtained employing 120 L of H_2O (until removing of whole sugars), 100 L of 20% EtOH:H_2O (for UV-active molecules), and 230 L of EtOH (Figure 20). The phytochemical profiles of fractions were checked via qualitative analysis. After fractionation, the saponin rich fractions were combined and the solvent was evaporated under vacuum at 50°C by a rotary. In the second step, process was carried out with the same manner with the first step except that applying 4.2 kg of the extract and using 143 L of H_2O, 100 L of 20% EtOH:H_2O and 170 L of EtOH elution.

Figure 20. Photos of resin column; A) H_2O elution, B) 20% EtOH:H_2O elution, C) EtOH elution

2.2.3.3. Purification Step

Isolation studies on the saponin rich fraction were started with open CC using 17.7 kg of silica gel that was conditioned with 50 L of $CHCl_3$:MeOH:H_2O (80:20:0.2). Silica gel was loaded into a glass column (V = 70 L). 4 kg of saponin rich fraction was adsorbed onto 4.2 kg of silica gel by mixing and subjected to the column as dry spotting. The column was developed employing $CHCl_3$:MeOH:H_2O (80:20:0.2; 160 L, 75:25:2.5; 108 L, 70:30:3, 174 L).to give subfractions (Figure 21). Phytochemical profiles of the fractions were tracked with TLC. The column was washed by 2.5 L of MeOH and 5 L of acetone when TLC results were indicated that AST VII bands disappeared. AST VII rich fractions according to TLC profiles were combined and solvents evaporated under vacuum at 60°C.

Isolation studies on AST VII rich fraction were continued with VLC using 1 kg of RP-C_{18} silica. The adsorbent dissolved with 3 L of MeOH was seated with 15 L of MeOH by using vacuum into a steel column. Column conditioning was performed with

25 L of H_2O. 810 g of AST VII rich fraction was adsorbed onto 2 kg of resin and was subjected onto column as dry spotting (Figure 22). The isolation was achieved by development of column using 30 L of H_2O, 13 L of 25% MeOH:H_2O, and 9 L of MeOH to give subfractions.

Figure 21. Photos of silica column

Isolation studies on AST VII rich fraction were finished with an open CC system using 10 kg of silica loaded into a glass column (V = 28 L). Adsorbent was conditioned with 90 L of $CHCl_3$:MeOH:H_2O (80:20:2). 525 g of AST VII rich fraction was subjected onto column as liquid spotting. The column was developed employing $CHCl_3$:MeOH:H_2O (80:20:2; 32 L, 75:25:2.5; 22 L, 70:30:3; 120 L) to give subfractions. Phytochemical profiles of the fractions were tracked with TLC. The column was washed by 20 L of MeOH when TLC results were indicated that AST VII spots disappeared.

In the final purification step, precipitation of AST VII has gradually performed with MeOH and acetone. Then pellet having AST VII and supernatant parts were separated by centrifugation (10 dk, 4000 rpm, 4°C) (Figure 23).

Figure 22. Photos of RP-C_{18} column

Figure 23. Photos of precipitation studies

CHAPTER 3

RESULTS AND DISCUSSIONS

The results were explained in this section and grouped under three main headings like in Chapter 2.

3.1. Results of Optimization Studies at Laboratory Scale

The results of studies were given and discussed under the subheadings. Optimum conditions of each step were determined considering scale-up concept and feasibility.

3.1.1. Optimization of Extraction

In the extraction studies, solvent, time, plant to solvent ratio, and plant particle size were selected parameters to be optimized.

3.1.1.1. Comparison of AST VII Content in Plant Parts

The powdered root (68.1 mg) and aerial parts (82.8 mg) were extracted using MeOH. TLC profiles were given in Figure 24 demonstrating phytochemical composition of the root and aerial part extracts.

Since phytochemical profiles of the extracts were similar to each other, a quantitative analysis was performed with UHPLC. The amount of AST VII was

calculated as 0.031 g/g in the root, whereas it was 0.036 g/g in the aerial part (Chromatogram 2) (Table 9).

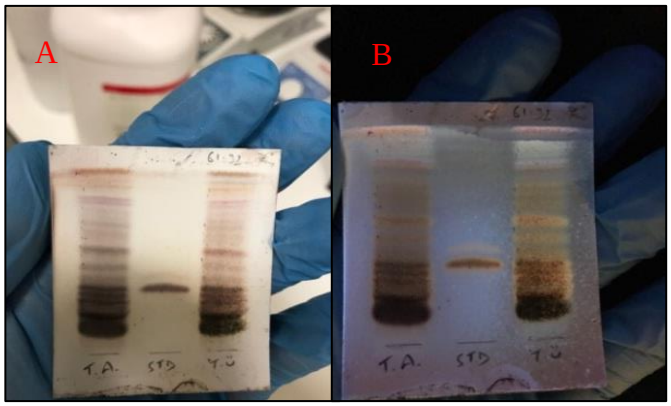

Figure 24. TLC profiles of the MeOH extracts of *A. trojanus* (TA. root part, TU. aerial part, STD. Standard) (A. day light B. under UV_{365}) (Normal Phase Silica Gel Plate, Mobile Phase; 61:32:7; $CHCl_3$:MeOH:H_2O) (Samples and standard (STD) were spotted 4 and 2 times, respectively)

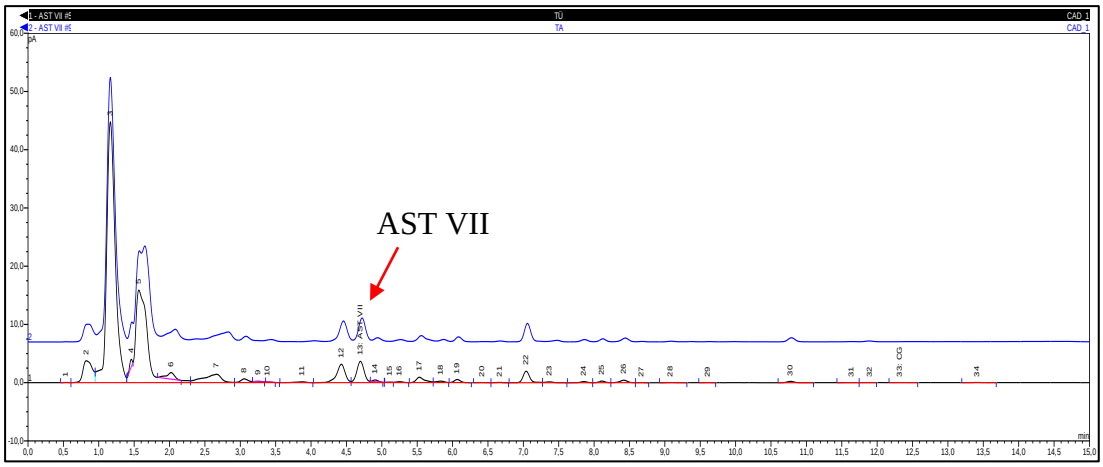

Chromatogram 2. UHPLC-CAD chromatogram of the MeOH extract of both plant parts (root. in blue; aerial. in black)

As the aerial part also contained a high amount of AST VII, the use of whole plant was considered thoroughly. The presence of chlorophyll in the aerial parts that might

cause purification problems in further steps, and about 5-fold mass difference between root and aerial parts for a whole plant were taken into consideration, and it was decided to continue with only root materials.

Table 9. AST VII content in the roots and aerial parts determined by UHPLC-DAD

ID	Absorbance at 205 nm	Concentration (ppm)	Amount of the Extract (mg)	Percent Yield of Extraction (g/g)	Percent of AST VII in the extract	Percent Yield of AST VII (g/g)
STD	0.1274	9.9				
Root Part	0.1176	2140	68.1	6.81	0.42	0.031
Aerial Part	0.1162	2040	82.8	8.28	0.43	0.036

3.1.1.2. Extraction Studies

The quantitative results of the extracts obtained from factor screening experiments were given in Response-1 column (Table 10). ANOVA was performed on data set, and parameters used in RSM studies were chosen according to these results.

The quantitative results of the extracts obtained from factor optimization experiments were given in Response-1 column of Table 11. Optimized conditions for each parameter was determined based on ANOVA results.

Table 10. Percent yield of AST VII data for factor screening

STD Number	Run Number	Block	Factor 1-Solvent	Factor 2-Time (h)	Factor 3-Plant:Solvent Ratio (g/mL)	Factor 4–Plant Particle Size (mm)	Response 1–Percent Yield of AST VII (g/g)
1	61	Block 1	MeOH	4	0.1	2-5	0.141
2	65	Block 2	MeOH	4	0.1	2-5	0.164

(cont. on next page)

Table 10. (cont.)

STD Number	Run Number	Block	Factor 1- Solvent	Factor 2- Time (h)	Factor 3- Plant:Solvent Ratio (g/mL)	Factor 4– Plant Particle Size (mm)	Response 1– Percent Yield of AST VII (g/g)
3	27	Block 3	MeOH	4	0.1	2-5	0.200
4	80	Block 1	EtOH	4	0.1	2-5	0.051
5	66	Block 2	EtOH	4	0.1	2-5	0.179
6	24	Block 3	EtOH	4	0.1	2-5	0.192
7	14	Block 1	50% EtOH:H_2O	4	0.1	2-5	0.151
8	70	Block 2	50% EtOH:H_2O	4	0.1	2-5	0.224
9	41	Block 3	50% EtOH:H_2O	4	0.1	2-5	0.218
10	96	Block 1	n-BuOH	4	0.1	2-5	0.035
11	8	Block 2	n-BuOH	4	0.1	2-5	0.081
12	58	Block 3	n-BuOH	4	0.1	2-5	0.075
13	75	Block 1	MeOH	12	0.1	2-5	0.163
14	71	Block 2	MeOH	12	0.1	2-5	0.183
15	32	Block 3	MeOH	12	0.1	2-5	0.213
16	10	Block 1	EtOH	12	0.1	2-5	0.070
17	29	Block 2	EtOH	12	0.1	2-5	0.192
18	6	Block 3	EtOH	12	0.1	2-5	0.076
19	16	Block 1	50% EtOH:H_2O	12	0.1	2-5	0.184
20	53	Block 2	50% EtOH:H_2O	12	0.1	2-5	0.238
21	94	Block 3	50% EtOH:H_2O	12	0.1	2-5	0.311
22	20	Block 1	n-BuOH	12	0.1	2-5	0.297
23	88	Block 2	n-BuOH	12	0.1	2-5	0.162
24	50	Block 3	n-BuOH	12	0.1	2-5	0.160
25	9	Block 1	MeOH	4	0.03	2-5	0.121
26	79	Block 2	MeOH	4	0.03	2-5	0.143
27	74	Block 3	MeOH	4	0.03	2-5	0.111
28	46	Block 1	EtOH	4	0.03	2-5	0.061
29	93	Block 2	EtOH	4	0.03	2-5	0.117
30	23	Block 3	EtOH	4	0.03	2-5	0.139
31	42	Block 1	50% EtOH:H_2O	4	0.03	2-5	0.132
32	82	Block 2	50% EtOH:H_2O	4	0.03	2-5	0.179
33	44	Block 3	50% EtOH:H_2O	4	0.03	2-5	0.212

(cont. on next page)

Table 10. (cont.)

STD Number	Run Number	Block	Factor 1- Solvent	Factor 2- Time (h)	Factor 3- Plant:Solvent Ratio (g/mL)	Factor 4– Plant Particle Size (mm)	Response 1– Percent Yield of AST VII (g/g)
34	76	Block 1	n-BuOH	4	0.03	2-5	0.035
35	95	Block 2	n-BuOH	4	0.03	2-5	0.019
36	35	Block 3	n-BuOH	4	0.03	2-5	0.070
37	11	Block 1	MeOH	12	0.03	2-5	0.144
38	40	Block 2	MeOH	12	0.03	2-5	0.187
39	51	Block 3	MeOH	12	0.03	2-5	0.191
40	33	Block 1	EtOH	12	0.03	2-5	0.063
41	54	Block 2	EtOH	12	0.03	2-5	0.172
42	31	Block 3	EtOH	12	0.03	2-5	0.074
43	49	Block 1	50% EtOH:H_2O	12	0.03	2-5	0.188
44	22	Block 2	50% EtOH:H_2O	12	0.03	2-5	0.230
45	90	Block 3	50% EtOH:H_2O	12	0.03	2-5	0.268
46	91	Block 1	n-BuOH	12	0.03	2-5	0.026
47	3	Block 2	n-BuOH	12	0.03	2-5	0.038
48	48	Block 3	n-BuOH	12	0.03	2-5	0.116
49	59	Block 1	MeOH	4	0.1	0.5-1	0.193
50	63	Block 2	MeOH	4	0.1	0.5-1	0.290
51	60	Block 3	MeOH	4	0.1	0.5-1	0.264
52	5	Block 1	EtOH	4	0.1	0.5-1	0.064
53	77	Block 2	EtOH	4	0.1	0.5-1	0.067
54	87	Block 3	EtOH	4	0.1	0.5-1	0.125
55	89	Block 1	50% EtOH:H_2O	4	0.1	0.5-1	0.145
56	43	Block 2	50% EtOH:H_2O	4	0.1	0.5-1	0.376
57	47	Block 3	50% EtOH:H_2O	4	0.1	0.5-1	0.141
58	15	Block 1	n-BuOH	4	0.1	0.5-1	0.021
59	78	Block 2	n-BuOH	4	0.1	0.5-1	0.048
60	34	Block 3	n-BuOH	4	0.1	0.5-1	0.079
61	57	Block 1	MeOH	12	0.1	0.5-1	0.240
62	81	Block 2	MeOH	12	0.1	0.5-1	0.327
63	2	Block 3	MeOH	12	0.1	0.5-1	0.258
64	18	Block 1	EtOH	12	0.1	0.5-1	0.100

(cont. on next page)

Table 10. (cont.)

STD Number	Run Number	Block	Factor 1- Solvent	Factor 2- Time (h)	Factor 3- Plant:Solvent Ratio (g/mL)	Factor 4– Plant Particle Size (mm)	Response 1– Percent Yield of AST VII (g/g)
65	68	Block 2	EtOH	12	0.1	0.5-1	0.197
66	7	Block 3	EtOH	12	0.1	0.5-1	0.078
67	56	Block 1	50% EtOH:H_2O	12	0.1	0.5-1	0.258
68	67	Block 2	50% EtOH:H_2O	12	0.1	0.5-1	0.231
69	45	Block 3	50% EtOH:H_2O	12	0.1	0.5-1	0.128
70	52	Block 1	n-BuOH	12	0.1	0.5-1	0.040
71	36	Block 2	n-BuOH	12	0.1	0.5-1	0.047
72	55	Block 3	n-BuOH	12	0.1	0.5-1	0.109
73	62	Block 1	MeOH	4	0.03	0.5-1	0.135
74	19	Block 2	MeOH	4	0.03	0.5-1	0.348
75	13	Block 3	MeOH	4	0.03	0.5-1	0.206
76	21	Block 1	EtOH	4	0.03	0.5-1	0.075
77	85	Block 2	EtOH	4	0.03	0.5-1	0.288
78	73	Block 3	EtOH	4	0.03	0.5-1	0.180
79	17	Block 1	50% EtOH:H_2O	4	0.03	0.5-1	0.173
80	37	Block 2	50% EtOH:H_2O	4	0.03	0.5-1	0.299
81	4	Block 3	50% EtOH:H_2O	4	0.03	0.5-1	0.238
82	92	Block 1	n-BuOH	4	0.03	0.5-1	0.038
83	83	Block 2	n-BuOH	4	0.03	0.5-1	0.371
84	1	Block 3	n-BuOH	4	0.03	0.5-1	0.060
85	72	Block 1	MeOH	12	0.03	0.5-1	0.227
86	38	Block 2	MeOH	12	0.03	0.5-1	0.269
87	64	Block 3	MeOH	12	0.03	0.5-1	0.346
88	28	Block 1	EtOH	12	0.03	0.5-1	0.092
89	84	Block 2	EtOH	12	0.03	0.5-1	0.206
90	12	Block 3	EtOH	12	0.03	0.5-1	0.379
91	39	Block 1	50% EtOH:H_2O	12	0.03	0.5-1	0.055
92	86	Block 2	50% EtOH:H_2O	12	0.03	0.5-1	0.316
93	69	Block 3	50% EtOH:H_2O	12	0.03	0.5-1	0.449
94	25	Block 1	n-BuOH	12	0.03	0.5-1	0.065
95	30	Block 2	n-BuOH	12	0.03	0.5-1	0.068
96	26	Block 3	n-BuOH	12	0.03	0.5-1	0.083

Table 11. Percent yield of AST VII data for factor optimization

STD Number	Run Number	Block	Factor 1– Time (h)	Factor 2- Plant:Solvent Ratio (g/mL)	Factor 3-Plant Particle Size (mm)	Response 1– Percent yield of AST VII (g/g)
1	11	Block 1	8	0.1	0.75	0.259
2	13	Block 1	12	0.1	0.75	0.253
3	14	Block 1	8	0.03	0.75	0.236
4	9	Block 1	12	0.03	0.75	0.234
5	15	Block 1	8	0.05	0.50	0.354
6	16	Block 1	12	0.05	0.50	0.360
7	2	Block 1	8	0.05	1.00	0.366
8	8	Block 1	12	0.05	1.00	0.352
9	17	Block 1	10	0.1	0.50	0.278
10	12	Block 1	10	0.03	0.50	0.293
11	3	Block 1	10	0.1	1.00	0.276
12	6	Block 1	10	0.03	1.00	0.304
13	7	Block 1	10	0.05	0.75	0.357
14	1	Block 1	10	0.05	0.75	0.362
15	5	Block 1	10	0.05	0.75	0.370
16	10	Block 1	10	0.05	0.75	0.355
17	4	Block 1	10	0.05	0.75	0.364

3.1.1.3. Design of Experiment

The ANOVA table for factor screening was shown in Figure 25. According to the table; solvent, time and plant particle size, as main factors, showed significant effects on the percent yield of AST VII while the plant:solvent ratio had no significant effect (significance level, $\alpha = 0.05$) but the interactions of factor C (plant:solvent ratio) with other factors had significant effects on the yield. Therefore, plant to solvent ratio was selected as a main factor for optimization studies. The R^2 value representing the fitted regression line was acceptable (R^2=0.8454). However, predicted (Pred.) and adjusted (Adj.) R^2 values were needed to be increased if model was intended to be used as a strong predictive tool for AST VII isolation procedure (Adj. R^2=0.7681; Pred. R^2=0.6294). Plots

including residuals of experiments showed that the experiments were performed randomly (Figure 26c), the deviation of the standardized residuals from the predicted values were ranged in the interval(-3,3) (Figure 26b), and Figure 26a and 26b showed no unusual pattern or discrepant values. There was one standardized residual slightly outside the interval (–3, 3).

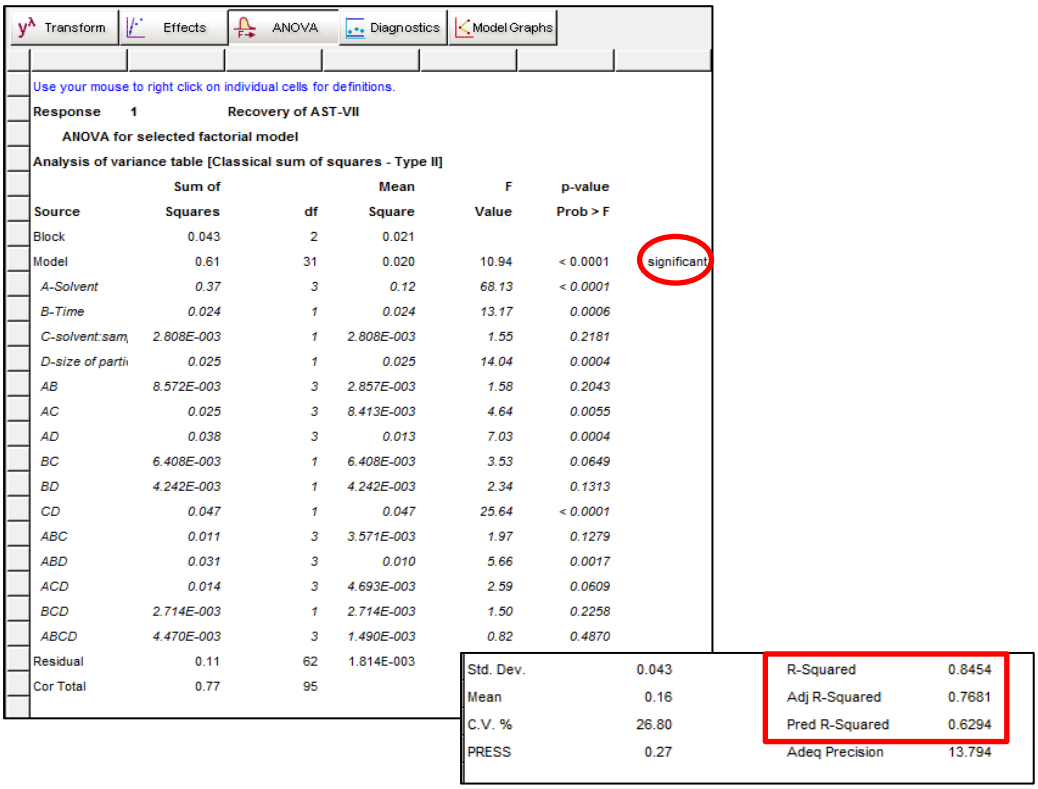

Figure 25. ANOVA table and R^2-values for factor screening studies

Figure 27 showed the graphs including results of factor screening. According to Figure 27, solvent, time and plant particle size had a significant effect on the yield as seen in the ANOVA table for factor screening (Figure 25). Although the yield increases with longer extraction time, it was rational to keep it between 8 and 12 h in the optimization studies considering pilot production shifts. Also, the smaller plant particle size resulted in higher yield due to increased plant surface area. Finally, comparisons amongst the solvents indicated that the MeOH and 50% EtOH:H_2O extracts contained higher AST VII content than the other solvents. Different solvent extracts were analyzed quantitively to

determine whether the solvent may affect the contents of crude extracts. For this purpose; chromatograms of MeOH (SN 15), EtOH (SN 18), 50% EtOH:H_2O (SN 21) and n-BuOH extracts (SN 24) were evaluated in Chromatogram 3.

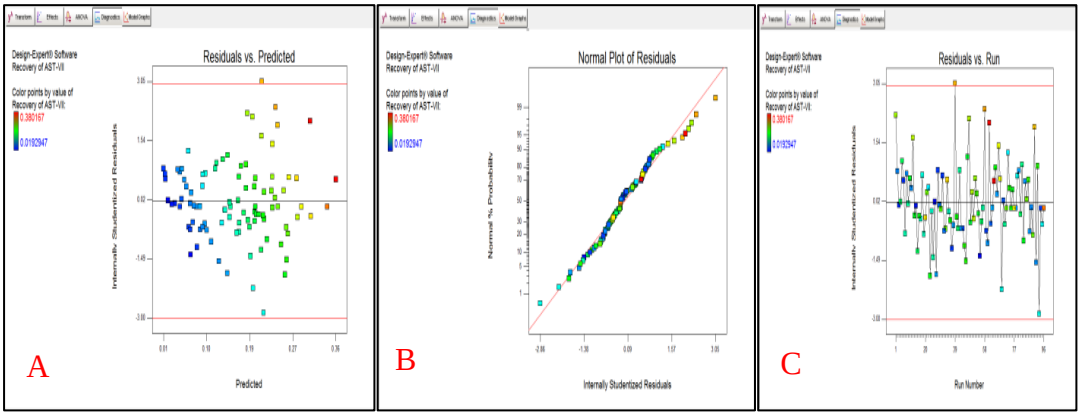

Figure 26. Plots for factor screening A. Residuals vs Predicted, B. Normal plot of residuals, C. Residuals vs Run

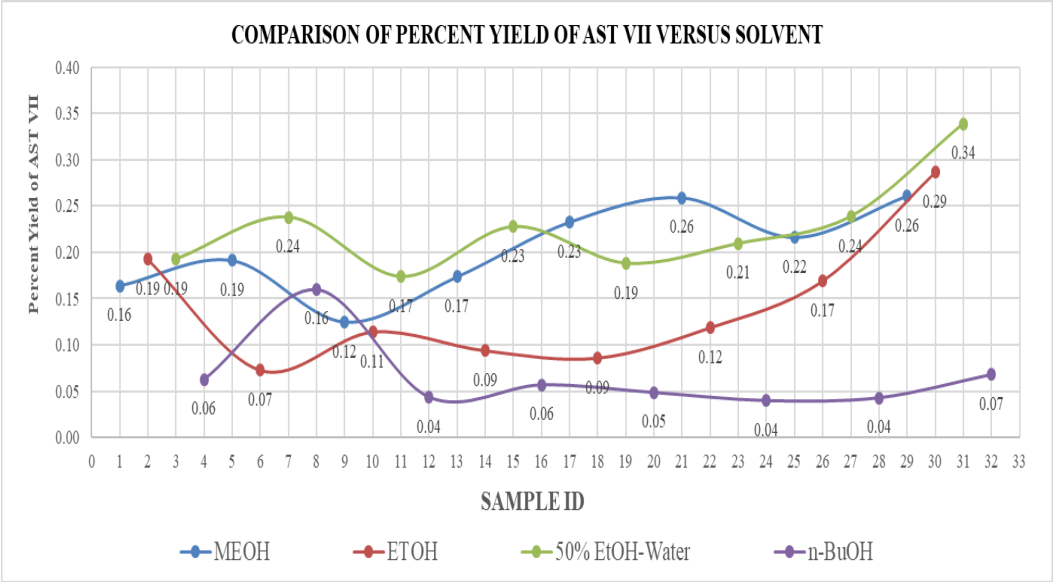

Figure 27. Comparisons of percent yield of AST VII versus main factors

(cont. on next page)

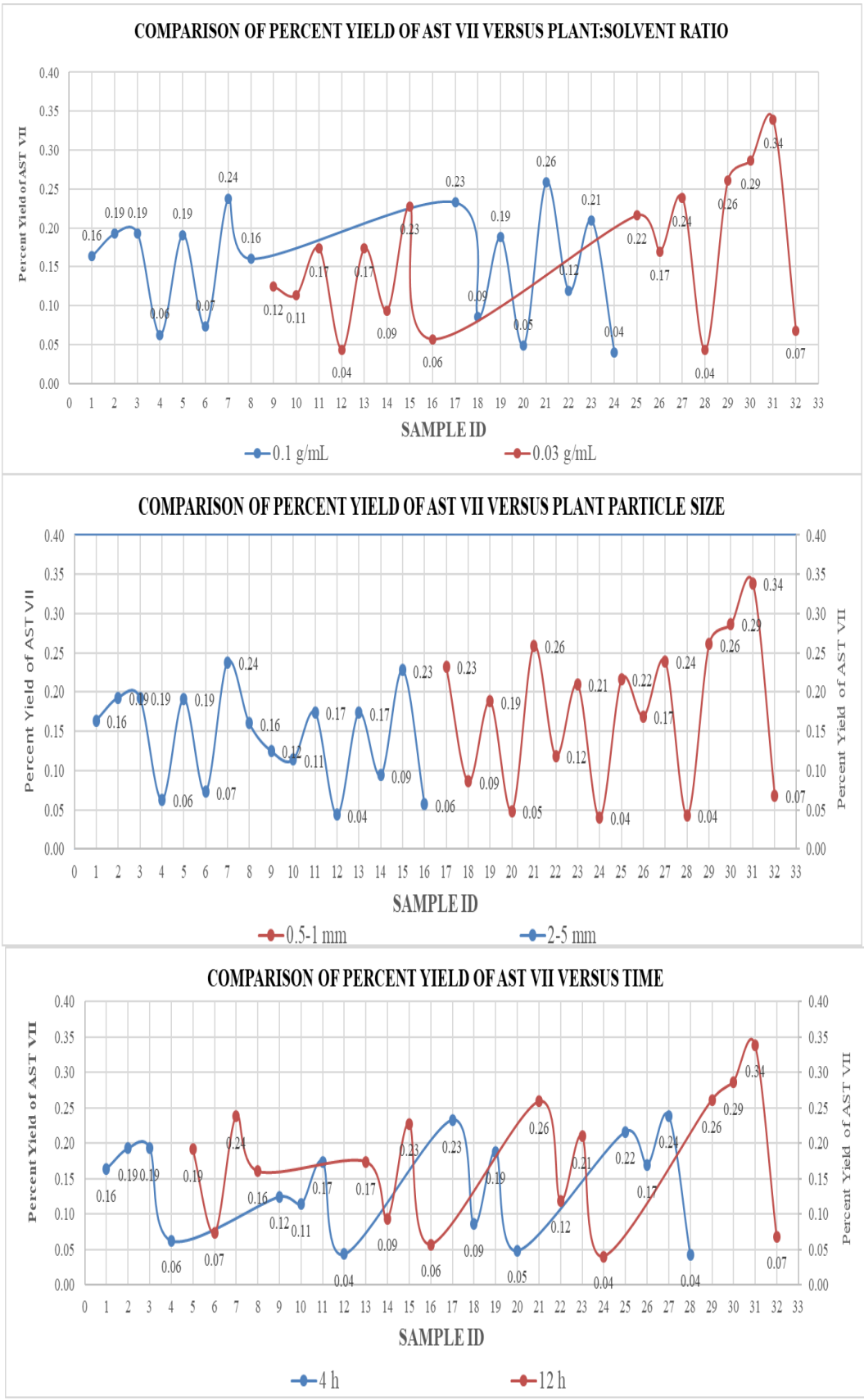

Figure 27. Comparisons of percent yield of AST VII versus main factors (cont.)

Chromatogram 3 showed that the phytochemical profiles of extracts of different solvents were similar. Therefore, it could be concluded that the solvent would not provide any advantages in downstream (separation-purification) processes. The water-free solvent systems are preferred in downstream process since the usage of aqueous systems in a large-scale process increases energy cost as long as do not make a significant difference in yield. MeOH generally provided higher percent yield of AST VII, it is cheaper than n-BuOH and it has high volatility. Consequently, MeOH was decided to use in extraction step. In addition, 0.5-1 mm of particle size was found appropriate since it offered higher yield than 2-5 mm range.

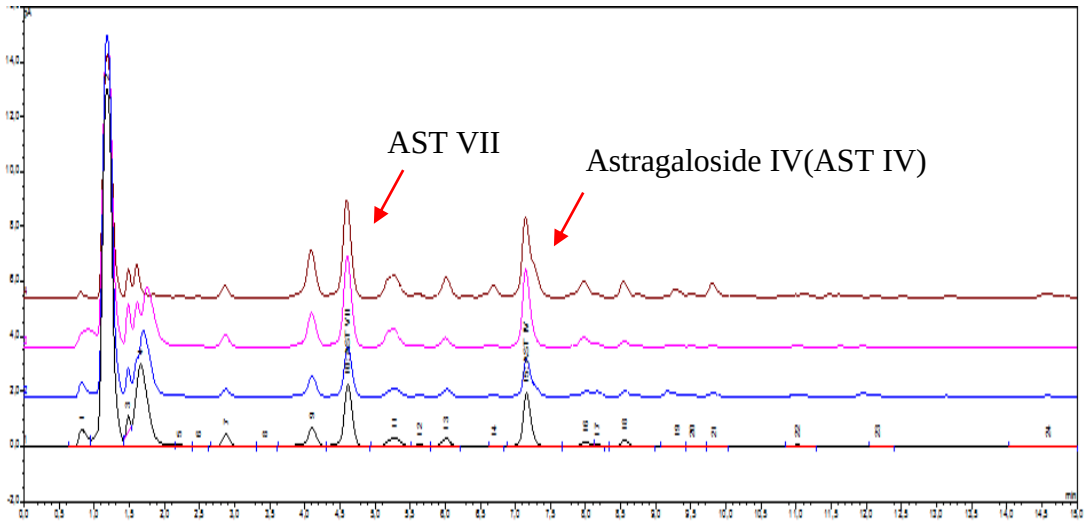

Chromatogram 3. UHPLC-CAD chromatogram of four samples (STD 15. in black; STD 18. in blue, STD 21. in pink, STD 24. in red)

In analysis of optimization studies, Quadratic vs. 2FI model was suggested by Design Expert 7.0.0 (Figure 28). For this model; cubic expressions were not included in the ANOVA analysis. The ANOVA table for factor optimization was shown in Figure 29. According to the table; the model was found to be significant, however the main factors was not significant ($p < 0.05$). The R^2 value was satisfactory ($R^2 = 0.9890$). In addition, other R^2 were found sufficient for modeling and optimization (Adj. $R^2 = 0.9748$, Pred. $R^2 = 0.8844$). Plots including residuals of experiment showed that the experiments were performed randomly (Figure 30c), the deviation of the standardized residuals from

the predicted values were ranged in interval (-3,3) (Figure 30b), and the results were found to be normal (Figure 30a and 30b).

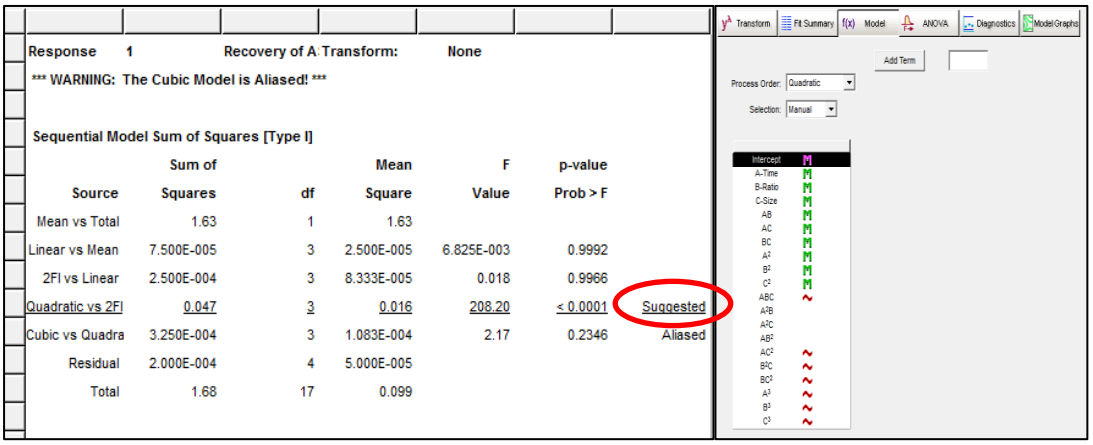

Response 1 Recovery of A Transform: None

*** WARNING: The Cubic Model is Aliased! ***

Sequential Model Sum of Squares [Type I]

Source	Sum of Squares	df	Mean Square	F Value	p-value Prob > F	
Mean vs Total	1.63	1	1.63			
Linear vs Mean	7.500E-005	3	2.500E-005	6.825E-003	0.9992	
2FI vs Linear	2.500E-004	3	8.333E-005	0.018	0.9966	
Quadratic vs 2FI	0.047	3	0.016	208.20	< 0.0001	Suggested
Cubic vs Quadra	3.250E-004	3	1.083E-004	2.17	0.2346	Aliased
Residual	2.000E-004	4	5.000E-005			
Total	1.68	17	0.099			

Figure 28. Model formation in Design Expert 7.0.0

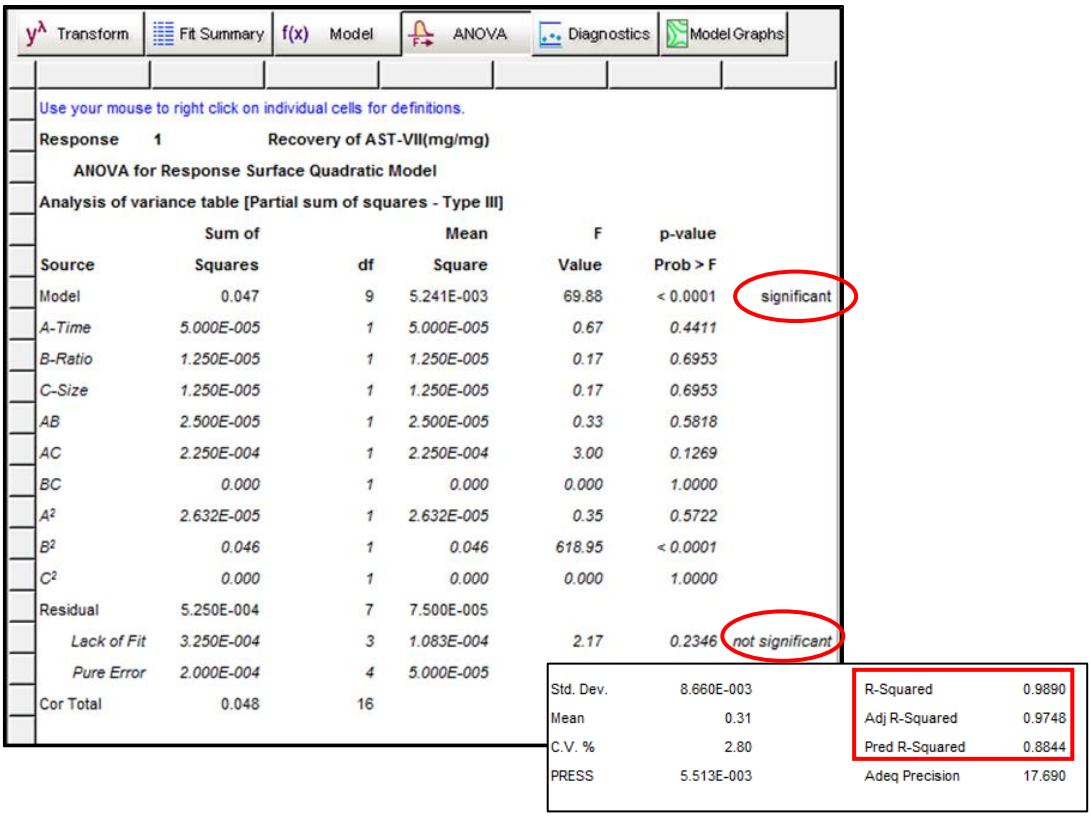

Use your mouse to right click on individual cells for definitions.

Response 1 Recovery of AST-VII(mg/mg)

ANOVA for Response Surface Quadratic Model

Analysis of variance table [Partial sum of squares - Type III]

Source	Sum of Squares	df	Mean Square	F Value	p-value Prob > F	
Model	0.047	9	5.241E-003	69.88	< 0.0001	significant
A-Time	*5.000E-005*	*1*	*5.000E-005*	*0.67*	*0.4411*	
B-Ratio	*1.250E-005*	*1*	*1.250E-005*	*0.17*	*0.6953*	
C-Size	*1.250E-005*	*1*	*1.250E-005*	*0.17*	*0.6953*	
AB	*2.500E-005*	*1*	*2.500E-005*	*0.33*	*0.5818*	
AC	*2.250E-004*	*1*	*2.250E-004*	*3.00*	*0.1269*	
BC	*0.000*	*1*	*0.000*	*0.000*	*1.0000*	
A^2	*2.632E-005*	*1*	*2.632E-005*	*0.35*	*0.5722*	
B^2	*0.046*	*1*	*0.046*	*618.95*	*< 0.0001*	
C^2	*0.000*	*1*	*0.000*	*0.000*	*1.0000*	
Residual	5.250E-004	7	7.500E-005			
Lack of Fit	*3.250E-004*	*3*	*1.083E-004*	*2.17*	*0.2346*	*not significant*
Pure Error	*2.000E-004*	*4*	*5.000E-005*			
Cor Total	0.048	16				

Std. Dev.	8.660E-003	R-Squared	0.9890
Mean	0.31	Adj R-Squared	0.9748
C.V. %	2.80	Pred R-Squared	0.8844
PRESS	5.513E-003	Adeq Precision	17.690

Figure 29. ANOVA table and R^2-values for factor optimization studies

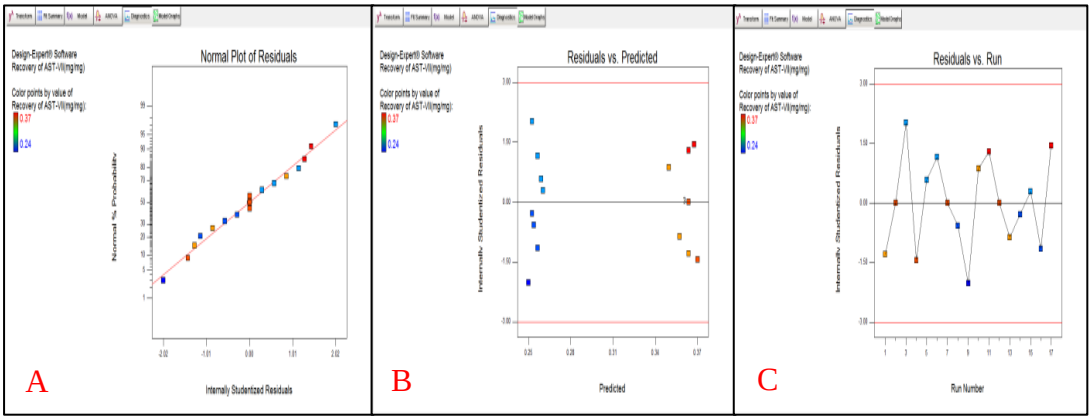

Figure 30. Plots for factor optimization; A) Residuals vs Predicted, B) Normal plot of residuals, C) Residuals vs Run

According to the 3D surface graph shown in Figure 31, the yield was slightly increased by time. However, we determined that 8-10 h was appropriate since extraction time used by BIONORM for *Astragalus* products were taken into consideration. Also, the plant:solvent ratio was determined as 0.05 g/mL which gave the high response. As a result, we noticed that determined values had the high efficiencies were in the center points of factors. Since runs formed with center points were replicated 5 times, optimum percent yield of AST VII was determined 0.036±0.001% as an average of responses of 5 runs.

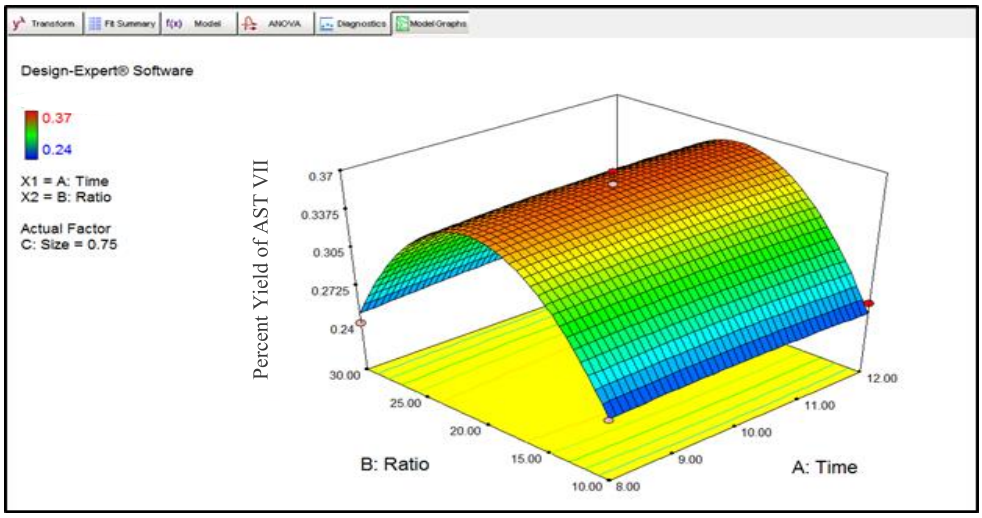

Figure 31. 3D surface graph for the percent yield of AST VII

3.1.2. Optimization of Pre-purification

In the pre-purification studies, liquid-liquid extraction, resin fractionation, and saponin precipitation were selected methods to be screened on removing some impurities from the crude extract and parameters of the superior method were determined to be optimized.

3.1.2.1. Liquid-Liquid Extraction

EtOAc:H_2O partition was used to remove non-polar impurities from the crude extract in SCES. TLC images were given in Figure 32 and comparisons of AST VII contents of the EtOAc and H_2O phases were presented in Table 12.

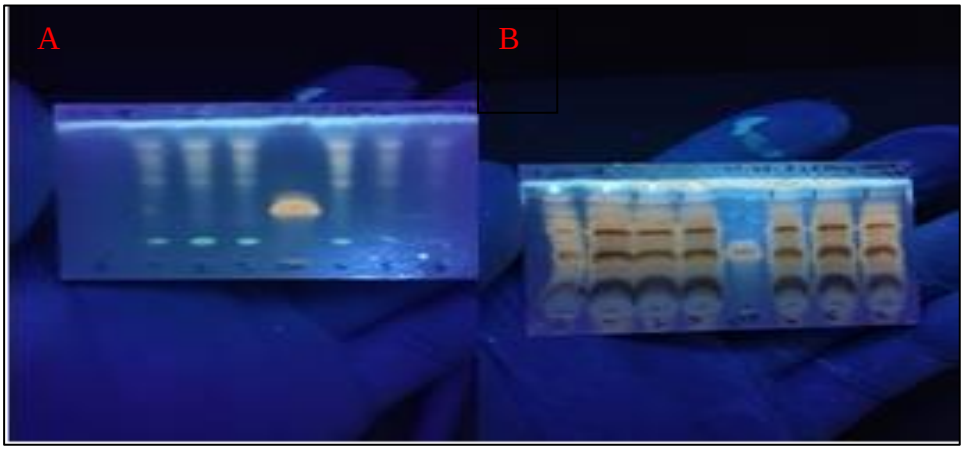

Figure 32. TLC profiles for EtOAc:H_2O partition in SCES (0. Sample at 0^{th} min, 1. Sample at 5^{th} min, 2. Sample at 10^{th} min, 3. Sample at 15^{th} min, 4. Sample at 20^{th} min, 5. Sample at 25^{th} min, 6. Sample at 30^{th} min) (A. view of EtOAc phase under UV_{365} B. view of H_2O phase under UV_{365}) (Normal Phase Silica Gel Plate, Mobile Phase; 61:32:7; $CHCl_3$:MeOH:H_2O)

According to UHPLC results, AST VII content remaining in H_2O phase was averagely 62-fold higher than EtOAc phase in the A_{205} detector. This was actually

intended but TLC profiles demonstrated that the non-polar molecules could not be sufficiently removed by EtOAc.

Table 12. UHPLC results of EtOAc:H_2O partitions in SCES

Sample ID	**Extract Amount (mg)**	**Concentration (ppm)**	**A_{205}**	**Percent Content of AST VII (g/g)**
EtOAc-H_2O-1-EtOAc Phase	1100	2000	N/A	N/A
EtOAc-H_2O-1-H_2O Phase	3900	2180	0.3106	0.58
EtOAc-H_2O-2-EtOAc Phase	1000	2000	0.0126	0.02
EtOAc-H_2O-2-H_2O Phase	4000	2140	0.3545	0.68
EtOAc-H_2O-3-EtOAc Phase	1000	2000	0.0067	0.01
EtOAc-H_2O-3-H_2O Phase	4000	2120	0.3106	0.60
Average of EtOAc Phases	1033.3±57.7			0.01±0.01
Average of H_2O Phases	3966.7±57.7			0.62±0.05

n-BuOH:H_2O partition was used to remove sugar impurities were intended from the crude extract in SCES. TLC images were given in Figure 33 and comparisons of AST VII contents of the phases were presented in Table 13.

Table 13. UHPLC results of n-BuOH:H_2O partitions in SCES

Sample ID	**Extract Amount (mg)**	**Concentration (ppm)**	**A_{205}**	**Percent Content of AST VII (g/g)**
n-BuOH:H_2O-1-n-BuOH Phase	2100	2020	0.5575	1.13
n-BuOH:H_2O-1-H_2O Phase	2900	2040	0.3139	0.63
n-BuOH:H_2O-2-n-BuOH Phase	2050	2040	0.4472	0.90
n-BuOH:H_2O-2-H_2O Phase	2950	2080	0.3038	0.60
n-BuOH:H_2O-3-n-BuOH Phase	2130	2120	0.6455	1.25
n-BuOH:H_2O-3-H_2O Phase	2870	2020	0.2898	0.59
Average of n-BuOH Phases	2093.3±40.4			1.09±0.18
Average of H_2O Phases	2906.7± 40.4			0.60± 0.02

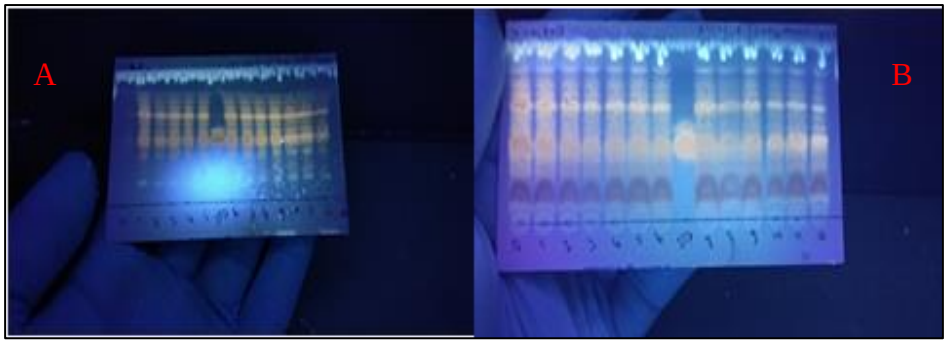

Figure 33. TLC profiles of n-BuOH:H_2O partition in SCES (0. Sample at 0^{th} min, 1. Sample at 5^{th} min, 2. Sample at 10^{th} min, 3. Sample at 15^{th} min, 4. Sample at 20^{th} min, 5. Sample at 25^{th} min, 6. Sample at 30^{th} min, 7. Sample at 35^{th} min, 8. Sample at 40^{th} min, 9. Sample at 45^{th} min, 10. Sample at 50^{th} min, 11. Sample at 55^{th} min, 12. Sample at 60^{th} min) A. view of n-BuOH phase under UV_{365} B. view of H_2O phase under UV_{365}) (Normal Phase Silica Gel Plate, Mobile Phase; 61:32:7; $CHCl_3$:MeOH:H_2O)

The purpose of the EtOAc:H_2O partition in SF was the same as of the EtOAc:H_2O partition in SCES. TLC images were given in Figure 34 and comparisons of AST VII contents were presented in Table 14.

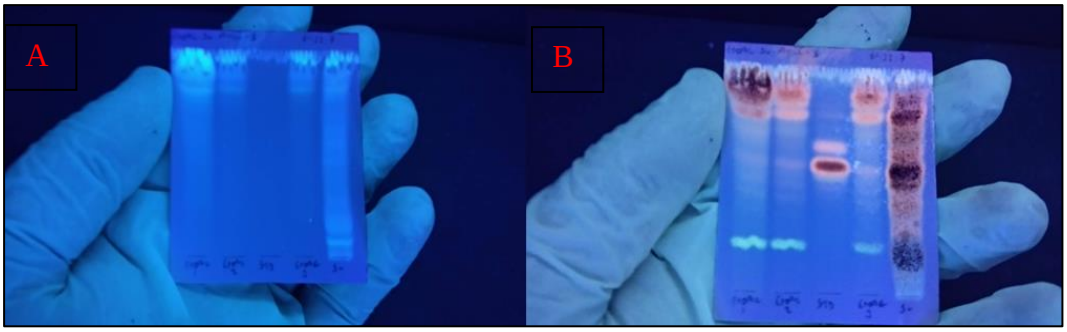

Figure 34. TLC profiles of EtOAc:H_2O partition in SF (From left to right; EtOAc-1, EtOAc-2, STD, EtOAc-3, H_2O) (A. view under UV_{365} before spraying 20% sulfuric acid, B. view under UV_{365} after spraying) (Normal Phase Silica Gel Plate, Mobile Phase; 61:32:7; $CHCl_3$:MeOH:H_2O)

Figure 34 and Table 14 showed that non-polar impurities were removed, and AST VII content was increased in each step, but the desired level of impurities could not be obtained by EtOAc:H_2O partition.

Table 14. UHPLC results for EtOAc:H_2O partitions in SF (Data in each row contained average of triplicate)

Sample ID	Extract Amount (mg)	Concentration (ppm)	A_{CAD}	Percent Content of AST VII (g/g)
EtOAc-H_2O-EtOAc-1 Phases	70.6±1.3	2050±10	0.0013±0.0002	0.005±0.002
EtOAc-H_2O-EtOAc-2-Phases	23.5±1	2070±30	0.0091±0.0004	0.024±0.001
EtOAc-H_2O-EtOAc-3-Phases	17.5±0.3	2100±100	0.0122±0.0037	0.032±0.008
EtOAc-H_2O-H_2O Phases	830±20	2100±20	0.4870±0.0055	1.291±0.03

The purpose of the n-BuOH:H_2O partition in SF was the same as of the n-BuOH:H_2O partition in SCES. TLC images were given in Figure 35 and comparisons of AST VII contents were presented in Table 15.

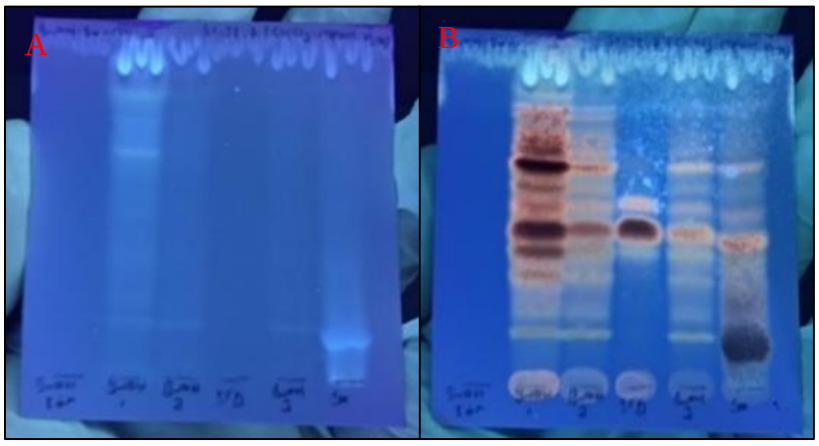

Figure 35. TLC profiles of n-BuOH:H_2O partition in SF (From left to right; Blank, n-BuOH-1, n-BuOH-2, STD, n-BuOH-3, H_2O) (A. view under UV_{365} before spraying, B. view under UV_{365} after spraying) (Normal Phase Silica Gel Plate, Mobile Phase; 61:32:7; $CHCl_3$:MeOH:H_2O)

The results were shown that sugar impurities were successfully kept in H_2O phase in n-BuOH:H_2O partition. In addition, UHPLC results were presented the percent content of AST VII remaining in n-BuOH phase was averagely 11-fold higher than H_2O phase in UV_{205} detector. Unlike these good results, some amount of AST VII remained in H_2O phase. This was an undesirable result because it may lead to loss of yield.

Table 15. UHPLC results of n-BuOH:H_2O partitions in SF (Values in each row contained average of triplicate)

Sample ID	Extract Amount (mg)	Concentration (ppm)	A_{205}	Percent Content of AST VII (g/g)
n-BuOH:H_2O-n-BuOH-1 Phases	345.5±10	2070±70	0.5415±0.045	1.08±0.125
n-BuOH:H_2O-n-BuOH-2-Phases	85.2±6	2080±20	0.9556±0.078	1.88±0.14
n-BuOH:H_2O-n-BuOH-3-Phases	65.5±20	2140±40	0.9394±0.065	1.79±0.15
n-BuOH:H_2O-H_2O Phases	447±14	2040±20	0.0684±0.023	0.14 ±0.05

As a result, liquid-liquid partition studies were not found as feasible for pre-purification step considering scale-up. Partition with EtOAc was not efficiently removed non-polar impurities from the crude extract. Also, partition with n-BuOH was not entirely extracted AST VII from crude extract.

3.1.2.2. Resin Fractionation

The TLC profile showing the molecular contents of the collected fractions to optimize the elution system was given in Figure 36. [Fr: 1-4] consisted of sugar impurities and [Fr: 5-16] consisted of saponin rich groups were independently combined due to similar profiles. After lyophilization, 34.4 mg of [Fr: 1-4] and 64.1 mg of [Fr: 5-18] were obtained. As a result, it was determined that the load of the columns to be used in the further purification steps could be reduced by 35.9% with H_2O elution. Nevertheless, it was decided that using 70-75% EtOH:H_2O to elute saponin rich fractions from resin surface. Because recovery of EtOH, up to 78.5% EtOH content, does not require further distillation.

TLC profile showing the chemical profiles of the collected fractions in the fractionation process with D-101 resin was given in Figure 37.

[Fr: 1-3] consisted of sugar impurities and [Fr: 4-18] consisted of saponin rich fractions were combined due to similar profiles. After lyophilization, 3.061 g of [Fr: 1-3]

and 3.632 g of [Fr: 4-18] were obtained. As a result, it was determined that the load of the columns to be used in the further purification steps could be reduced by 40.8% with H_2O elution. In addition, UHPLC analysis was performed to determine the amount of AST VII in fractions [Fr: 1-3] and [Fr: 4-18] (Table 16).

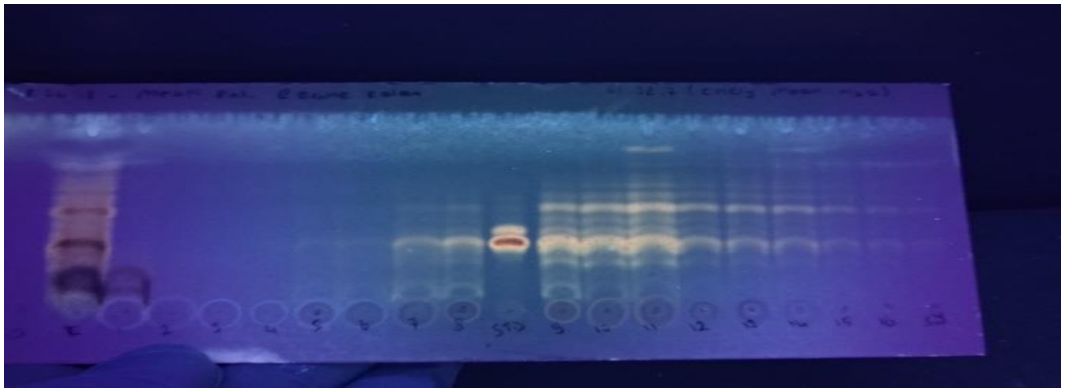

Figure 36. TLC profiles of the fractions under UV_{365} (Numbers. Numbers of fractions, E. MeOH extract of *A.trojanus*, SY. Wash) (Normal Phase Silica Gel Plate, Mobile Phase; 61:32:7; $CHCl_3$:MeOH:H_2O)

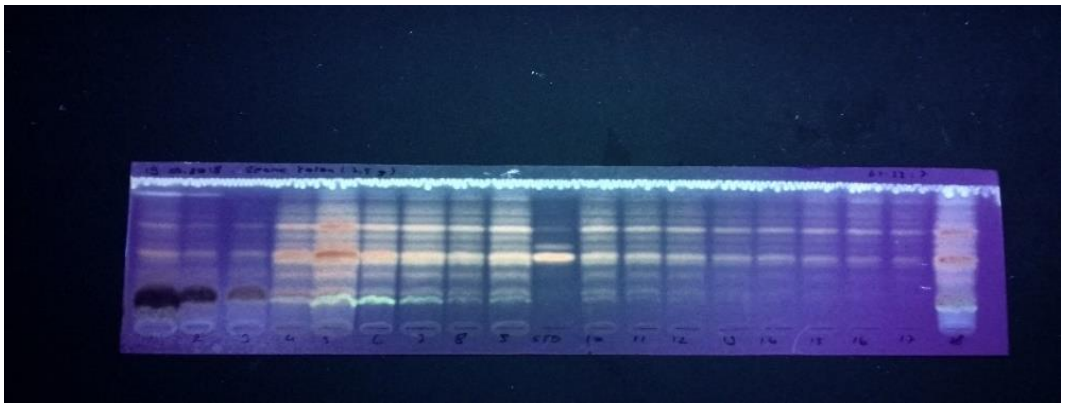

Figure 37. TLC profiles of fractions obtained after resin column (Numbers. Numbers of fractions) (Normal Phase Silica Gel Plate, Mobile Phase; 61:32:7; $CHCl_3$:MeOH:H_2O)

According to UHPLC results, AST VII existing in H_2O elution indicated that the crude extract was not enough adsorbed by resin. Thus, a kinetic study was carried out for

loading rate. First kinetic study was performed to find out the optimum ratio of the saponin rich fraction to resin. TLC profiles were given in Figure 38.

Table 16. UHPLC results of fractions obtained after resin column

Sample ID	Extract Amount (g)	Concentration (ppm)	A_{205}	Percent Content of AST VII (g/g)
STD 1	-	9.9	0.1375	-
[Fr: 1-3]	3.061	2040	0.0919	0.3182
STD 2	-	9.9	0.1578	-
[Fr: 4-18]	3.632	2020	1.3562	4.1321

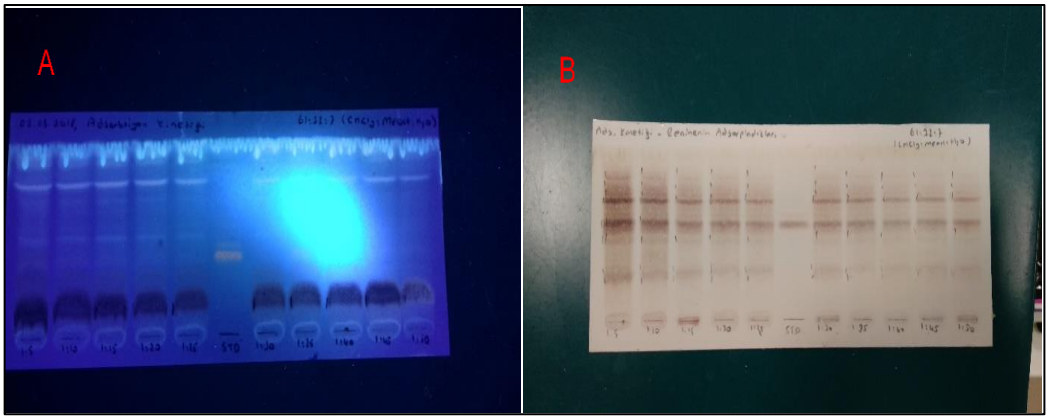

Figure 38. TLC profiles of first kinetic study (A. view of the phytochemical profile non-adsorbed by the resin under UV_{365} after (sugars in the MeOH extract), B. view of the phytochemical profile adsorbed by the resin under day light) (Normal Phase Silica Gel Plate, Mobile Phase; 61:32:7; $CHCl_3$:MeOH:H_2O)

Based on TLC profiles, 1:5 and 1:10 ratios were found to be similar. Then, it was decided to focus on a range from 1:1 to 1:10 and a second kinetic study was conducted. As results of second kinetic study, no profile differences were observed between 1:1 and 1:10.

As a result, D-101 resin fractionation studies were found to be feasible for pre-purification step considering scale-up. It was determined that the load of the columns to

be used in the further purification steps could be reduced by in a range of 30-40% with H_2O elution. In addition, sugar impurities were effectively eliminated using H_2O elution with minimum loss of AST VII. D-101 resin can be effectively loaded by any ratio from 1:1 to 1:10 (extract:resin).

3.1.2.3. Saponin Precipitation

Acetone precipitation was tested on crude extract and [Fr: 4-18] to obtain saponin-rich fractions (Figure 39 and 40).

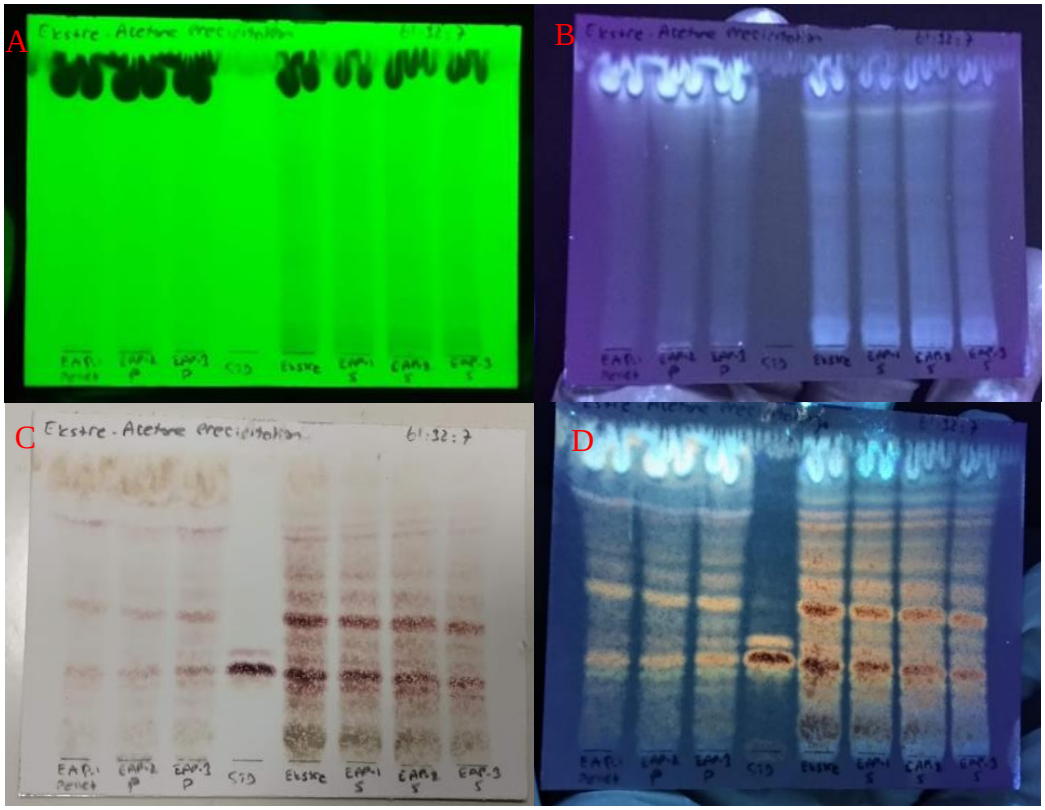

Figure 39. TLC profiles of precipitation studies with crude extract (from left to right; Pellet of 1st experiment, Pellet of 2nd experiment, Pellet of 3th experiment, STD, Extract, Supernatant of 1st experiment, Supernatant of 2nd experiment, Supernatant of 3th experiment)(A. under UV_{254} before spraying, B. under UV_{365} before spraying, C. view under day light after spraying, D. after under UV_{365} spraying) (Normal Phase Silica Gel Plate, Mobile Phase; 61:32:7; $CHCl_3$:MeOH:H_2O)

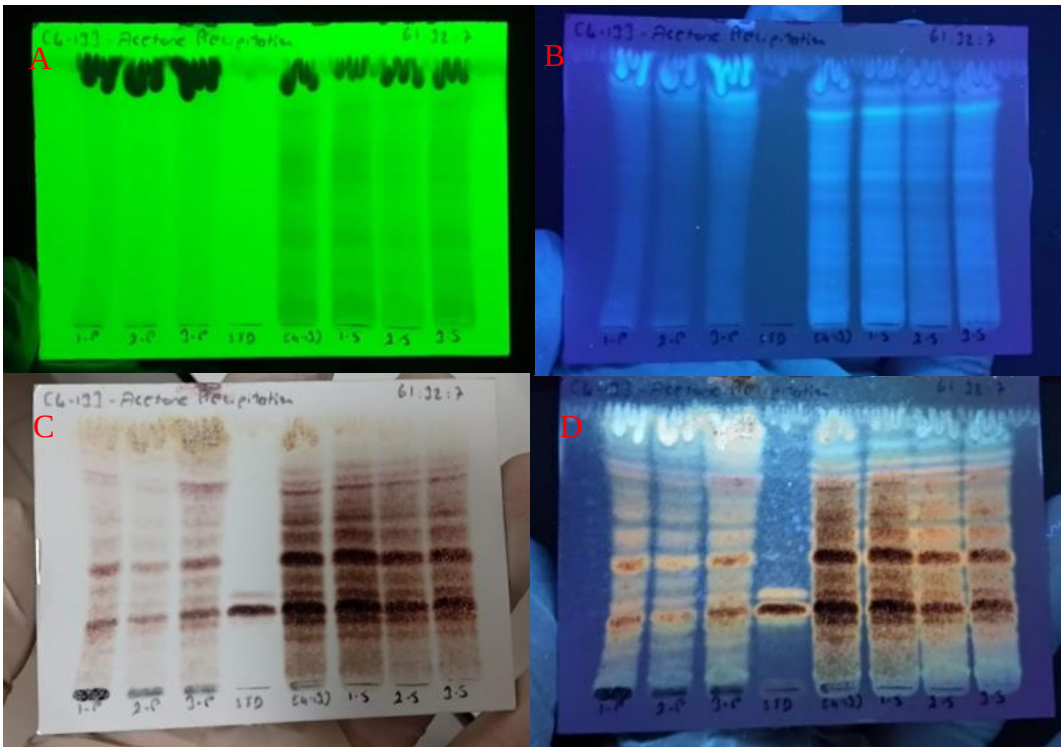

Figure 40. TLC profile of precipitation studies with [4-18] obtained after resin column (from left to right; Pellet of 1st experiment, Pellet of 2nd experiment, Pellet of 3th experiment, STD, [4-18], Supernatant of 1st experiment, Supernatant of 2nd experiment, Supernatant of 3th experiment)(A. view below 254 nm before spraying, B. view below 365 nm before spraying, C. view under day light after spraying, D. view below 365 nm after spraying) (Normal Phase Silica Gel Plate, Mobile Phase; 61:32:7; $CHCl_3$:MeOH:H_2O)

According to TLC profiles, it was observed that the precipitation process was not good option and no further analytical (UHPLC) studies were required.

3.1.3. Optimization of Purification

In the purification studies, mobile phase system and adsorbent were selected parameters to be optimized (Figure 41).

Silica gel was preferred for initial purification studies, because it is cheap as an adsorbent and can be regenerated. When mobile phases were compared, $CHCl_3$:MeOH:H_2O systems provided better separation than EtOAc:MeOH:H_2O.

However, EtOAc:MeOH:H_2O (100: 17.5: 13.5) solvent system was preferred because it does not contain halogen, much less hazardous than $CHCl_3$:MeOH:H_2O, and showed similar resolution with chloroform contained systems.

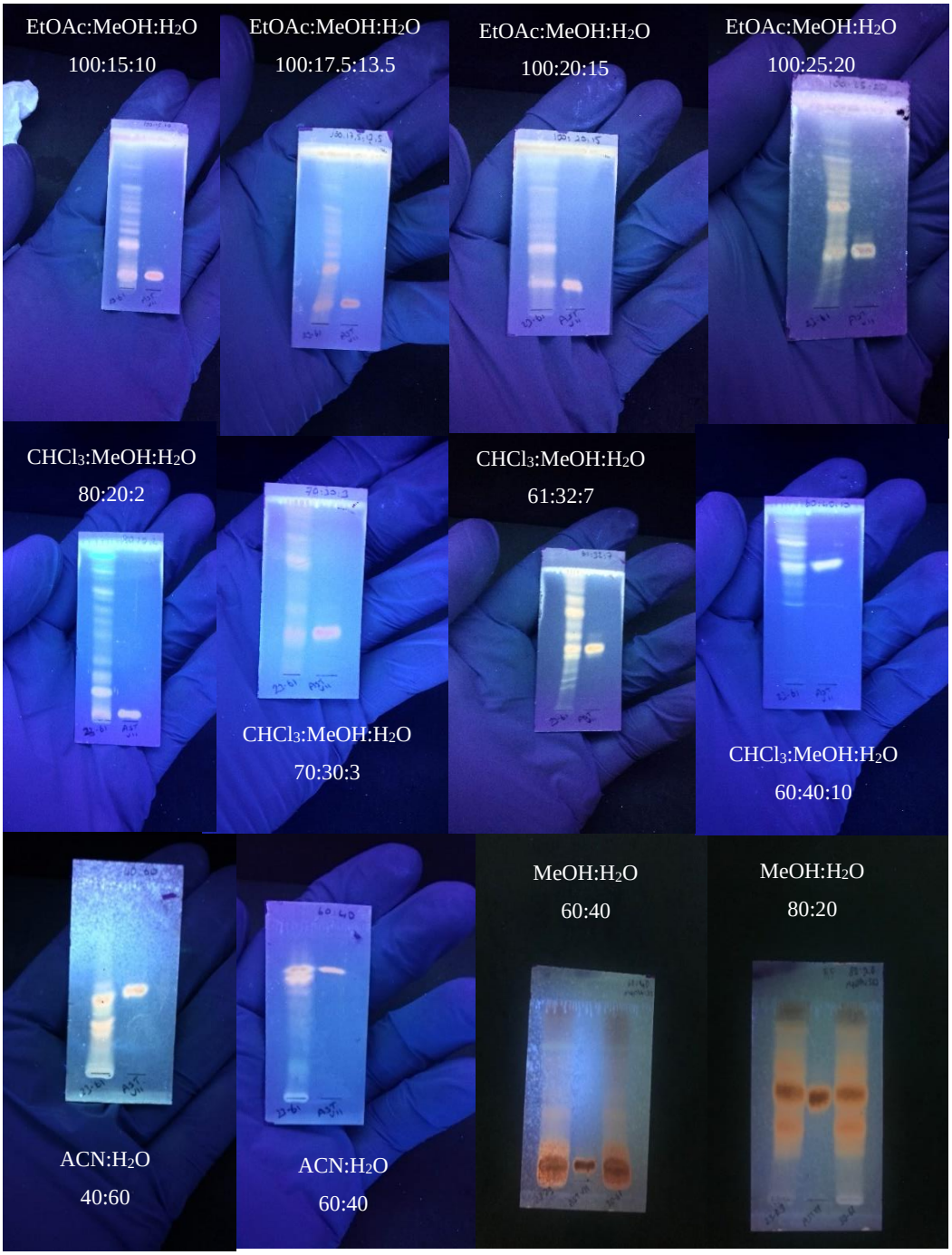

Figure 41. TLC profiles of fraction of [Fr: 23-61] spotted on different adsorbents and developed with different mobile phase system (RP-C_{18}: MeOH: H_2O and ACN:H_2O; Silica gel: EtOAc:MeOH:H_2O and $CHCl_3$:MeOH:H_2O)

3.1.4. Optimization of Final Purification

In the precipitation and crystallization studies, MeOH, EtOH, ACN and acetone were selected solvents to be screened. To precipitate AST VII, the superior solvent was selected as a mixture of MeOH and acetone.

3.2. Results from the Production of AST VII at Laboratory Scale

The results were explained below in the subheadings. Production of AST VII was successfully carried out by making slight changes in the optimized process.

3.2.1. Extraction Step

191.75 g extract was obtained from 1 kg of *A.trojanus*. Results were consistent with previous results obtained in optimization studies. Even though the percent yield of extraction (g extract/g plant) was averagely 17.4% in the optimization studies, higher extraction yield (19.2%) was obtained at laboratory scale.

3.2.2. Pre-purification Step

The crude extract was subjected to open column chromatography using D-101 resin to give 2 main fractions ([Fr: 0-22] and [Fr: 23-61]). [Fr: 0-22] consisted of sugar impurities and they were removed. [Fr: 23-61] (107 g) consisted of saponin rich groups and they were combined due to similar TLC profiles (Figure 42).

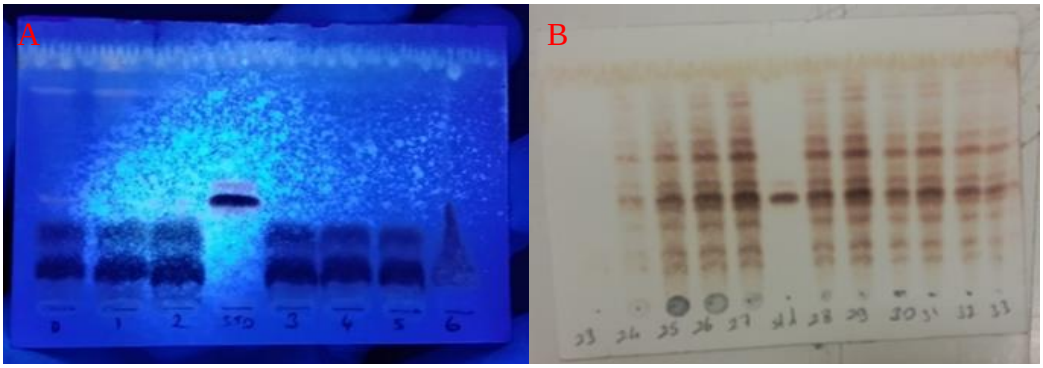

Figure 42. TLC profiles of some fractions obtained after resin column (A. [Fr:0-6] under UV_{365} after spraying, B. [Fr:23-33] under UV_{365} after spraying) (Normal Phase Silica Gel Plate, Mobile Phase; 61:32:7; $CHCl_3$:MeOH:H_2O)

As a result, the load of the columns to be used in the further purification steps was reduced up to 44.3% by using D-101 resin. Also, results were consistent with previous results obtained in optimization studies.

3.2.3. Purification Step

[Fr: 37-54] (24.7 g) was obtained as AST VII rich fraction from first silica gel column and subjected to further steps (Figure 43).

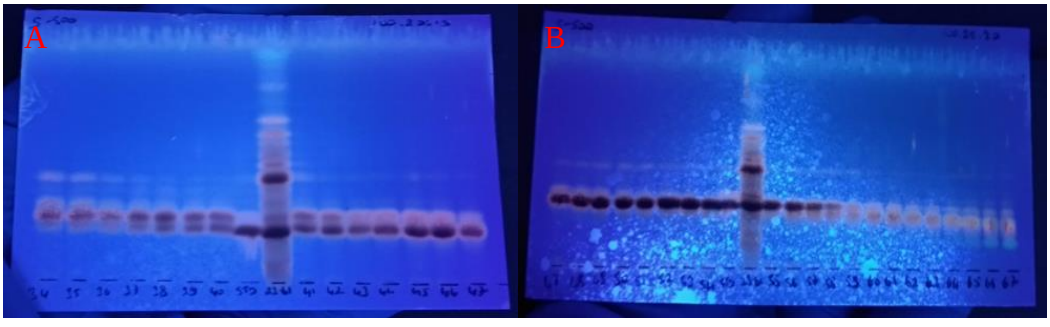

Figure 43. TLC profiles of AST VII rich fractions (view of A. [Fr: 34-47] under UV_{365} after spraying, B. [Fr: 47-67] under UV_{365} after spraying) (Normal Phase Silica Gel Plate, Mobile Phase; 100:20:15 (for A); 100:25:20 (for B), EtOAc:MeOH:H_2O)

[Fr: 71-110] (21.7 g) (Figure 44) were combined to afford enriched AST VII fractions from second silica gel column and re-chromatographed over RP-C_{18} column to give [Fr: 121-176] (6.78 g).

To imaging of phytochemical profiles of fractions taken from RP-C_{18} silica gel column, normal silica gel TLC plates was developed. In normal silica TLC plates, it was observed that pure AST VII was obtained from the silica gel column using EtOAc:MeOH:H_2O system. To control this purity, normal silica gel HPTLC plate was used. As shown in Figure 45, saponins with very close polarity to AST VII were found and the fractions were not pure. Subsequently, all fractions were analyzed on both HPTLC and RP TLC plates to check AST VII purity. Compounds with very close polarity to AST VII were observed on the HPTLC using $CHCl_3$:MeOH:H_2O systems. Therefore, $CHCl_3$:MeOH:H_2O systems were preferred as solvent system in the following stages.

Lastly, [Fr: 121-176] (6.78 g) was purified on silica gel using $CHCl_3$:MeOH:H_2O systems to afford [Fr:78-94] and [Fr: 95-104]. These fractions were determined to be of high purity in TLC controls and 3.5 g of AST VII was totally obtained in >%95 purity.

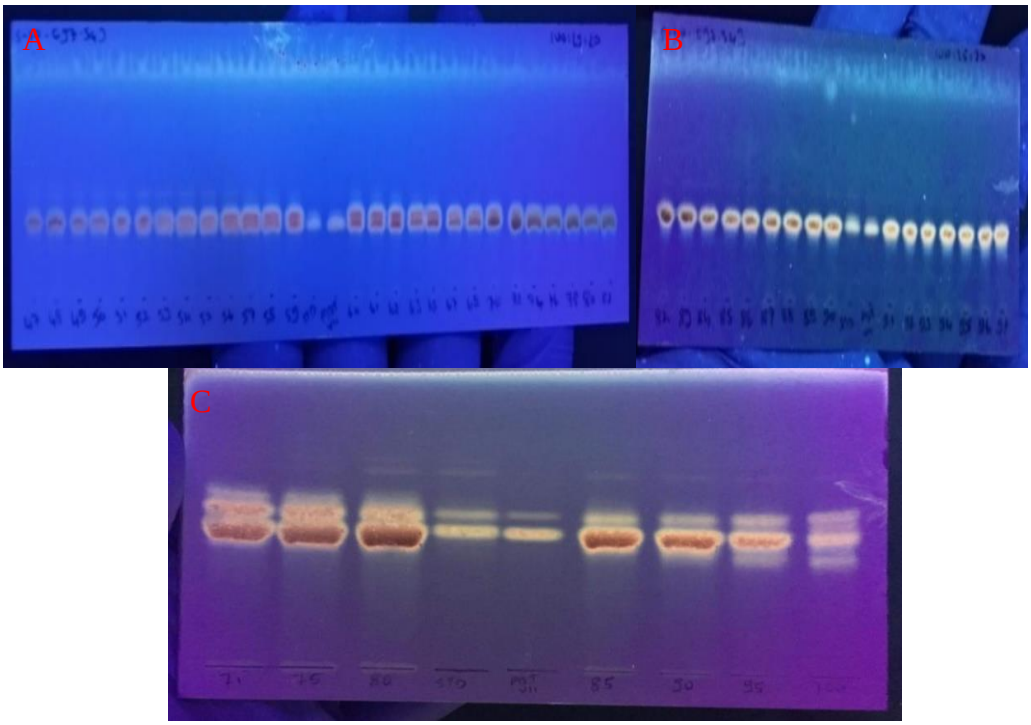

Figure 44. TLC profiles of the AST VII richest fraction (view of **A**. [Fr: 47-83] under UV_{365} after spraying, **B.** [Fr: 84-97] under UV_{365} after spraying, **C**. [Fr: 71-100] under UV_{365} after spraying) (Normal Phase Silica Gel Plate, Mobile Phase; 100:25:20; 90:25:20 (for HPTLC), EtOAc:MeOH:H_2O)

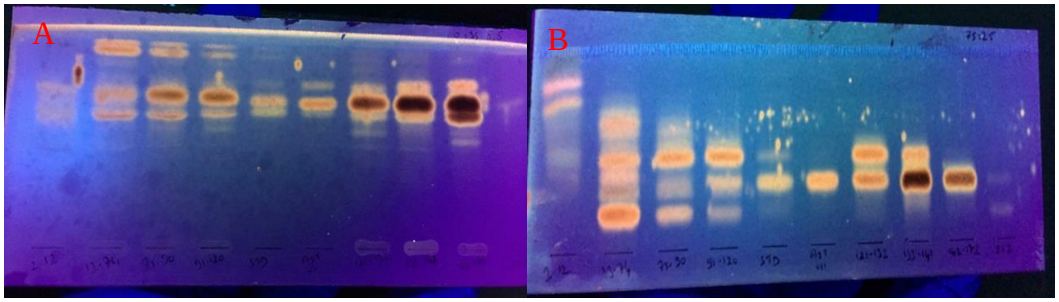

Figure 45. TLC profiles of combined fractions after RP-C_{18} column (view of A. HPTLC under UV_{365} after spraying, B. RP-TLC under UV_{365} after spraying) (from left to right, [Fr: 2-12], [Fr: 13-74], [Fr: 75-90], [Fr: 91-120], STD, AST VII, [Fr: 121-132], [Fr: 133-141], [Fr: 142-172], [Fr: 217]) (Mobile Phases; 60:35:8.5 (for HPTLC), $CHCl_3$:MeOH:H_2O, 75:25 (for RP-TLC), MeOH:H_2O)

3.3. Results from the Production of AST VII at Semi-Pilot Scale

The target which is the production of 100 g of AST VII from 100 kg of plant was nearly achieved. The stepwise purification of fractions containing ASTVII was shown in the TLC (Figure 46). Also, the results obtained during production of AST VII were clearly described below in the headings.

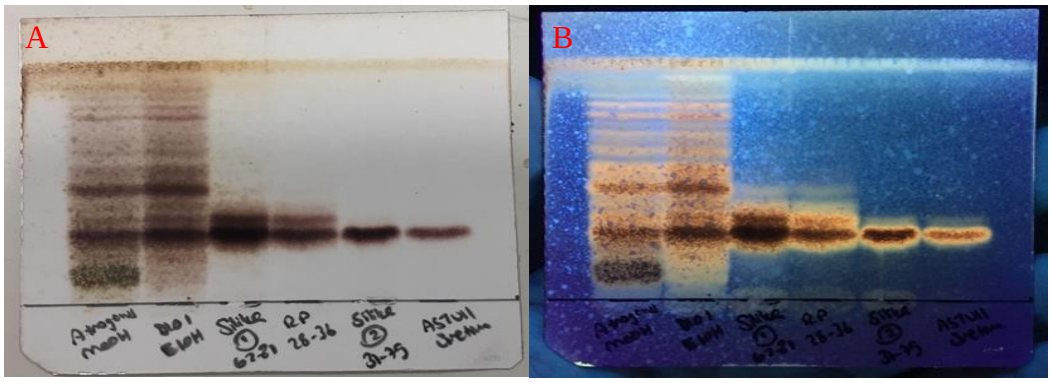

Figure 46. TLC profiles of main fractions obtained in different stages during the isolation of AST VII (from Extraction to Precipitation) (view of A. TLC under day light, B. TLC under UV_{365} after spraying) (Normal Phase Silica Gel Plate, Mobile Phase; 61:32:7; $CHCl_3$:MeOH:H_2O)

3.3.1. Extraction Step

12.6 kg of MeOH extract was obtained from 100 kg *A.trojanus*. UHPLC chromatogram of the MeOH extract and AST VII reference was given in chromatogram 4. Percent yield of AST VII was calculated as 0.25% in regard to results of the analysis. The reason of the decrease in yield could be the failure to perform the extraction under optimum conditions.

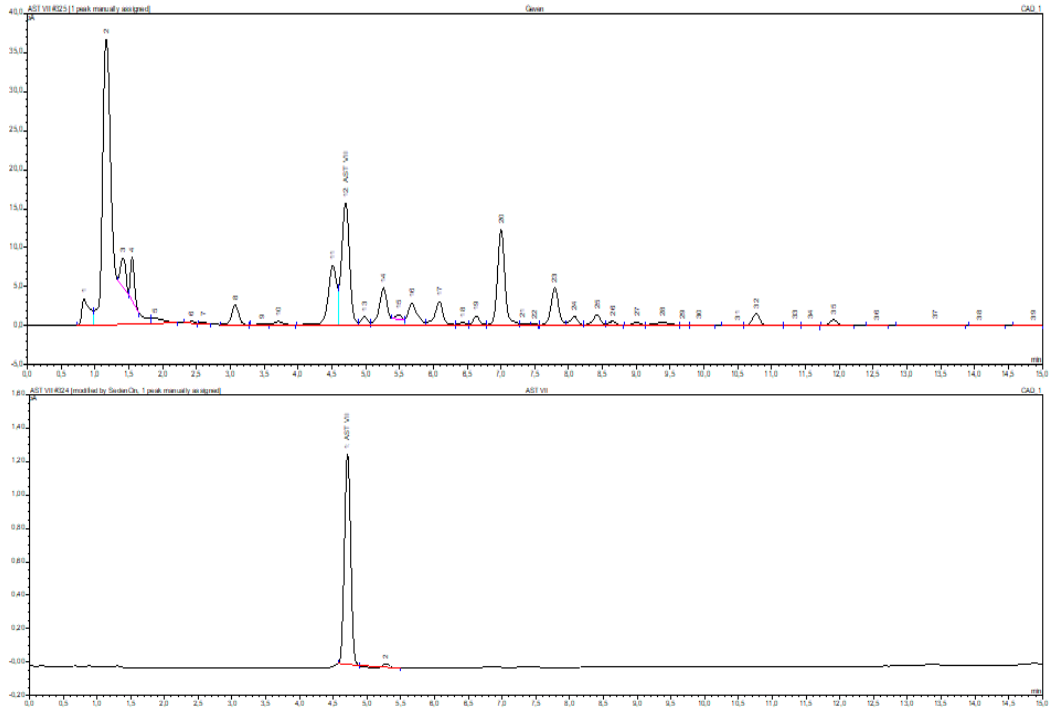

Chromatogram 4. UHPLC-CAD chromatogram of MeOH extract of *A.trojanus* and pure AST VII

3.3.2. Pre-purification Step

The crude extract was fractionated into 3 main fractions as sugar rich fractions, UV-active compound rich fractions, and saponin rich fractions. 4 kg of saponin rich fraction was obtained after resin fractionation. The load of the columns to be used in the

further purification steps was reduced about 53.8% by elution from the D-101 resin. As a result, AST VII content was enriched 2-fold in comparison with the crude extract.

3.3.3. Purification Step

[Fr: 62-81] (810 g) was isolated as AST VII rich fraction from first silica column and subjected to VLC using RP-C_{18} (Figure 47). Moreover, [Fr: 82-95] was directly precipitated in order to obtain pure AST VII.

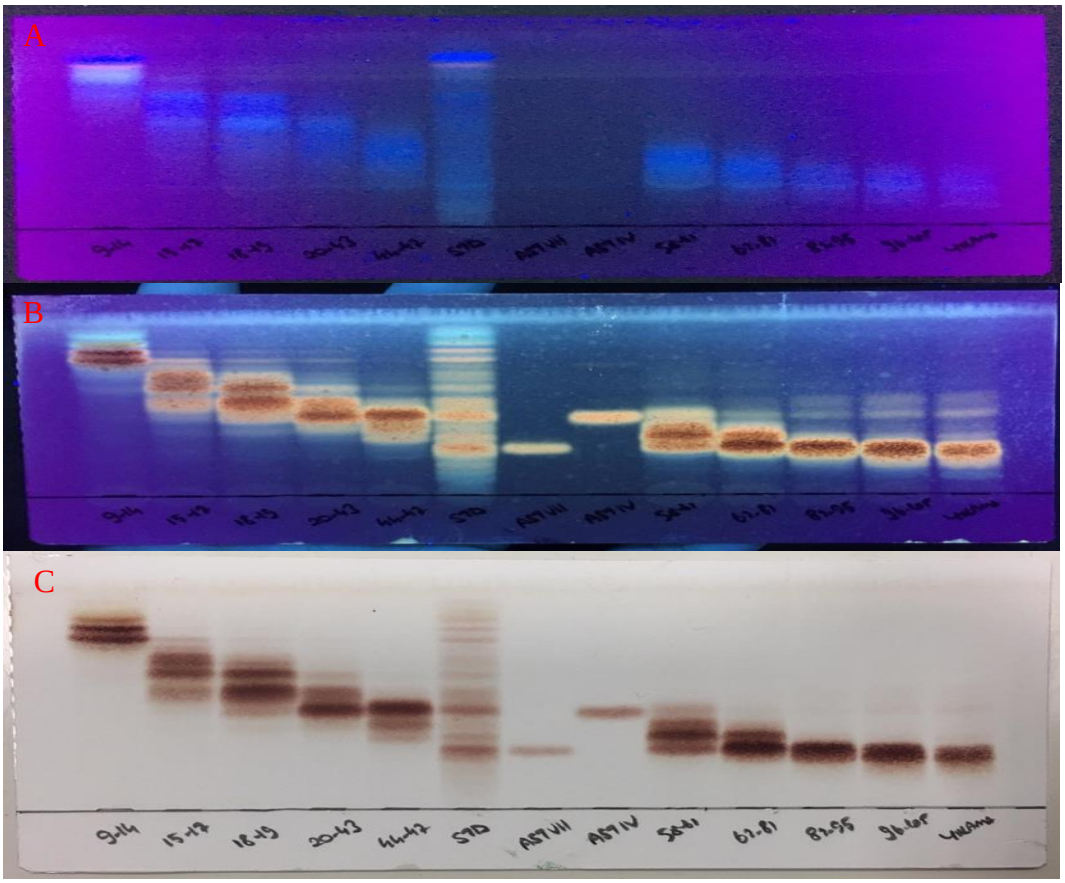

Figure 47. TLC profiles of combined fractions after first silica column (From left to right, [Fr: 9-14], [Fr: 15-17], [Fr: 18-19], [Fr: 20-43], [Fr: 44-47], STD, AST VII, AST IV, [Fr: 58-61], [Fr: 62-81], [Fr: 82-95], [Fr: 96-108], Wash) (view of A. under UV_{365} before spraying, B. under UV_{365} after spraying, C. under day light) (Normal Phase Silica Gel Plate, Mobile Phase; 61:32:7; $CHCl_3$:MeOH:H_2O)

HPLC chromatogram of [Fr: 62-81] was given in chromatogram 5. According to analysis data, AST VII content after first silica column was enriched 5-fold in comparison with saponin rich fraction.

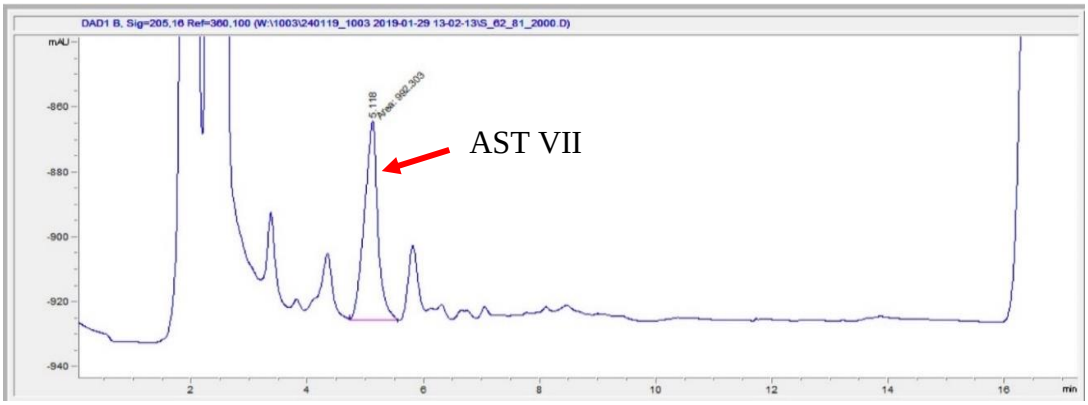

Chromatogram 5. HPLC-DAD chromatogram of [Fr: 62-81] isolated from first silica column

[Fr: 28-36] (525 g) was isolated as AST VII rich fraction from RP-C_{18} column and subjected to second silica gel column. HPLC chromatogram of [Fr: 28-36] was given in chromatogram 6. According to analysis data, AST VII content after RP-C_{18} column was enriched 1.5-fold in comparison with previous isolation step.

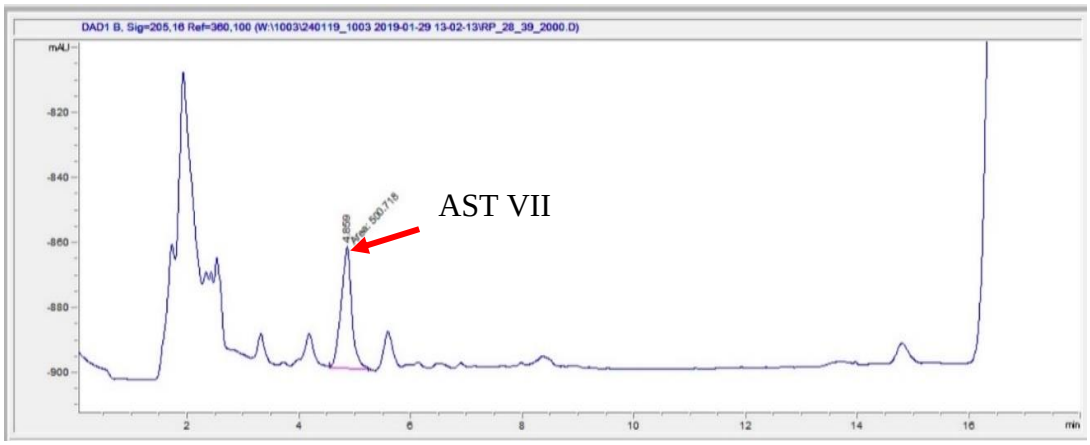

Chromatogram 6. HPLC-DAD chromatogram of [Fr: 28-36] isolated from RP-C_{18} silica

At the end of the last purification step, [Fr: 39-50], [Fr: 51-60], [Fr: 61-67] and [Fr: 68-79] were found to be high purity in TLC controls. HPLC chromatogram of [Fr: 61-67] was given in chromatogram 7. According to analysis data, AST VII content after second silica column was enriched 1.5-fold in comparison with previous isolation step.

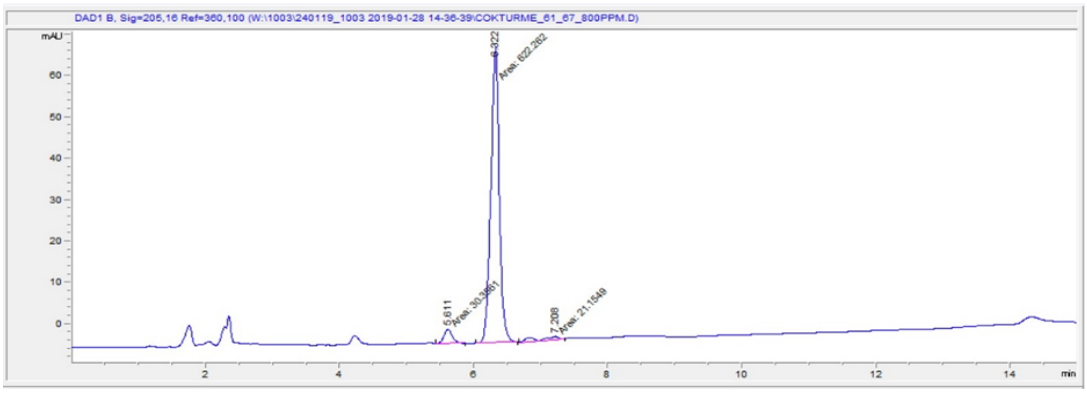

Chromatogram 7. HPLC-DAD chromatogram of [Fr: 61-67] isolated after second silica column

[Fr: 39-50], [Fr: 51-60], [Fr: 61-67] and [Fr: 68-79] were precipitated using MeOH and acetone. 18 g of AST VII from [Fr: 39-50], 58.6 g of AST VII from [Fr: 51-79], and 35 g of AST VII from [Fr: 82-95] was successfully purified. Total amount of AST VII was 93.6 g in >%95 purity according to HPLC results (Chromatogram 8).

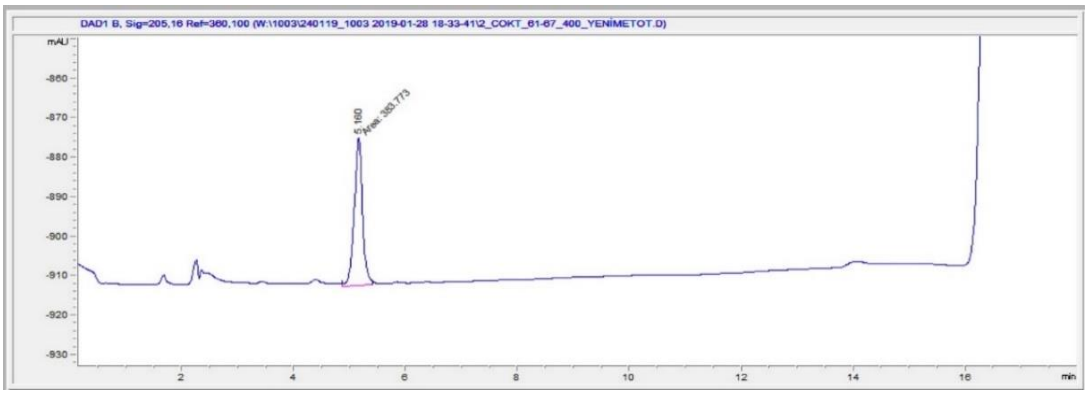

Chromatogram 8. HPLC-DAD chromatogram of [Fr: 61-67] purified after precipitation

The structure and purity of obtained AST VII were confirmed by TLC (Figure 48), HPLC and NMR spectra (^{1}H and ^{13}C) (Spectrum 1,2,3, and 4).

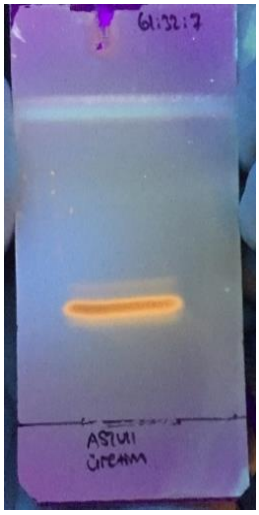

Figure 48. HPTLC profile of AST VII obtained from precipitation of [Fr: 51-79] (Normal Phase Silica Gel Plate, Mobile Phase; 61:32:7; $CHCl_3$:MeOH:H_2O)

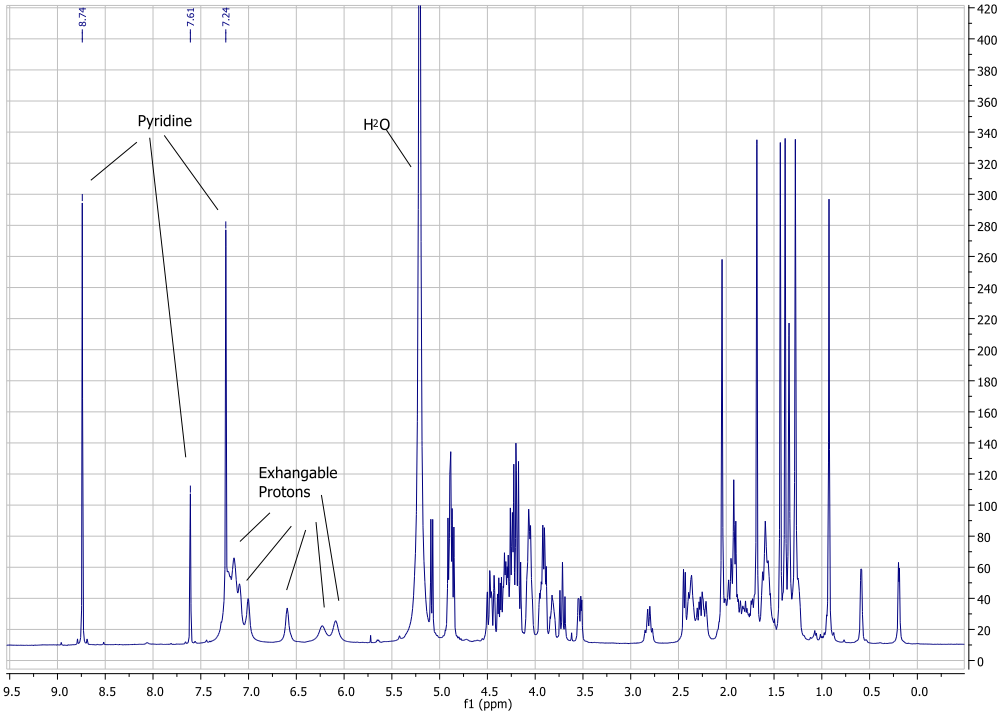

Spectrum 1. ^{1}H NMR spectrum of AST VII obtained from precipitation of [Fr: 51-79]

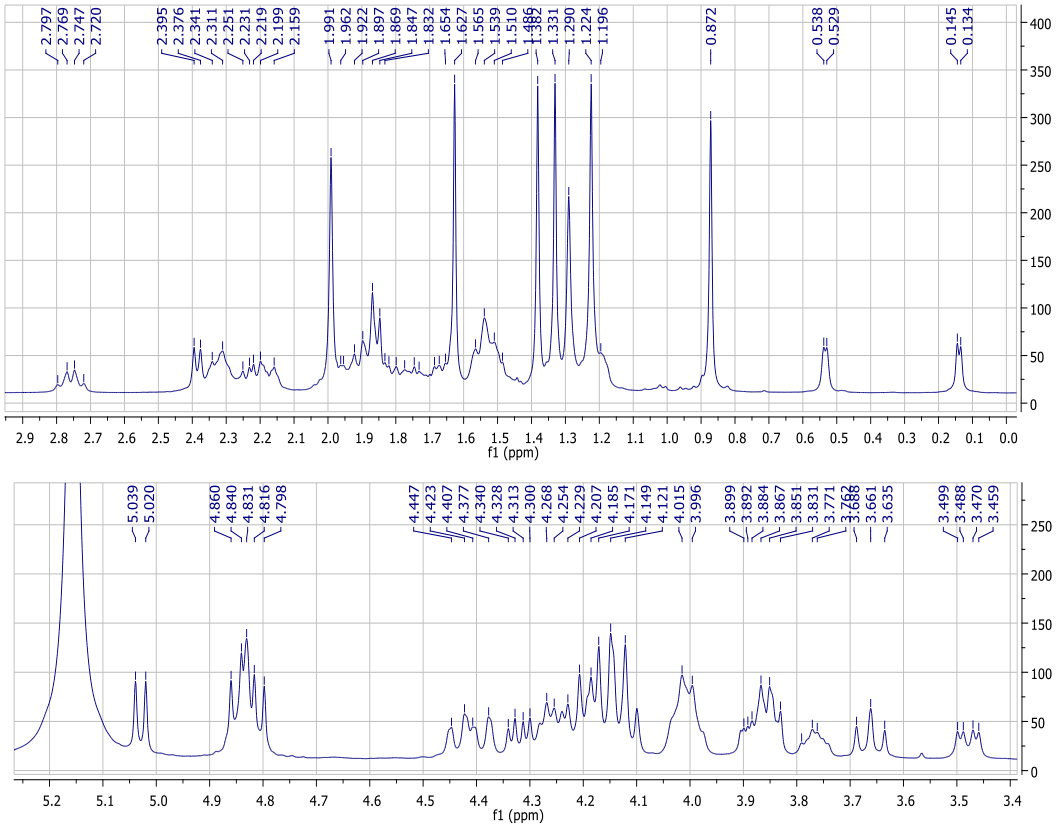

Spectrum 2. Expanded ^{1}H NMR spectrum of [Fr: 51-79]

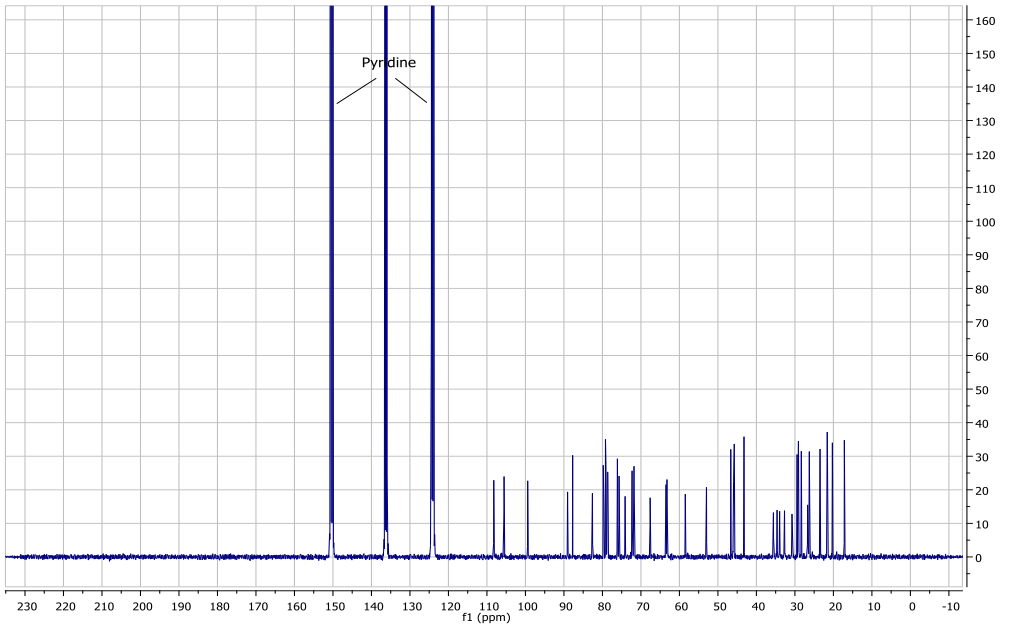

Spectrum 3. ^{13}C NMR spectrum of AST VII obtained from precipitation of [Fr: 51-79]

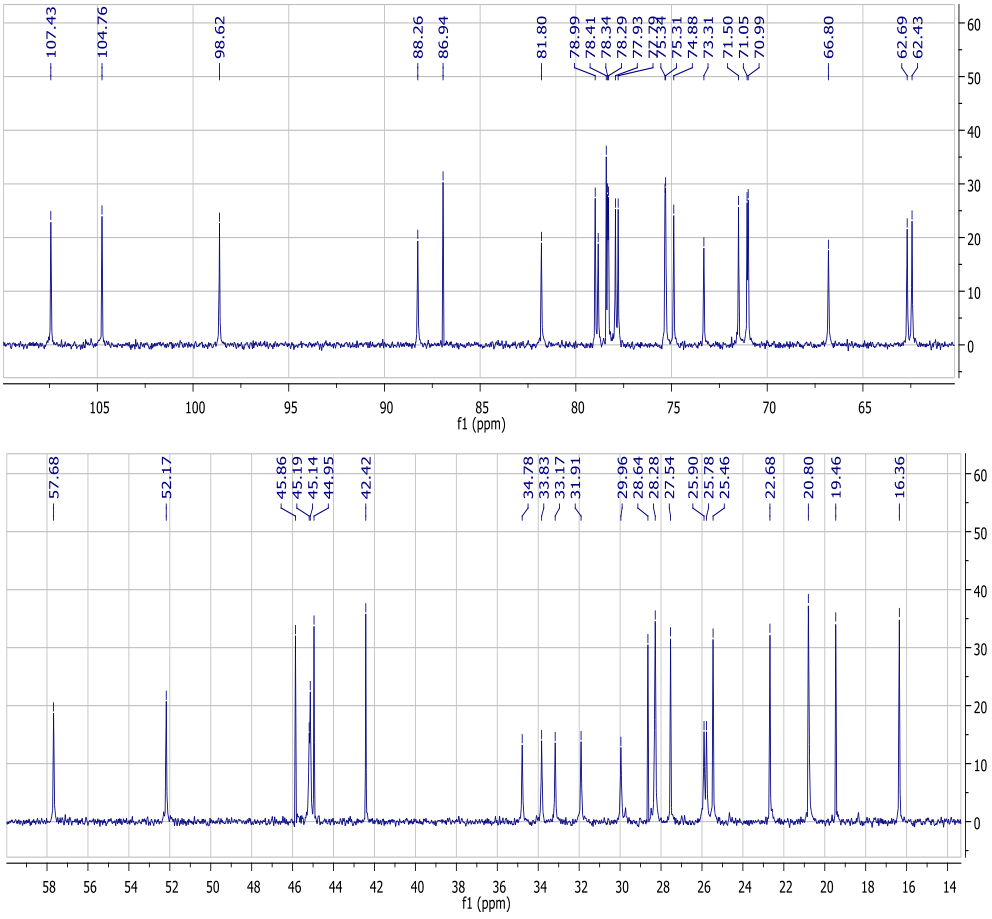

Spectrum 4. Expanded ^{13}C NMR spectrum of [Fr: 51-79]

^{1}H and ^{13}C NMR (400 MHz, C_5D_5N) data was superimposable on those reported in the literature (Bedir 1998, Kitagawa, Wang, and Yoshikawa 1983).

CHAPTER 4

CONCLUSION

As AST VII is a promising compound to become a vaccine adjuvant and/or immunotherapy agent, the main objective of this thesis has been to establish an efficient isolation process to obtain AST VII at large scale. We developed a new method, reliable and stable, to isolate AST VII from *A.trojanus* for pilot-scale production in high purity (Figure 49). To accomplish production of AST VII in +95% purity, a series of processes was optimized and utilized from laboratory scale to semi-pilot scale including extraction, isolation and purification.

The Soxhlet-type extraction is easy to operate and efficient to obtain high yields compared to the conventional methods, and it is more adoptable to pilot-scale than assisted-extraction systems. Thus, it was method of choice during extraction studies. The MeOH extraction optimization studies helped us to determine the important parameters including plant to solvent ratio (0.05 g/mL), plant particle size (0.5-1.0 mm) and duration (8-10 hours) yielding high concentrations of AST VII (3.6‰ g AST VII/g plant).

In the case of isolation process, D-101 resin as a preliminary fractionation provided satisfactory results, and H_2O, 20% EtOH and EtOH elution was found to be superior than other elution ratios. This pre-fractionation not only helped to remove saccharidic and UV-active impurities efficiently but also reduced further load on silica column about 30-40%.

Multistage purification steps are always required for saponin or sapogenin productions at small and large scales due to the presence of close polarity secondary metabolites to be excluded from the target compound as in the case of AST VII.

Accordingly, further chromatographic steps needed to be undertaken to enrich AST VII. Utilization of normal (employing EtOAc:MeOH:H_2O and $CHCl_3$:MeOH:H_2O systems) and reversed phase (RP) (C_{18}; employing MeOH:H_2O systems) silica gel column chromatographies, 85-90% purity was achievable.

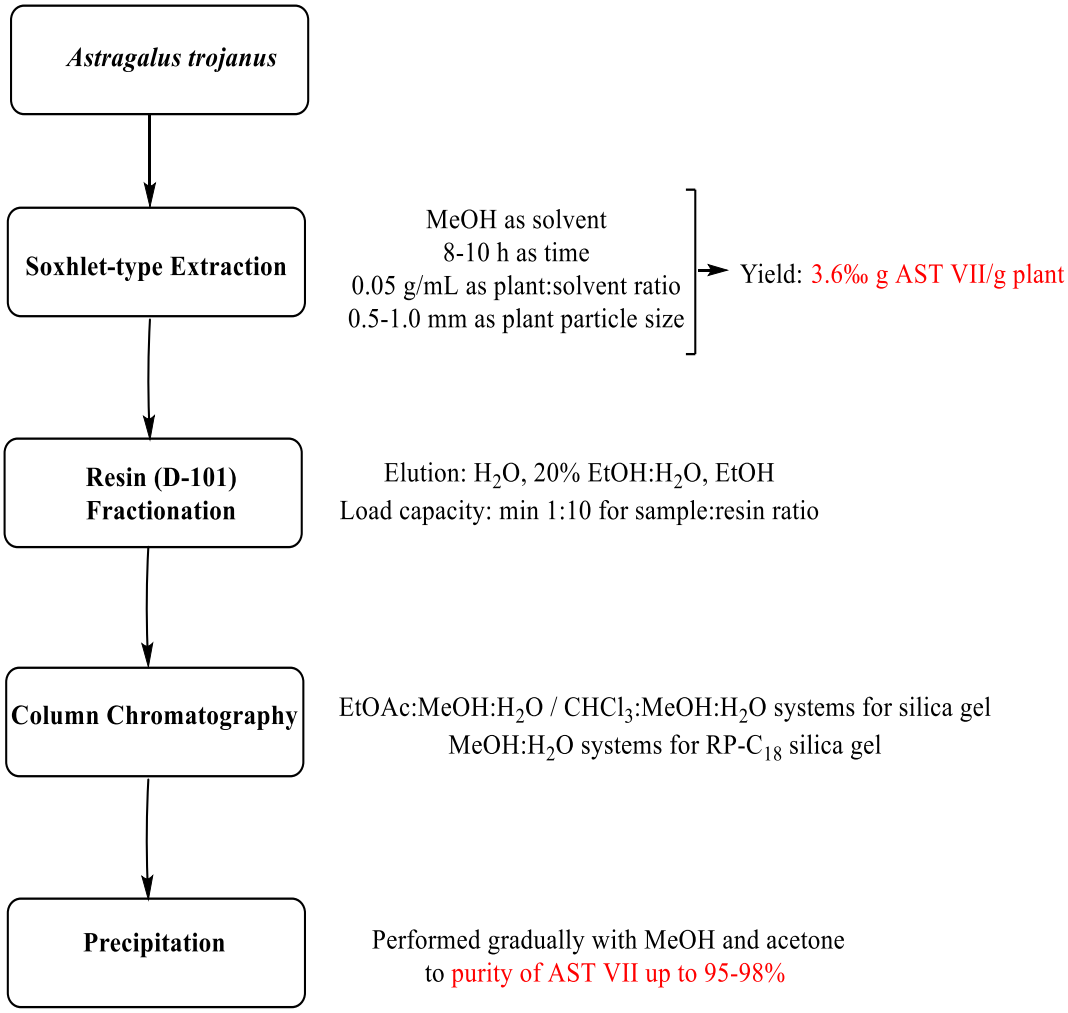

Figure 49. The flow chart of developed method for isolating AST VII in high purity from *A.trojanus*

To obtain natural products or synthetic compounds in their purest form, developing a precipitation or crystallization step is a must to meet the pharmaceutical specifications in regards to purity/impurity ratio. Thus, in the last step, a precipitation method was developed for AST VII production, using MeOH and acetone to afford 98% purity.

The developed method at lab scale (3.5 g) was successfully transferred to semi-pilot scale (~100 g) with minor modifications, and a crucial step towards large-scale isolation (kg) of AST VII was accomplished.

We believe that our studies are important for several reasons. Firstly, AST VII is a promising candidate for immunotherapy and vaccination. If planned clinical trials are

successful to be used as an adjuvant in human vaccines, AST VII will be one of the most valuable compounds exported from our country as high-volume chemical. As the starting plant material is an endemic plant source (*A. trojanus*), the success of the molecule will encourage adaptation and cultivation studies on Astragalus plants and will be an alternative agricultural crop for our farmers in the future.

From a commercial point of view, AST VII's estimated market price would be around 12.000-15.000 USD/kg (98% purity) upon successful production at the pilot scale for large scale orders. The production of AST VII at competitive prices in Republic of China is almost impossible due to the absence or too low content of AST VII in cultivated A*stragalus membranaceus*. The major competitor of AST VII would be QS-21, a binary isomeric mixture obtained from *Quillaja saponaria*, as a marketed adjuvant. The major commercial disadvantages of QS-21 against AST VII is its high price (+100,000 USD/kg) due to purification difficulties, and low stability due to the existence of ester bonds. Based on these, one can state that AST has several advantages over QS-21 when introduced to the market.

As conclusion, the optimization and method development studies towards production of AST VII from *A. trojanus* were carried out from laboratory (mg) to semi-pilot (100 g) scale for the first-time. The data obtained in this study would make a significant contribution to literature for the isolation and scale-up studies of similar molecules. Lastly, the developed method is currently being transferred to the pilot scale (kg) as part of a TUBITAK 1003 project (116Z958).

REFERENCES

Aguilar, JC, and EG Rodriguez. 2007. "Vaccine adjuvants revisited." *Vaccine* 25 (19):3752-3762.

Aprile, Marie A, and AC Wardlaw. 1966. "Aluminium compounds as adjuvants for vaccines and toxoids in man: a review." *Canadian Journal of Public Health/Revue Canadienne de Sante'e Publique* 57 (8):343-354.

Arda, M, A Minbay, N Aydın, Ö Akay, M İzgür, and K İmmunoloji Diker. 1994. Medisan Yayınevi. Ankara.

Bedir, Erdal. 1998. "Bazı Astragalus Türlerinin Sikloartan Triterpenik Saponozitleri Üzerinde Farmakognozik Araştırmalar." Saglık Bilimleri Enstitüsü, Hacettepe Üniversitesi.

Bedir, Erdal, Ihsan Calis, Rita Aquino, Sonia Piacente, and Cosimo Pizza. 1998. "Cycloartane triterpene glycosides from the roots of Astragalus brachypterus and Astragalus microcephalus." *Journal of natural products* 61 (12):1469-1472.

Bedir, Erdal, Ihsan Çalis, Rita Aquino, Sonia Piacente, and Cosimo Pizza. 1999a. "Secondary metabolites from the roots of Astragalus trojanus." *Journal of natural products* 62 (4):563-568.

Bedir, Erdal, Ihsan Çalis, Rita Aquino, Sonia Piacente, and Cosimo Pizza. 1999b. "Trojanoside H: a cycloartane-type glycoside from the aerial parts of Astragalus trojanus." *Phytochemistry* 51 (8):1017-1020.

Bedir, Erdal, Ihsan Calis, Chuck Dunbar, Rudraksh Sharan, John K Buolamwini, and Ikhlas A Khan. 2001. "Two novel cycloartane-type triterpene glycosides from the roots of Astragalus prusianus." *Tetrahedron* 57 (28):5961-5966.

Bedir, Erdal, Ihsan Calis, and Ikhlas A Khan. 2000. "Macrophyllosaponin E: a novel compound from the roots of Astragalus oleifolius." *Chemical and pharmaceutical bulletin* 48 (7):1081-1083.

Bedir, Erdal, Ihsan Calis, Sonia Piacente, Cosimo Pizza, and Ikhlas A Khan. 2000. "A new flavonol glycoside from the aerial parts of Astragalus vulneraria." *Chemical and pharmaceutical bulletin* 48 (12):1994-1995.

Bedir, Erdal, Nirmal Pugh, Ihsan Calis, David S PASCO, and Ikhlas A KHAN. 2000. "Immunostimulatory effects of cycloartane-type triterpene glycosides from Astragalus species." *Biological and Pharmaceutical Bulletin* 23 (7):834-837.

Bedir, Erdal, Irem Iffet Tatli, Ihsan Calis, and Ikhlas Ahmad Khan. 2001. "Trojanosides I—K: New cycloartane-type glycosides from the aerial parts of Astragalus trojanus." *Chemical and pharmaceutical bulletin* 49 (11):1482-1486.

Chaves-Mora, Fernando, M Chacón, Beatriz Badilla-Baltodano, and Carolina Arévalo-Valdes. 2007. "Effect of Echinacea purpurea (Asteraceae) aqueous extract on antibody response to Bothrops asper venom and immune cell response. Efecto del extracto acuoso de Echinacea purpurea en la respuesta de los anticuerpos murinos al veneno de la serpiente Bothrops asper." *Revista de Biología Tropical.* 55 (1):113-119.

Coffman, Robert L, Alan Sher, and Robert A Seder. 2010. "Vaccine adjuvants: putting innate immunity to work." *Immunity* 33 (4):492-503.

Cox, SJ, PV Barnett, P Dani, and JS Salt. 1999. "Emergency vaccination of sheep against foot-and-mouth disease: protection against disease and reduction in contact transmission." *Vaccine* 17 (15-16):1858-1868.

Davis, PH. 1970. Flora of Turkey and East Aegean Islands. Vol: 3, 518-531. University Press, UK: Edinburg.

Davis, PH, and U Plitmann. 1970. Vicia L. Flora of Turkey and East Aegean Islands, Vol. 3. Edinburgh University Press, Edinburgh.

Diker, KS. 1998. "İmmunoloji." *Ankara: Medisan Yayınevi*.

Djimtombaye, Basile-Jimmy, Özgen Alankuş-Çalışkan, Derya Gülcemal, Ikhlas A Khan, Hüseyin Anıl, and Erdal Bedir. 2013. "Unusual secondary metabolites from Astragalus halicacabus LAM." *Chemistry & biodiversity* 10 (7):1328-1334.

Donnelly, John J. 1997. "New developments in adjuvants." *Mechanisms of ageing and development* 93 (1-3):171-177.

Edelman, R. 2000. "An Overview of Adjuvant Use [in:] Vaccine Adjuvants." *Preparation Methods and Research Protocols*:1-29.

Fernández-Tejada, Alberto. 2017. Design, synthesis and evaluation of optimized saponin variants derived from the vaccine adjuvant QS-21. In *Pure and Applied Chemistry*.

Garçon, Nathalie, Patrick Chomez, and Marcelle Van Mechelen. 2007. "GlaxoSmithKline Adjuvant Systems in vaccines: concepts, achievements and perspectives." *Expert review of vaccines* 6 (5):723-739.

Garcon, Nathalie, and Marcelle Van Mechelen. 2011. "Recent clinical experience with vaccines using MPL-and QS-21-containing adjuvant systems." *Expert review of vaccines* 10 (4):471-486.

Glenny, AT. 1926. "The antigenic value of toxoid precipitated by potassium alum." *J. Pathol. Bacteriol.* 29:38-45.

Gülcemal, Derya, Özgen Alankuş-Çalışkan, Angela Perrone, Fevzi Özgökçe, Sonia Piacente, and Erdal Bedir. 2011. "Cycloartane glycosides from Astragalus aureus." *Phytochemistry* 72 (8):761-768.

Gülcemal, Derya, Behnaz Aslanipour, and Erdal Bedir. 2019. "Secondary Metabolites from Turkish Astragalus Species." In *Plant and Human Health, Volume 2,* 43-97. Springer.

Gülcemal, Derya, Milena Masullo, Erdal Bedir, Michela Festa, Tamer Karayıldırım, Ozgen Alankus-Caliskan, and Sonia Piacente. 2012. "Triterpene glycosides from Astragalus angustifolius." *Planta medica* 78 (07):720-729.

Gülcemal, Derya, Milena Masullo, Assunta Napolitano, Tamer Karayıldırım, Erdal Bedir, Özgen Alankuş-Çalışkan, and Sonia Piacente. 2013. "Oleanane glycosides from Astragalus tauricolus: isolation and structural elucidation based on a preliminary liquid chromatography-electrospray ionization tandem mass spectrometry profiling." *Phytochemistry* 86:184-194.

Gupta, Rajesh K. 1998. "Aluminum compounds as vaccine adjuvants." *Advanced drug delivery reviews* 32 (3):155-172.

Gupta, Rajesh K, and George R Siber. 1995. "Adjuvants for human vaccines—current status, problems and future prospects." *Vaccine* 13 (14):1263-1276.

Horo, Ibrahim, Erdal Bedir, Milena Masullo, Sonia Piacente, Fevzi Özgökçe, and Özgen Alankuş-Çalışkan. 2012. "Saponins from Astragalus hareftae (NAB.) SIRJ." *Phytochemistry* 84:147-153.

Horo, İbrahim, Erdal Bedir, Angela Perrone, Fevzi Özgökçe, Sonia Piacente, and Özgen Alankuş-Çalışkan. 2010. "Triterpene glycosides from Astragalus icmadophilus." *Phytochemistry* 71 (8-9):956-963.

Karabey, Fatih, Ikhlas A Khan, and Erdal Bedir. 2012. "Cycloartane-type glycosides from Astragalus schottianus." *Phytochemistry letters* 5 (2):320-324.

Kensil, Charlotte A, and Dante J Marciani. 1991. Saponin adjuvant. Google Patents 5057540.

Kensil, Charlotte R, MJ Newman, RT Coughlin, S Soltysik, D Bedore, J Recchia, JY Wu, and DJ Marciani. 1993. "The use of Stimulon adjuvant to boost vaccine response." *Vaccine Res* 2 (4):273-81.

Kitagawa, Isao, Huikang Wang, and Masayuki Yoshikawa. 1983. "Saponin and sapogenol. XXXVII. Chemical constituents of astragali radix, the root of Astragalus membranaceus Bunge.(4). Astragalosides VII and VIII." *Chemical and pharmaceutical bulletin* 31 (2):716-722.

Lee, Sujin, and Minh Trang Nguyen. 2015. "Recent advances of vaccine adjuvants for infectious diseases." *Immune network* 15 (2):51-57.

Lindblad, EB. 1995. "Aluminium adjuvants." *The theory and practical application of adjuvants* 2:21-35.

Mamedova, RP, and MI Isaev. 2004. "Triterpenoids from Astragalus plants." *Chemistry of natural compounds* 40 (4):303-357.

Marty-Roix, Robyn, Gregory I. Vladimer, Kimberly Pouliot, Dan Weng, Rachel Buglione-Corbett, Kim West, John D. MacMicking, Jonathan D. Chee, Shixia Wang, Shan Lu, and Egil Lien. 2016. "Identification of QS-21 as an Inflammasome-activating Molecular Component of Saponin Adjuvants." *The Journal of biological chemistry* 291 (3):1123-1136. doi: 10.1074/jbc.M115.683011.

Nalbantsoy, Ayşe, Tuna Nesil, Seçil Erden, İhsan Çalış, and Erdal Bedir. 2011. "Adjuvant effects of Astragalus saponins macrophyllosaponin B and astragaloside VII." *Journal of ethnopharmacology* 134 (3):897-903.

Nalbantsoy, Ayşe, Tuna Nesil, Özlem Yılmaz-Dilsiz, Güzide Aksu, Shabana Khan, and Erdal Bedir. 2012. "Evaluation of the immunomodulatory properties in mice and in vitro anti-inflammatory activity of cycloartane type saponins from Astragalus species." *Journal of ethnopharmacology* 139 (2):574-581.

National Center for Biotechnology Information. PubChem Database. Unii-61H83wzx3U, CID=73652135, https://pubchem.ncbi.nlm.nih.gov/compound/Unii-61H83wzx3U, (accessed on Jan. 14, 2020).

O'Hagan, Derek T. 2000. *Vaccine adjuvants: Preparation methods and research protocols*. Vol. 42: Springer Science & Business Media.

Petrovsky, Nikolai, and Julio César Aguilar. 2004. "Vaccine adjuvants: current state and future trends." *Immunology and cell biology* 82 (5):488-496.

Polat, Emre, Erdal Bedir, Angela Perrone, Sonia Piacente, and Ozgen Alankus-Caliskan. 2010. "Triterpenoid saponins from Astragalus wiedemannianus Fischer." *Phytochemistry* 71 (5-6):658-662.

Polat, Emre, Ozgen Caliskan-Alankus, Angela Perrone, Sonia Piacente, and Erdal Bedir. 2009. "Cycloartane-type glycosides from Astragalus amblolepis." *Phytochemistry* 70 (5):628-634.

Puder, Carsten H., Herbert Graef, Markus J. Thumerer, and Markus Heitzmann. 2007. "Improved method for the production of betulinic acid". Canada Patent 2 626996.

Rajput, Zahid Iqbal, Song-hua Hu, Chen-wen Xiao, and Abdullah G Arijo. 2007. "Adjuvant effects of saponins on animal immune responses." *Journal of Zhejiang University Science B* 8 (3):153-161.

Ramon, G. 1925. "Sur l'augmentation anormale de l'antitoxine chez les chevaux producteurs de serum antidiphterique." *Bull Soc Centr Med Vet* 101:227-234.

Ramon, G. 1926. "Procedes pour acroitre la production des antitoxins." *Ann Inst Pasteur* 40:1-10.

Reddy, L Harivardhan, and Patrick Couvreur. 2009. "Squalene: A natural triterpene for use in disease management and therapy." *Advanced drug delivery reviews* 61 (15):1412-1426.

Richou, R, R Jensen, and C Belin. 1964. "Research on saponin, an adjuvant substance which stimulates immunity. I." *Revue d'immunologie et de therapie antimicrobienne* 28:49.

Roberts, David S. 2000. Multicomponent clostridial vaccines using saponin adjuvants. Google Patents.

Sivakumar, SM, Mohammed M Safhi, M Kannadasan, and N Sukumaran. 2011. "Vaccine adjuvants–current status and prospects on controlled release adjuvancity." *Saudi Pharmaceutical Journal* 19 (4):197-206.

Spriggs, Dale R, and Wayne C Koff. 1990. *Topics in vaccine adjuvant research*: CRC Press.

Stewart-Tull, DES. 1989. "Recommendations for the assessment of adjuvants (immunopotentiators)." In *Immunological adjuvants and vaccines*, 213-226. Springer.

Sun, Hong-Xiang, Yong Xie, and Yi-Ping Ye. 2009. "Advances in saponin-based adjuvants." *Vaccine* 27 (12):1787-1796.

Tabanca, Nurhayat, Erdal Bedir, Ozgen Alankus-Caliskan, and Ikhlas A Khan. 2005. "Cycloartane triterpene glycosides from the roots of Astragalus gilvus Boiss." *Biochemical systematics and ecology*.

Yeo, Jinmo, and Kyu Il Kim. 1997. "Effect of feeding diets containing an antibiotic, a probiotic, or yucca extract on growth and intestinal urease activity in broiler chicks." *Poultry Science* 76 (2):381-385.

Yesilada, Erdem, Erdal Bedir, İhsan Çalış, Yoshihisa Takaishi, and Yasukazu Ohmoto. 2005. "Effects of triterpene saponins from Astragalus species on in vitro cytokine release." *Journal of ethnopharmacology* 96 (1-2):71-77.

Yurdakök, Kadriye, and Tolga İnce. 2008. "Aşı adjuvanları." *Çocuk Sağlığı ve Hastalıkları Dergisi* 51 (4):225.

Zeybek, N. 1985. Pharmaceutical Botany, No 1. Ege University Press, Izmir.

Zhang, Guanfu. 2015. "Extraction process of ginseng saponin Rd". Chinese Patent 1046100410A.

Zhiming, Zhang, Yang Xiangyu, Erdun bayar, An Xiaodong, and Lian canal. 2017. "Industrial production method of rough glycyrrhizic acid". China Patent 106279345A.